Trace Explosive Sensor Devices Based on Semiconductor Nanomaterials

Danling Wang

A dissertation

submitted in partial fulfillment of the

requirements for the degree of

Doctor of Philosophy

University of Washington

2014

Reading Committee:

Lih Y. Lin, Chair

Antao Chen

Bill Asher

Program Authorized to Offer Degree:

Department of Electrical Engineering

University of Washington

ABSTRACT

Trace Explosive Sensor Devices Based on Semiconductor Nanomaterials

Danling Wang

Chair of the Supervisory Committee:

Professor Lih Y. Lin

Department of Electrical Engineering

This dissertation discusses an explosive sensing device based on semiconductor nanomaterials. Here, we mainly focus on two kinds of materials: titanium dioxide nanowires and silicon nanowires to detect explosive trace vapor. Herein, methods for the synthesis, fabrication, design of nanostructured sensing materials using low-cost hydrothermal process are present. In addition, the nanomaterials have been systemically tested on different explosive. The first part of dissertation is focused on the fabrication of TiO_2(B) dominant nanowires and testing the response to explosives. It was found that the high porous TiO_2(B) nanowires when mixed anatase TiO_2, exhibit a very fast and highly sensitive response to nitro-containing explosives. The second part of dissertation has studied the basic sensing mechanism of TiO_2(B) nanowire sensor to detect explosives. It shows the specific surface characteristics of TiO_2 responsible for the nitro-containing explosives. This information is then used to propose a method using UV illumination to reduce the effect of water vapor on TiO_2(B) nanowires. The third part discussed an explosive sensor based on silicon nanowires. We analyzed the mechanism of silicon nanowires to detect

nitro-related explosive compounds. In order to further investigate the sensing mechanism of TiO_2, the fourth part of dissertation studies the effect on sensor performance by using different crystal phases of TiO_2, different microstructure of TiO_2, surface modification of TiO_2, and different kinds of nanostructured semiconductors such as ZnO nanowires, TiO_2 coated ZnO nanowires, V_2O_5 nanowires, and CdS nanowires to detect explosives. It is found that only TiO_2 related semiconductor shows good response to explosives.

Table of Contents

List of Figures

List of Tables

ACKNOWLEGEMENTS

First and foremost I want to thank my research advisor, Dr. Antao Chen, for giving me the opportunity to join his group. Since 2008, Dr. Chen has supported me not only by providing a research assistantship over 5 years, but also motivating me a great interest in exploring explosive sensors using nanomaterials. My dissertation cannot be done without his excellent guidance, invaluable advice, constant support and great encouragement. I feel very grateful and extremely fortunate for all my life to have this opportunity to work under such a knowledgeable and helpful advisor. I also would like to thank Prof. Lih Y. Lin, my academic advisor. She has helped me much greatly through my PhD study in the Department of Electrical Engineering since 2008. For the reason of a big extension from physics to electrical engineering, I had a very difficult time in the beginning of my Ph.D. study. Without Prof. Lin's warm and moral support, I could not overcome it.

I am very thankful my committee members, Dr. Bill Asher in Applied Physics Laboratory, Prof. Bruce Darling in the department of Electrical Engineering, Prof. Alex K.-Y. Jen in the Department of Materials Science & Engineering, and Prof. Munira Khalil in the Department of Chemistry, for providing me with great advice and suggestions to improve my dissertation and defense. It has been an honor to learn from them. I also want to thank Prof. Guozhong Cao in the Department of Materials Science & Engineering for helping initialize this project in regard of material fabrication. I appreciate Dr. Eric Thorsos in Applied Physics Laboratory. He provided valuable suggestion for the improvement of my dissertation.

The members of photonics group have provided me with many useful discussions and valuable suggestions to my research. Here, I would like to thank the past and present members: Dr. Haishan Sun, Dr. Hassan Arbab, Charles Elliott, Dr. Philip Colosimo, and Alan Yao. It was so nice to work with all of you.

Finally, I want to thank my parents. Without their support, I cannot be here. Last but not least, I want to thank my husband, Qifeng Zhang, for his constant support in these years.

DEDICATION

To my parents, my husband (Qifeng), and my daughters (Windy and Sunny)

Chapter 1

INTRODUCTION

1.1 Background

1.1.1 The importance of explosive detection

In recent years, terrorism has grown very quickly and nearly every terrorist attack involves explosives because explosive-based weapons are simple, easy to deploy, and can cause enormous damage [1, 2]. Therefore, in order to protect the society from the increasing terrorist threat, effective techniques to detect high-explosive materials commonly used in terrorist attacks such as TNT (2,4,6-trinitrotoluene), RDX (cyclotrimethylene trinitramine), PETN (pentaerythritol tetranitrate), picric acid (2,4,6-trinitrophenol) at trace levels in luggage, vehicles, mail, aircraft and soils are very necessary. However, explosives detection is very challenge due to many reasons, such as, very low vapor pressure of most explosives [3], physical state of the sample to be detected (solid, liquid and gas), complicating or inhibiting the detection due to degradation by-products of explosives, and interferences leading to false signal due to other chemicals in the environment and the lack of selectivity of the detection techniques.

1.1.2 Properties of Explosives

It is important to understand the physical and chemical properties of explosives since these will affect how the explosives may be detected. There are three main characteristics of explosives that are relevant [4].

1) Explosives may be broken down into two general groups: **nitro/nitrate-based** and **non nitro/nitrate-based**. Nitro/nitrate-based explosives include ***aliphatic nitro compounds***, such as nitromethane, hydrazine nitrate; ***Nitroaromatic compounds***, such as 2,4,6-trinitrotoluene (TNT), 2,4-dinitrobenzene (DNB), 2,4,6-trinitrophenol (TNP, also called picric acid); ***Nitramines or nitrosamines***, such as octahydro-1,3,5,7-tetranitro-1,3,5,7-tetrazocane (HMX) or hexahydro-1,3,5-trinitro-1,3,5-triazine (RDX); ***Nitrate esters***, such as pentaerythritol tetranitrate (PETN); and acid salts, such as ammonium nitrate. Non-nitro/nitrate-based explosives are derived from materials such as peroxides, e.g., triacetone triperoxide (TATP), perchlorates, and azides. Since the military primarily uses nitro-based explosives, our studies mainly focused on nitro/nitrate-based explosives.

2) The vapor pressures of most explosives at ambient temperature are extremely low, ranging from parts per million (ppm) to less than parts per quadrillion (ppq) like HMX [5]. Table 1.1 shows the vapor pressures of common explosives. The very low vapor pressures indicate that these molecules are very sticky and tend to adsorb to surfaces very easily. The sticky nature of explosive molecules on surfaces at room temperature can condensation of the molecules in delivery lines into sensor systems. Therefore, trace sampling of these explosives can be even hard because of the small number of molecules in a sampling volume. The detection of explosives in techniques becomes very limited.

3) Nitro/nitrate-based explosives all have nitro-groups and are high electronegativity.

Table 1.1 Vapor pressures and molecular weights of some explosives [5].

Explosive	Molecular weight (g/mol)	Vapor pressure at 20°C (Torr)
Ethylene glycol dinitrate (EGDN)	152.1	5.2×10^{-2}
2,4,6-trinitrotoluene (TNT)	227.1	4.8×10^{-6}
Pentaerythritol tetranitrate (PETN)	316.1	6.2×10^{-8}
2,4,6-trinitrophenol (picric acid)	229.1	3.1×10^{-8}
Tetranitro-triazacyclohexane (RDX)	222.3	8.3×10^{-10}
Tetranitro-N-methylamine (Tetryl)	287.1	3.7×10^{-10}

However, larger surface energy materials such as metal oxides, or materials with large surface area can absorb more explosive molecules and make the detection of explosives easier.

1.1.3 Sensor and Its parameters

A sensor is a **device** that converts a signal from one form to another or detects a signal, physical condition or chemical compounds. In this dissertation, we mainly discuss a sensor device to detect chemical compounds. When target molecules chemically adsorb on the sensor surface, they alter the surface state and change the sensor resistance. Therefore, sensors that detect analytes by monitoring resistance change are also called chemiresistors. Increasing the surface-to-volume ratio or enhancing the surface adsorption is the most important way to improve the sensitivity of chemiresistors. Generally, there are several parameters which can be used to evaluate the performance the sensor devices. Table 1.2 shows commonly used sensor performance of parameters. Since the vapor pressures of explosives are very low, trace explosive detection needs a sensor with ***high sensitivity*** and a ***low limit of detection (LOD)*** because of the

relatively small amount of explosive molecules that can be collected and detected. In order to continuously operate sensing device with low power consumption, the explosive sensor should be ***stable, fast response time*** and ***readily reversible*** at room temperature. Also, ***high selectivity*** is important in order to avoid false response.

Table 1.2 Definition of performance parameters for sensors [5]

Performance Parameter	Definition
Sensitivity	The slope of a calibration curve or change in unit sensor response with change in unit analyte concentration
Limit of detection (LOD)	Lowest analyte concentration value that can be detected
Resolution	Smallest concentration variation that can be detected when the concentration is continuously changed
Dynamic range	The analyte concentration from LOD to maximum concentration that can be reliably detected
Selectivity	The ability to detect a specific analyte in the presence of other interfering molecules
Reversibility	The ability of the sensor to return back to its original value when the analyte is removed
Response time	The time required to respond to a change from zero analyte concentration to a step in the concentration
Linearity	The range where the sensor response is in direct proportion to the analyte concentration
Hysteresis	The difference in sensor characteristics for increasing and decreasing analyte concentrations

1.1.4 Development and challenge of current techniques of trace explosive detection

Techniques to detect hidden explosives can be classified into two categories [6]: bulk detection and trace detection. Bulk detection detects bulk quantities of explosives while trace detection is able to detect the invisible residues of explosives on vehicles, persons, packages, mail, baggage, and other items handled by a person who has been exposed to explosives. In the past years, the most common techniques for bulk and trace explosives detection include trained canines [7], X-ray and gamma ray imaging techniques [8, 9], Terahertz spectroscopy based detection [10, 11], fluorescence based detection [12-14], mass spectrometry or Gas chromatography–mass spectrometry [15] and surface acoustic wave [16]. A brief review of most representative detecting technologies is described below.

1) *Trained dogs to detect explosive*

As early as 1971, Dr. Philips at University of Mississippi has done a systemically study to train dogs efficiently detecting explosives [7]. Although there are a lot of advantages to use trained dogs rapid and efficiently detecting several different kinds of explosives, this technique is still complicated and can cause uncontrolled performances. This is because this method not only needs to spend a lot of time training dogs but also a well-trained handler is needed. Also, the dogs are only fit for duty for couple of hours or so before needing to be rested.

2) *X-ray and gamma ray imaging techniques*

X-ray technique is used for bulk explosive detection, which involves irradiation of target item with X-rays, followed by detection of images created by X-rays that are either transmitted or backscattered by the item [8]. This technique provides 2D or 3D quality images. For example,

2D transmission approach, as shown in Fig.1.1, can clearly provide the information of a given object such as location, orientation and volume. However, X-ray technique is only sensitive to shapes, densities and absorption patterns of materials and cannot identify the type of material. Considering this limitation, gamma ray imaging technique is used to detect explosives [9]. It can measure relative content of nitrogen, oxygen and carbon by identifying their molecular weight. Therefore, gamma ray imaging technique is ability to identify the type and location of the target. However, both X-ray and gamma ray imaging techniques require expensive instruments.

3) *Terahertz spectroscopy based detection [10, 11]*

As early as in 2003, terahertz spectroscopic technique was firstly applied in the explosive detection. Since then, a considerable amount of research and development has carried out and continues to be. This is because terahertz spectroscopy can nondestructively and nonintrusively discriminate different explosives as well as identify them in comparison with other materials. The most commonly used methods for terahertz spectroscopy are Fourier transform infrared (FTIR) spectroscopy and terahertz time-domain spectroscopy (TDS). As shown in Fig.1.2, most explosives such as TNT, RDX, HMX, PETN, PE4, and Semtex, have distinctive spectral features. This confirms that terahertz spectroscopy can effectively detect different explosives without strongly affected by other materials or environmental temperature change [10].

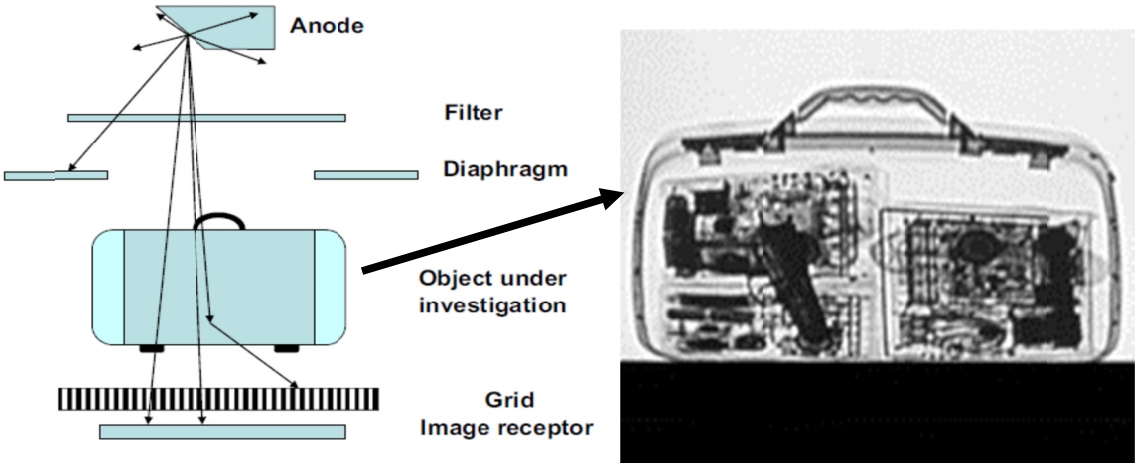

Figure 1.1 Schematic of a standard projection radiography set-up providing for imaging of bulky item [10].

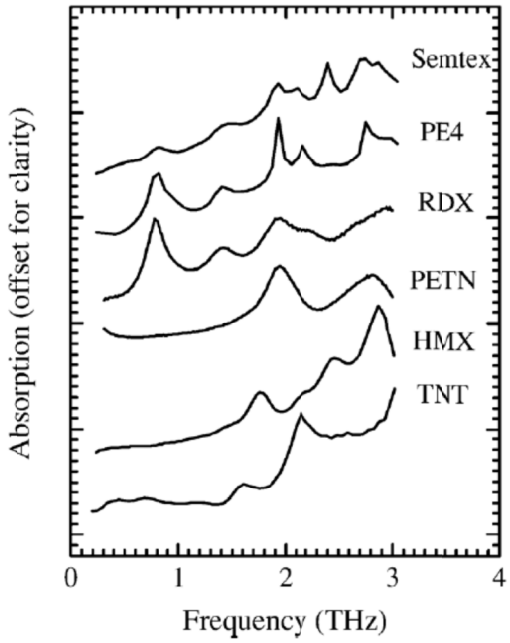

Figure 1.2 Terahertz transmission spectra of the raw explosive materials TNT, HMX, PETN and RDX together with the spectra of the compound explosives PE4 and Semtex [11].

4) *Fluorescence based technique [12, 13]*

Fluorescence sensors are kind of sensing system to be capable of not only trace nitroaromatic explosives detection but also field deployment. Also, they can be scalable to relative small sizes, and inexpensive. The main mechanism of fluorescence based explosive sensors is due to the ability of nitroaromatic and nitramine molecules to act as electron acceptors, quenching the emission of nearby excited fluorescence species, such as fluorescent polymer (FP) (Fig.1.3) [14, 15].

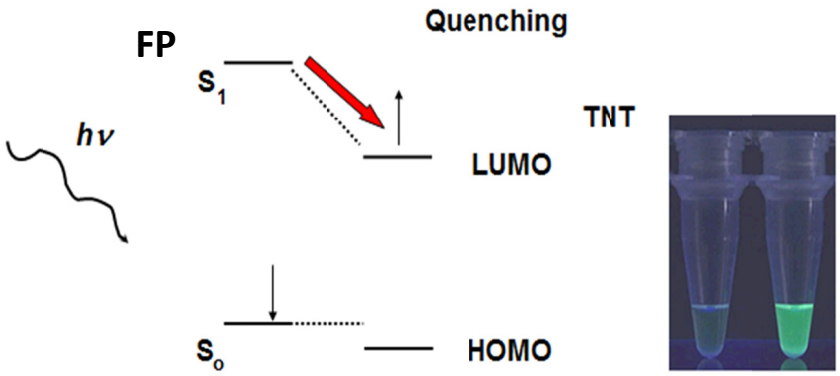

Figure 1.3 The schematic shows the mechanism of fluorescent polymer to detect TNT. The transfer of excited electrons from the conjugated polymer or namely FP to the lowest unoccupied molecule orbital (LUMO) of the target molecule (TNT) leads to quenching of fluorescence intensities of the polymer.

Those techniques have provided feasible and vast diversity of methods to detect and analyze explosives. However, detection systems based on those techniques are usually bulky, expensive, high-power consumption and requiring a careful maintenance by qualified personnel. These factors limit their applications in explosives detection [17-19]. Therefore, their common feature

is a high degree of complexity that adversely affects their compatibility with miniature mass-deployable devices.

1.2 Metal-Oxide Semiconductors as Gas Sensors

Considering the challenges of above techniques, it is very necessary to develop a new technique which could allow detecting explosives with high sensitivity, selectivity, stability, small size, and low-cost. The development of semiconductor materials, such as tin oxide, zinc oxide, aluminum oxide and indium oxide etc., provides a well-suited way of sensing application in gas detection. This is because the semiconductor based gas sensors have several unique advantages such as low cost, small size, measurement simplicity, durability, ease of fabrication, and low detection limits (< ppm levels). Therefore, nowadays, semiconductors become the most widely used gas sensors. While, nanotechnology based on semiconductor materials further provides a feasible solution for building substantially smaller, highly sensitive and selective sensing devices [20]. Due to high surface to volume ratio, nanostructured semiconductors favor the adsorption of gases on the sensor and can increase the sensitivity and response time of the device because of stronger interaction between the analytes and the sensing material and more measurable response (especially at low concentration) [21-25].

1.2.1 Working Principle

The fundamental mechanism of semiconductor as a sensor device is that the electrical resistance is very sensitive to the presence of impurities in its volume or at the surface. In most case, the change of conductivity in semiconductor by trapping electrons from the bulk once target gas molecules adsorb at the surface of the metal oxides. The overall effect of this trapping is

increasing the resistance of the sensor, for n-type materials, or decreasing it, for p-type materials [26]. Therefore, semiconductor sensors are also called chemiresistor sensors. As shown in Fig.1.4, for example, a schematic diagram of the reactions occurs at the surface of an n-type semiconductor. When a reducing species such as CO is present, it oxidizes and releases a negative charge, which decreases the depleted region and then increases the conductivity of the material. While, in the present of an electronegative compound such as NO_2 or O_2, the charges are attached to the adsorbed molecules, which decreases the conductivity of the semiconductor material. This change is recorded and the signal is correlated to the concentration of the target gas.

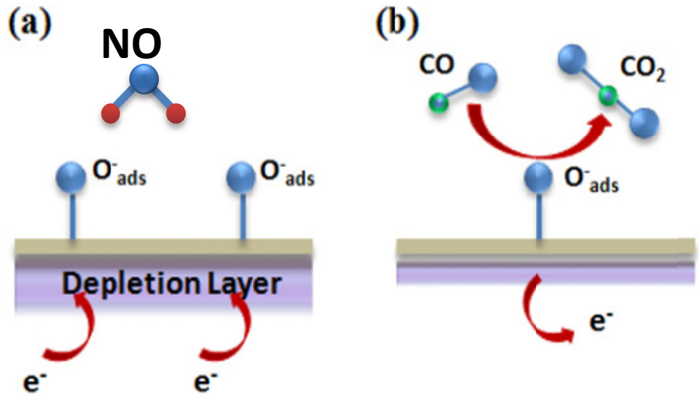

Figure 1.4 Schematic diagram of the reactions occurring at the surface of an n-type semiconductor metal oxide. (a) Adsorption of NO_2 at the surface creates surface acceptor sites, creating a depletion layer. (b) Reducing gases, such as CO, remove surface bound oxygen atoms, releasing electrons, reducing the thickness of the depletion layer [27].

Although the fundamental mechanisms of semiconductors causing a gas response are still unclear, t**rapping of electrons** at adsorbed molecules and **band bending** induced by these charged molecules are considered to be the essential reasons of a change in conductivity of semiconducting metal-oxides. In the ideal case, only oxygen presents and humidity is not

involved, oxygen is ionosorbed on the metal oxide surface and forms charge species such as O^-, O_2^-, and O^{2-}. These ionosorbed species acting as electron acceptors are believed to be a key factor leading to a difference in the energy band structure between surface and bulk in metal-oxides. As shown in Figure 1.5, when O_2 molecules are adsorbed on the surface of metal oxides, they would extract electrons from the conduction band E_c and trap the electrons at the surface in the form of ions. This will lead to **band bending** and an **electron depleted region**. The electron-depleted region is so called space-charge layer, of which thickness is the length of band bending region. When other gas molecules adsorb on the surface of metal-oxides, it can change the thickness of the depleted region due to a charge transfer reaction and then cause a change of conductivity.

The reaction of semiconducting metal oxide with gas and the result of the conductometric changes were firstly observed in the early 1950's by Brattein et al. [29]. Then, in the early 1960s, the direct applications of the semiconductor as sensors to detect various gases were introduced by Seiyama et al. [30], which resulted in the fabrication of the first gas-sensing elements. Since that time, much technological effort has been made in order to improve the sensitivity, selectivity, stability, as well as the response and recovery time, which are the key parameters for the sensor performance. Researchers and engineers realized that sensing properties based on semiconductors can be enhanced by varying the crystal structure, dopants, fabrication techniques and operation temperature, etc. [31-34].

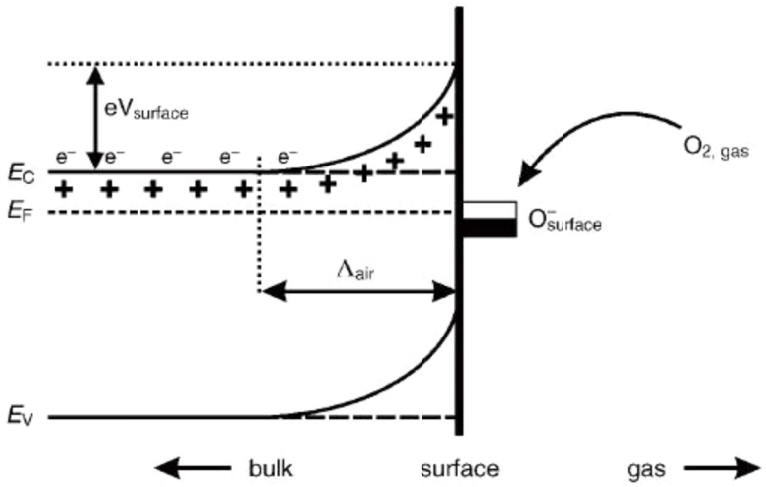

Figure 1.5 A diagram of band bending after chemisorptions of charged species (here the ionosorption of oxygen). E_c, E_v, and E_F are energy of the conduction band, valence band, and the Fermi level, respectively. Δ_{air} is the thickness of the depletion region, and $eV_{surface}$ is the surface potential barrier. The conducting electrons are presented by e^- and + means the donor sites [28].

1.2.2 Why Nanostructured Semiconductors are Important to Gas Sensors?

Even with the efforts of improving the sensing properties of semiconductors, the sensor devices made by bulk semiconductors still have a lot of limited characteristics, such as long-term signal drift, slow sensor response, and low sensitivity. In addition, semiconducting metal-oxide based sensors need to operate at high temperatures. This is because oxygen is ionosorbed on the surface predominantly as O_2^- ions below 147 °C or as O^- ions between 100 and 400 °C. Above 400 °C, the parallel formation of O^{2-} occurs. Such high operating temperature range also limits the use of this type of material in sensing detection.

With the progress in nanotechnology, nanostructured metal-oxides have attracted much attention in the sensing application since they have high surface to volume ratio, good chemical and thermal stabilities with minimal power consumption, charge confinement ability, less power

consumption and easy fabrication methods [35]. Based on the sensing mechanism of semiconducting metal-oxides as we discussed above, both surface state and morphology of the metal-oxides play important roles in gas sensing performance [36]. While, nanostructured semiconductors have unique surface state and controlled morphology. All these characteristics make nanostructured semiconductors be sensor devices not only robust but also high sensitivity, selectivity and reversibility in favorable operating condition.

- **High surface area/volume ratio:** since the response of gas sensor depends on the surface reaction or interaction between the metal oxide and the gas molecules, nanostructured metal-oxides favor the adsorption of gases on the sensor and exhibit an **increased sensitivity** as well as a **faster response and recovery time** compared to bulk semiconductor.

- **Difference in microstructure:** the influence of the microstructure, that is, **the film thickness** and its **porosity**, are critical factors on the response time and the sensitivity. Sensing layers are penetrated by oxygen and analyte molecules which form a concentration gradient. This concentration gradient depends on the equilibrium between the diffusion rates of reactants and their surface reaction and so the rate determines the response and recovery time. Therefore, a fast diffusion rate can be reached with smaller mean pore size at a certain working temperature. In addition, higher sensitivity will be achieved if more analyte molecules are involved. Thus, a lower film thickness together with a higher porosity contributes to a higher sensitivity and faster response time [37, 38].

- **Difference in morphology:** forms of 0-dimensional nanoparticles and 1-dimentional nanowires can result in different **sensing response** and **selectivity** [39]. Fig.1.6 gives an

example how the dimensionality of ZnS nanostructures affects its sensing characteristics on hydrogen. This is because different morphologies of nanostructured semiconductors have different exposed facets with different ability of chemisorption.

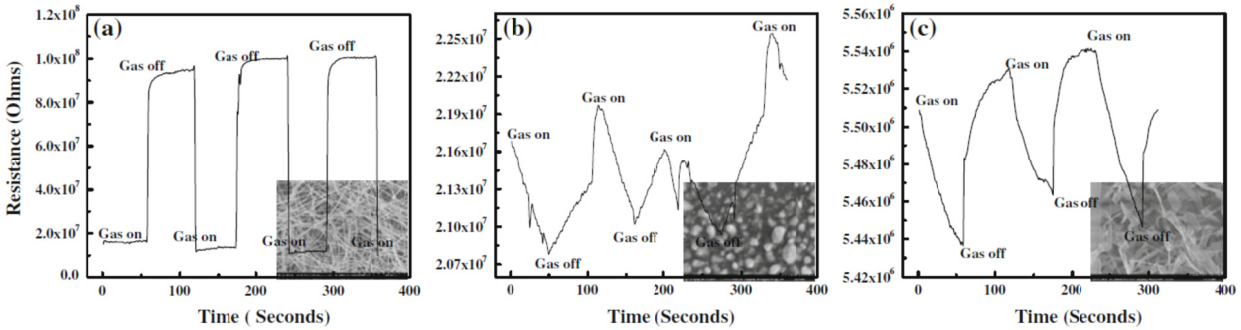

Figure 1.6 Sensing response of ZnS to 50,000 ppm H_2 gas at the working temperature of 230 °C; (a) nanowires (b) nanodots and (c) nanoleaves [39].

- **Shape controlled nanocrystallites**: it can provide energetically different adsorption sites for the analytes on different crystal facets. This can affect semiconductor surface energy to adsorb analyte molecules and then cause a change of sensing sensitivity and response time.

- **Surface modification and doping:** surface modification and doping on nanostructured semiconductors provide addition of catalytically active sites to the surface. Therefore, this process improves sensor performance by increasing the sensitivity, favoring the selective interaction with the target analyte and thus increasing the selectivity, and decreasing response and recovery time. Furthermore, surface modification and doping may enhance sensor's long-term stability and have lower power consumption. Moreover,

chemical sensitization of nanostructured metal-oxide surface can also improve metal-oxides sensing performance.

1.2.3 Nanostructured Semiconductors as Explosive Sensors

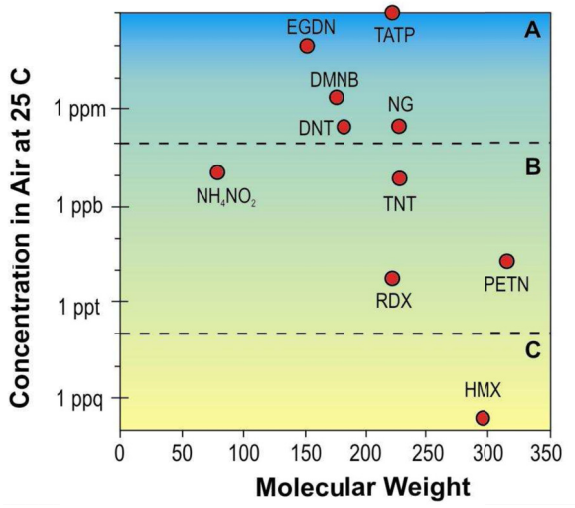

Figure 1.7 Vapor concentration of explosives (A, B, and C-high, medium and low respectively).

In this dissertation, we are focused on **trace vapor explosive detection**. So, the explosive is detected by chemical identification of microscopic residues of the explosive compound. These residues can be applied in either or both of two forms: vapor and particulate. While, vapor detection refers to gas-phase molecules emitted by a solid or liquid explosive. The concentration of explosives can be divided into three groups: high, medium, and low vapor pressure. Figure1.7 shows the maximal vapor concentrations of several explosives at room temperature [40]. Since vapor pressures of most explosives are extremely low, detecting trace vapors of explosives is a challenging task. Sensors based on nanoscience offer a way to detect trace explosive with satisfying this requirement. Other than this, nanostructured semiconductors provides a feasible

solution for building substantially smaller, highly sensitive, and selective trace explosive detectors.

Nanostructures of metal-oxide semiconductors such as SnO_2 and In_2O_3 are widely used as a base material for commercial gas sensors for the detection of toxic (e.g. CO) or dangerous (e.g. CH_4) gases [41]. The first explosive sensor based on single-walled carbon nanotubes was reported by E.S.Snow et al. in 2005 [42]. They used by thinly coating chemoselective materials to detect 2, 4-dinitrotoluene (2, 4-DNT) and found that the sensing response was strongly modified by surface interactions. In 2009, Banerjee *et al* developed an explosive sensor device based on surface sensitized titania nanotube arrays [43]. The response to explosive (triacetone triperoxide, TATP) is rapid and a signal of five to eight orders of magnitude is observed. In 2010, Engel et al demonstrated selective detection of TNT in solution by silicon nanowire arrays [44]. Recently, our group has carried out a series of study to detect trace explosives based on titania nanowires and silicon nanowires [45-49]. We found out that nanostructured TiO_2 based chemiresistive sensors can effectively detect explosives with detection limit below sub-ppb levels and response time below a second.

1.3 Outline of Thesis Contents

Chapter 2 describes different explosive sensing detection based on TiO_2 (B) nanowires. Chapter 3 focuses on a symmetrical study of sensing mechanism based on TiO_2 (B) nanowires to detect explosive. Chapter 4 discusses a method to reduce cross-sensitivity of humidity effect by using UV illumination. Chapter 5 has briefly described silicon nanowire based explosive sensor. Chapter 6 discusses several methods to further understand the sensor mechanism based on

nanostructured TiO_2 and improve TiO_2 nanowire sensing performance based on these understandings. Finally, in this Chapter, it presents the overall conclusions of this dissertation research and suggests possible future research directions.

Chapter 2

TITANIA (B) NANOWIRES BASED CHEMIRESISTIVE EXPLOSIVE SENSORS

2.1 Introduction

Compared to other wide band-gap metal oxides such as SnO_2, Ga_2O_3, ZnO and WO_2, titanium oxide (TiO_2) is an n-type semiconductor due to oxygen vacancies and exhibits unique chemical and electrical characteristics including superior photocatalytic properties and excellent chemical stability [50] and has been extensively used in gas sensing experiments [51-53]. Also, TiO_2 has found to have self-cleaning surfaces [54]. TiO_2 has four crystal polymorphs found in nature: rutile, anatase, brookite, and TiO_2(B) [55]. These different polymorphs can influence the sensing properties. The anatase phase is preferred over rutile and brookite in gas sensing due to its higher photocatalytic activity [56]. TiO_2(B) has the advantage over the other TiO_2 polymorphs due to a relatively open structure with significant voids and continuous channels, a higher electron mobility, and lower density. These make the TiO_2(B) structure an excellent host for adsorbates [57]. Recently, it has been reported that solids with mixed anatase and TiO_2(B) phases exhibit much higher photocatalytic activity than the solids of either pure anatase or TiO_2(B) phases [58]. Nanostructured TiO_2 especially is extensively studied in the field of solar cells, photochemical and photophysical applications, and gas sensors.

This chapter first introduces the fabrication of TiO_2(B) dominant nanowires. Then, a series sensing tests based on TiO_2(B) dominant nanowires have been carried out. Based on the results,

a sensing mechanism of TiO_2(B) dominant nanowires to detect explosive gas vapors has been discussed.

2.2 Nanostructured TiO_2 Fabrication and Characterization

TiO_2 can be prepared in the form of powders, crystals, or thin films. Both powders and films can be built up from crystallites ranging from a few nanometers to several micrometers. There are many methods to synthesize nanostructured TiO_2 such as solution routes including precipitation methods, Sol-gel methods, electrochemical synthesis, hydrothermal method, and so on. Here, single crystalline TiO_2(B) dominant nanowires were synthesized using the hydrothermal method [59, 60] because this method can control grain size, particle morphology, crystalline phase, and surface chemistry by regulating the solution composition, reaction temperature, pressure, solvent properties, additives, and processing time. In our case, the TiO_2(B) dominant nanowires were typically synthesized by a hydrothermal growth from TiO_2 nanoparticles in 10 M NaOH at 180 °C for 32 hours [61]. The precipitate was then repeatedly washed with a 0.1 M HCl aqueous solution followed by distilled water, until the pH of the water reached 7. In order to promote the phase transformation from titanate to TiO_2(B) and to remove Na^+ ions remaining in the titanate nano-products, a post-treatment was performed at 450 °C for one hour [62, 63].

The morphology of the films of TiO_2(B) nanowires was characterized with a Joel JSM-7000F scanning electron microscope (SEM). An SEM image of a typical film is shown in Figure 2.1a. The nanowires are approximately 50 ± 10 nm in diameter and 1.8 ± 0.3 μm in length. The thin film is made of an interconnected three-dimensional mesh of randomly orientated nanowires. An x-ray diffraction (XRD) pattern of "as-synthesized" TiO_2 nanowires was obtained with a Bruker

F8 Focus Power XRD to confirm the TiO_2(B) crystal structure. The XRD pattern shown in Figure 1.2b reveals that the TiO_2 nanowires are mainly in a crystalline TiO_2(B) phase [61, 62] by containing anatase phase. Here, we call it "TiO_2(B) dominant nanowires".

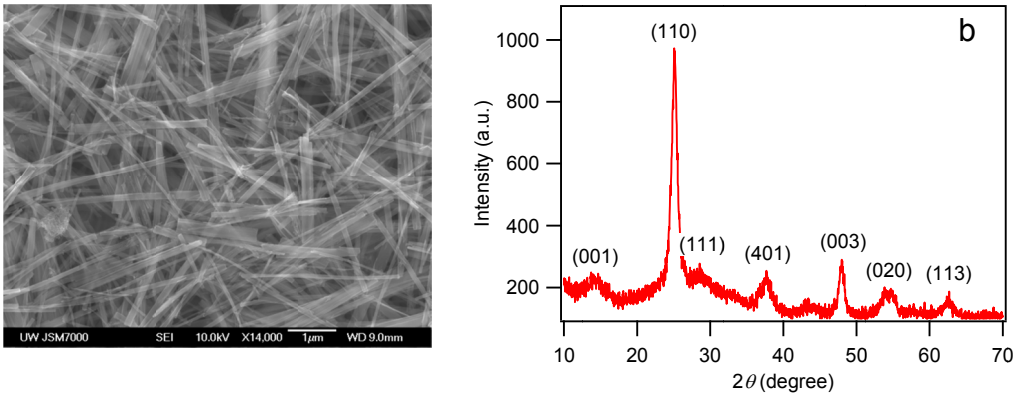

Figure 2.1 Characterization of TiO_2(B) nanowires. (a) SEM image showing an interconnected 3D mesh structure of a TiO_2(B) thin film (b) XRD pattern of synthesized TiO_2(B) nanowires. θ is the X-ray diffraction angle. The XRD pattern mostly matches the TiO_2(B) phase in literature.

2.3 Surface electrical and structural properties of nanostructured TiO_2

Since the sensing mechanism based on semiconducting metal-oxides is mainly due to the adsorption or reactions of molecules from the gas phase with the surface, conductivity will change by an upward or downward shift of the Fermi-level within the band-gap of these n-type materials. The Fermi-level shift is induced by charge transfer from the gas sensing material to an adsorbate. In a macroscopic view, this shift is caused by a band bending at the surface after adsorption of gas molecules. Therefore, understanding the surface structural and electrical characteristics of TiO_2 is very important to describe its sensing properties. The surface structures mainly depend on semiconductor crystalline status [64] and surface defects [65].

Surface defects have been recognized extensively in the literatures as point defects that exist as oxygen vacancy sites in conjunction with the conversion of Ti^{4+} to Ti^{3+} located within the bridging oxygen rows of the TiO_2 (110) surface. Liu et al [66] have shown that the dominant defects in TiO_2 surfaces are Ti^{3+} defects and oxygen vacancies. Compared to bulk TiO_2, more surface defects can be formed in the process of fabricating nanostructured TiO_2 [67]. The creation of Ti^{3+} defects has a profound effect on the electrical properties of TiO_2. Also, Ti^{3+} defects are considered to be the important active sites for many adsorbates [68]. Typically, there are two processes to form Ti^{3+} surface defects. One is using UV irradiation [69]. Under UV illumination, photogenerated electrons and holes are produced in TiO_2. The electrons can be trapped and tend to reduce Ti^{4+} to Ti^{3+}, and the holes oxidize O^{2-} anions giving rise to the formation of O^-. The other process for Ti^{4+} reduction to Ti^{3+} is usually accompanied by a loss of oxygen from the surface of TiO_2.

2.4 Explosive sensors based on TiO_2 (B) dominant nanowires

In this paragraph, TiO_2(B) dominant nanowires were studied to work as a chemiresistive sensor material for a detection of the nitroaromatic and nitroamine explosives [45].

As-synthesized nanowires were dispersed in ethanol to form a suspension. This suspension was then drop-cast on glass substrates and heated at 70 $^{\circ}$C to attain a thin film of nanowires about 10 μm in film thickness. To fabricate a sensor, as shown in Figure 2.2, patterned titanium electrodes were deposited through a shadow mask over the nanowire film by sputtering. The titanium electrodes have a circular shape and are 4 mm in diameter. The spacing between contacts is 1 cm

for the convenience of shadow mask patterning and probing during testing. The nominal thickness of the titanium electrodes is 200 nm.

Vapors of equilibrium concentration at room temperature were generated using glass beads coated with various explosives (Inert Products, LLC.) and a vapor generator based on [70], and confirmed by an HP 5797 gas chromatography-mass spectrometry (GC-MS). Vapor of lower concentration is obtained by diluting the saturated explosive vapor with air at the required ratio. The resistance change and response time of the sample is determined by measuring its resistance between two metal contacts with an electrometer (Keithley 617) when the gas applied to the thin film sample is cycled between air with vapor and pure air. The electrometer applies a constant current of 1 nA through the sample during resistance measurement, and the voltage across the sample is typically below 1 V. The resistance measurements were made at room temperature and in ambient air.

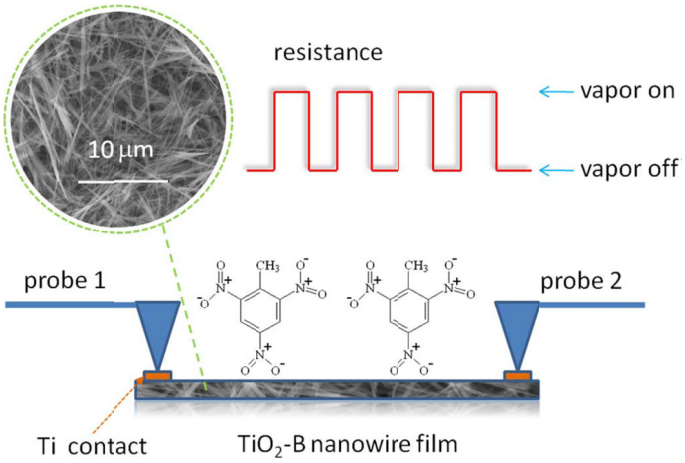

Figure 2.2 Schematic sketch of the chemiresistive effect of TiO_2(B) dominant nanowires to nitroaromatic and nitroamine explosives. Inset is a SEM image of the TiO_2(B) nanowire film. The film is fabricated on glass substrate and its resistance is modulated as the vapor (TNT) switches between "on" and "off".

1) Sensitivity and Response time

The SEM image in Figure 2.1a revealed that the thin film made by TiO_2 nanowires is very porous and has a large amount of free space between wires. All these characteristics make thin film highly permeable by vapors of analytes for rapid response.
The sensing performance of nanowire film samples were tested in ambient air, except for tests of temperature effects. During the test the resistance of the sample was recorded while air flow to the sample was alternately switched between pure air and air that contains explosive vapor at intervals of several seconds to a few tens of seconds. The chemiresistive response is defined as $S = (R_v-R_0)/R_0$, where R_v is the resistance when the sample is exposed to the vapor, and R_0 is the resistance of the fresh sample before it is exposed to any explosive vapor [5, 71]. The resistance of the nanowires increases to R_v upon exposed to explosive vapor. After the sample is returned to fresh air, its resistance decreases and reaches a stabilized value R_s, which is usually 0% to 100% higher than R_0 and is likely due to incomplete desorption of explosive molecules from the surface of nanowires. Subsequent switching cycles between vapor of the same concentration and pure air makes the resistance vary between R_v and R_s, as shown in Figure 2.3 and Figure 2.4. The recovery time of the resistance after the explosive vapor is replaced by pure air is almost same as the response time to the vapor. The incomplete desorption mentioned above can be eliminated by heating the sample at 80 to 100 ºC for several minutes, and the resistance of the sample returns to R_0.

Table 2.1 lists the percentage resistance change and response times of the TiO_2(B) dominant nanowire thin film for vapor of representative explosive compounds at equilibrium concentrations, where the values of equilibrium vapor concentration are referenced from

literature [72]. Significant and fast changes in resistance have been observed with all major explosives, including cyclotrimethylenetrinitramine (RDX) which has extremely low vapor pressure. The concentrations of TNT and RDX vapors were analyzed by HP 5797 GC-MS spectrum and compared with the results in literature [73]. Note that molecules of less mass produce faster response, because the response time is limited by the diffusion of the vapour molecules through the nanowire thin film and smaller molecules permeate the 3-D matrix of nanowires faster.

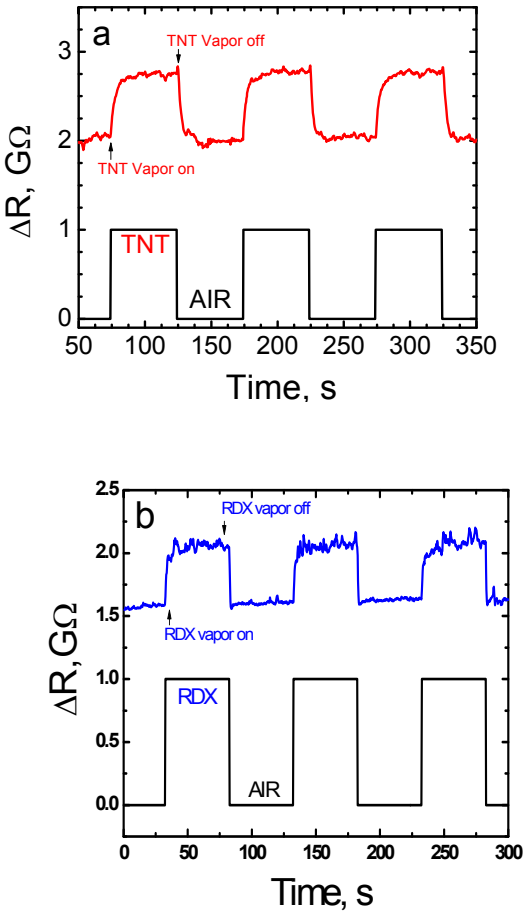

Figure 2.3 Typical resistance change of a TiO_2(B) dominant nanowire thin film in response to vapors. (a) 1 ppb of 2,4,6-trinitrotoluene (TNT). (b) 5 ppt of 1,3,5-Trinitroperhydro-1,3,5-triazine (RDX) at ambient conditions.

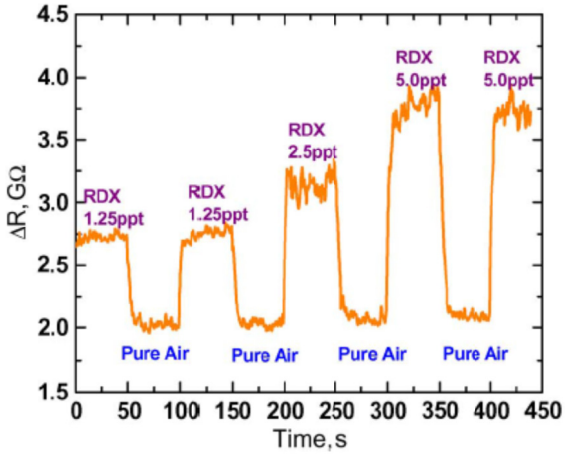

Figure 2.4 Chemisistive response to different concentration of RDX vapour at room temperature. The nanowires are 1.1 um in length and 50 nm in diameter. The noise-equivalent detection limit of RDX is 100 parts-per-quadrillio (ppq).

Table 2.1 Response of a TiO_2(B) dominant nanowire thin film to explosives.

Symbol	Equilibrium Vapor Concentration	Percentage Response ($100 \times (R_v - R_0)/R_0$)	Response Time (s)	Molar Mass (g/mol)
Nitrotoluene (NT)	130ppm	55	0.57	132
2,4-dinitrotoluene (DNT)	100ppb	38	0.64	182.13
2,4,6-trinitrotoluene (TNT)	5ppb	37	1.67	227.13
RDX	5ppt	30	2.35	222.12

(Response of a TiO_2 (B) dominant nanowire thin film sample to room temperature equilibrium vapor of common high explosives. ppm: parts-per-million; ppb: parts-per-billion; ppt: parts-per-trillion.)

Since the detection of explosives based on TiO_2(B) nanowires was conducted at room temperature, the interaction between explosive molecules and TiO_2(B) nanowires should be quite different from previous semiconductor gas sensors, which typically operate at elevated temperatures of 200 - 400 °C and their sensitivity is only at parts-per-million level with a slow

response on the order of a minute [23, 74, 75]. Their sensing mechanism at elevated operating temperatures was attributed to the chemical reduction-oxidation reactions via surface charged species [76] such as O^{2-}, O^{-} and O_2^{-}. On the other hand, explosive molecules are unlikely to be capable of producing significant and fast chemical reduction-oxidation reactions at room temperature to produce sensitivity below ppt level and a fast response on the order of a second, as shown in Figure 2.3. Therefore, a different sensing mechanism based on the specific surface properties of TiO_2(B) nanowires should play an important role in the surface interaction between and explosives.

2) Specificity and Stability

Figure 2.5 exhibits that TiO_2(B) nanowires has exceptional stability of sensing performance. Although the resistant baseline has a drift from 0.6 GΩ to 1.5 GΩ, the resistance change between R_v and R_s is found to be highly consistent over a long-term test of fifteen thousand switching cycles. Beside this, the nanowires are found to have good specificity (seen in Figure 2.5b) and are not sensitive to chemicals that are unrelated to explosives that cause false positives to other explosive detectors such as inert chemicals that have high nitrogen content (for example, urea).

3) Factors of influence on the sensing response of TiO_2(B) nanowires to explosives

In order to understand the influence of nanowire structures on its sensing properties, TiO_2(B) nanowire films with different diameters but same length (1.8 ± 0.3 μm) were prepared. Test samples of nanowires with the same diameter but different lengths were also fabricated. Here, the same film thickness and electrode spacing were used for all test samples. As shown in Figure 2.6c, wires of 50 nm ± 10 nm in diameter produced a response of 30%, higher than the 22%

response observed for wires of 100 nm ± 20 nm in diameter. This is because the sensing response of TiO_2 (B) nanowires to explosives is determined by the surface depletion region and thinner wires are more susceptible to surface depletion [77]. The response time is found to be independent of the diameter of nanowires. However, longer wires respond to the vapor at faster rate, as shown in Figure 2.6a and Figure 2.6b. The slower response for shorter wires can be attributed to the denser (less porous) structure. These test results confirm that the microstructures of nanomaterials can be a big factor to affect their sensing properties. In the case of TiO_2(B) dominated nanowires as explosive sensors, the wires with longer length and smaller diameter could have better sensing response: higher sensitivity and quicker response time. In addition, different metal electrodes including gold, aluminum, copper, and titanium have been used for the electrodes. It was found as indicated in Figure 2.7 that test samples with titanium electrodes exhibited a more linear current-voltage (I-V) relationship, characteristic of a good ohmic contact between the metal electrode and nanowires. The ohmic contact can rule out the effect due to the interface between the metal electrodes and nanowires in the chemiresistive response.

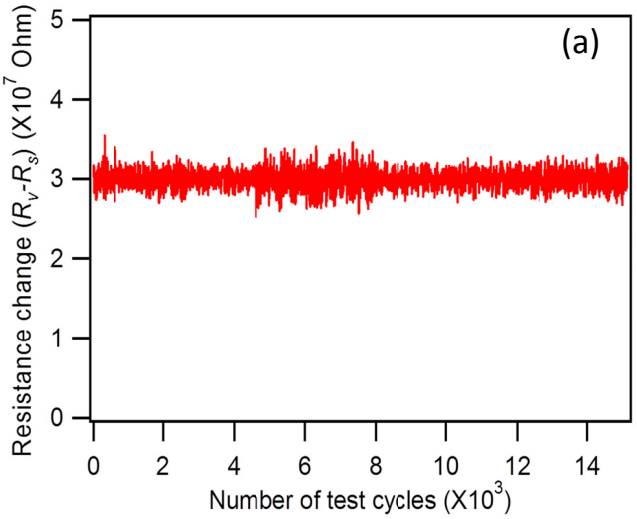

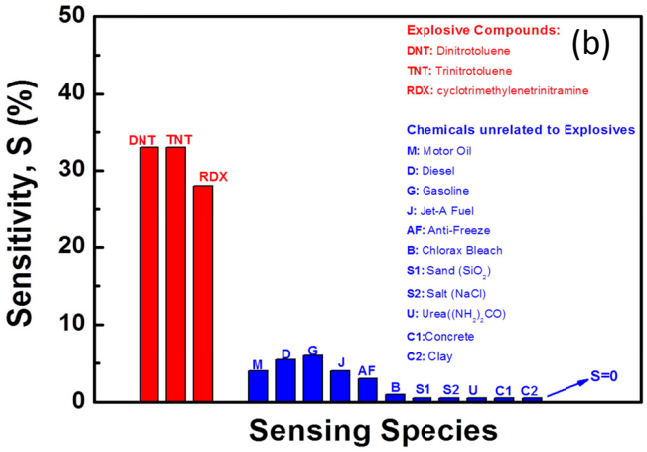

Figure 2.5 (a) Resistance change R_v–R_s over fifteen thousand continuous test cycles between vapor of 100 ppb of DNT and pure air. Each test cycle consists of 6 seconds of vapor and 6 seconds of air. (b) The sensing response of TiO_2 (B) nanowires to different chemical compounds.

2.5 Discussion and Conclusion

TiO_2(B) dominant nanowires show a fast and large increase of sensing response to sub-trace vapors of nitroaromatic and nitroamine explosive compounds at room temperature. The primal results indicate that the response originates from a depletion of electron carriers by the surface states produced by adsorbed molecules of electronegative explosive compounds. The achievement of TiO_2(B) dominant nanowires in detecting explosives is firstly considered due to the following reasons:

- The special characteristics of the nitroaromatic and nitroamine explosive compounds. As we discussed in the beginning of this thesis, nitro-related explosives are high electronegativity due to strong oxidizing groups: nitro groups and strong tendency to adsorb on the surface of objects due to extremely low vapor pressure.

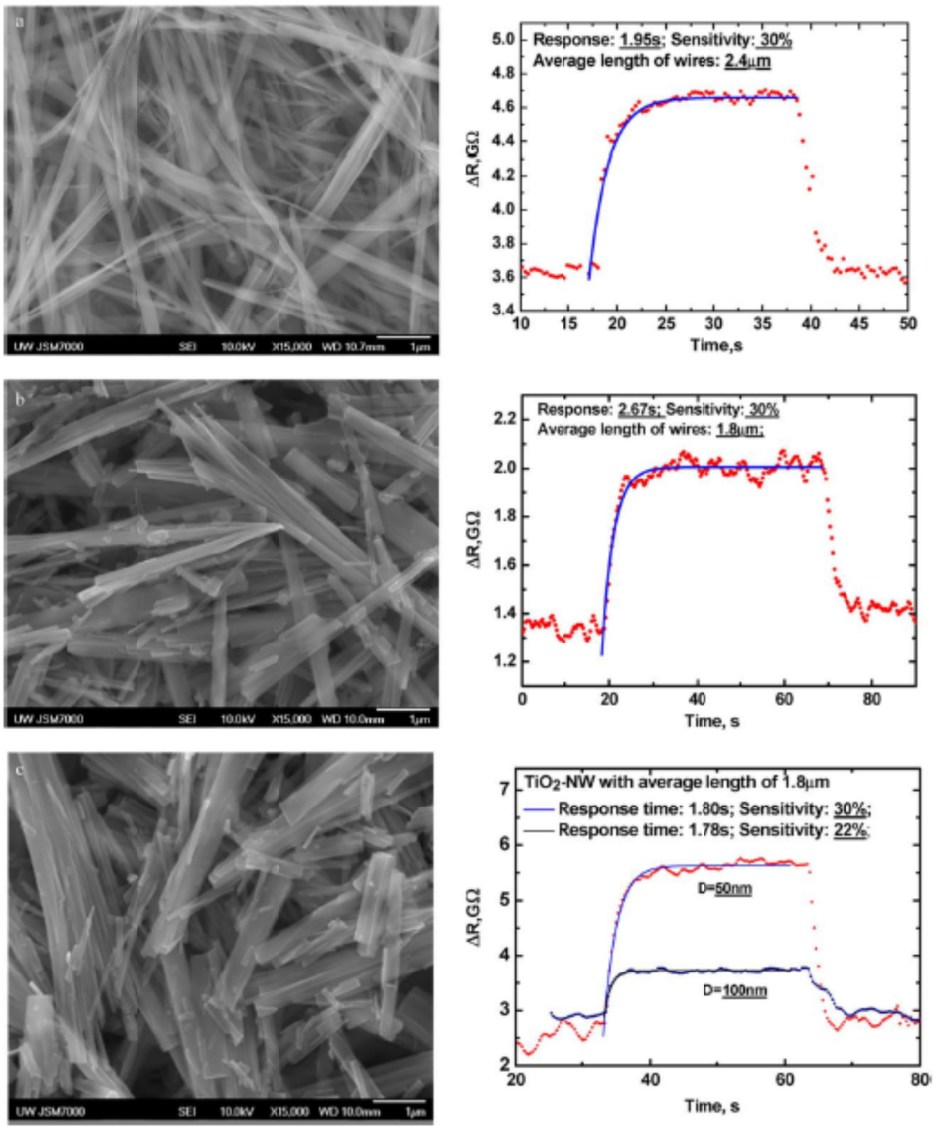

Figure 2.6 SEM images of nanowires of different length and diameter obtained through treatment and their sensing responses to TNT vapor (a) Nanowires with 2.2 μm in length and 50 nm in diameter with pre-ultrasonic treatment and reaction temperature of 180 ºC. The response shows 1.95s. (b) Shorter wires of 1.1 μm in length and 50 nm in diameter without pre-ultrasonic treatment and reaction temperature of 180 ºC. The response on the right is 2.67s. (c) Thicker wires of 100 nm in diameter and 1.1 μm in length obtained with reaction temperature of 150 ºC. The three images have the same scale of magnification. Comparing to (a), they exhibit the similar response time to TNT vapor but thinner wires are more sensitive.

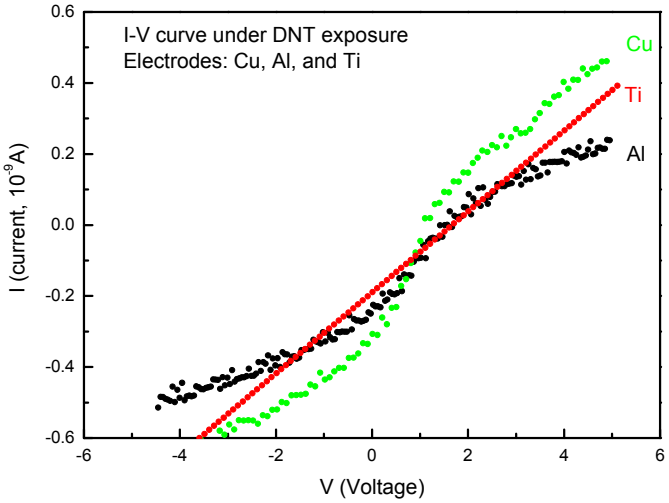

Figure 2.7 Current vs. voltage curves obtained for TiO_2(B) nanowires coated Cu, Al and Ti under DNT exposure.

- TiO_2 (B) dominant nanowires like other nanostructured materials have a high surface-to-volume ratio as well as a large surface area for molecule adsorption.

- Compared to other polymorphs of TiO_2, TiO_2(B) dominant nanowires has relative higher charger carrier transfer ability, less compact structure and higher level of surface defects such as oxygen vacancies.

In a word, good sensing response to explosives based on TiO_2(B) dominant nanowires at room temperature has been observed. Detection limit can be up to sub-ppt levels and response time is about a second. Initially, we ruled out the sensing mechanism based on TiO_2(B) dominant nanowires was due to chemical reduction-oxidation reactions via TiO_2(B) dominant nanowire surface charged species to give rise to a charge-transfer. High surface-to-volume ratio, high porous structures, higher levels of surface defects of nanowires and strong electronegativity of

explosive compounds determine the excellent sensing properties of TiO_2 (B) dominant nanowires to explosive detection.

However, a fully understanding of the sensing mechanism is still needed. In the following Chapters, a series experiments targeted on the sensing mechanism were designed and carried out.

Chapter 3

SENSING MECHANISM OF THE TiO_2(B) DOMINANT NANOWIRES AS EXPLOSIVE SENSOR

3.1 Introduction

In Chapter 2, the primal sensing results indicated that the TiO_2(B) dominant nanowires have great potential to detect concentration of nitroaromatic and nitroamine explosives. Detection limit below sub-ppb levels and response time below a second at room temperature were observed [45]. These unique sensing properties indicate the mechanism of TiO_2(B) dominant nanowires to detect explosives are quite different compared to other semiconductor gas sensors [41, 78] which are usually operating at elevated temperature. Therefore, sensing mechanism based on surface oxidization-reduction for other semiconductor gas sensor is not suitable for TiO_2(B) nanowires based explosive sensor. In addition, one issue observed with TiO_2(B) nanowires is that their chemiresistive responses to explosive vapours are affected by the humidity of the environment that the nanowires are exposed to [46]. All of these sensing characteristics have indicated a different mechanism needs to be revealed based on TiO_2(B) dominant nanowires as explosive sensors.

The goal of this Chapter is to design a series of sensing tests based on TiO_2(B) nanowires and nanowires with surface modification. The mechanism studies based on nanowire surface properties and chemical characteristics of the analytes were performed.

3.2 The role of surface hydroxyl groups on TiO_2(B) dominant nanowires to response explosives

3.2.1 Sensor samples preparation

The method of synthesized nanowires and testing setup have described in Chapter 2. The surface modifications of TiO_2(B) nanowire thin film were performed via surface plasma treatment (oxygen and hydrogen) and self-assembled monolayer of hydrophobic acids.

1) Oxygen and hydrogen plasma treatments of nanowires were carried out in a microwave plasma cleaner/etcher (Plasma-preen). The plasma treatments were made at pressure of 1 Torr and rf power of 300 W for 5 min, when the effect of plasma treatments became saturated.

2) Surface self- assembled hydrophobic acids were performed by immersing the nanowire thin films into hydrophobic acids such as stearic and benzoic acids and then rinsed with de-ionized water before drying the thin films in an oven.

3.2.2 Sensing tests and Results [46]

Here, a series of surface treatments to change the density of surface hydroxyl groups on TiO_2 (B) nanowires have been carried out in order to show how the density of hydroxyl groups on the TiO_2 (B) nanowires surface influence its chemiresistive response.

The as-synthesized TiO_2(B) nanowires are approximately 50 nm ±10 nm in diameter and 1.8 μm ± 0.3 μm in length. The nanowire thin film is made of an interconnected three-dimensional mesh of randomly orientated nanowires. The nanowire mesh has a highly porous structure desirable for

gas sensing. The porous structure provides a large surface area for the highly electronegative explosive compounds to adsorb onto, and results in a change in the resistivity of the nanowires.

In the sensing test of TiO_2(B) nanowires to explosive, it was noticed that their chemiresistive responses to explosive vapours are affected by the relative humidity (RH) of the environment that the nanowires are exposed to shown in Figure 3.1. The resistance increases when the RH in the environment decreases. This indicates that the hydroxyl groups on the surfaces of nanowires participate in the chemiresistive response, as it is known that the humidity strongly influences the density of hydroxyl groups on the surface of metal oxides [79]. So, it is necessary to study the role of surface hydroxyl groups to understand the sensing response of TiO_2(B) nanowires to explosives.

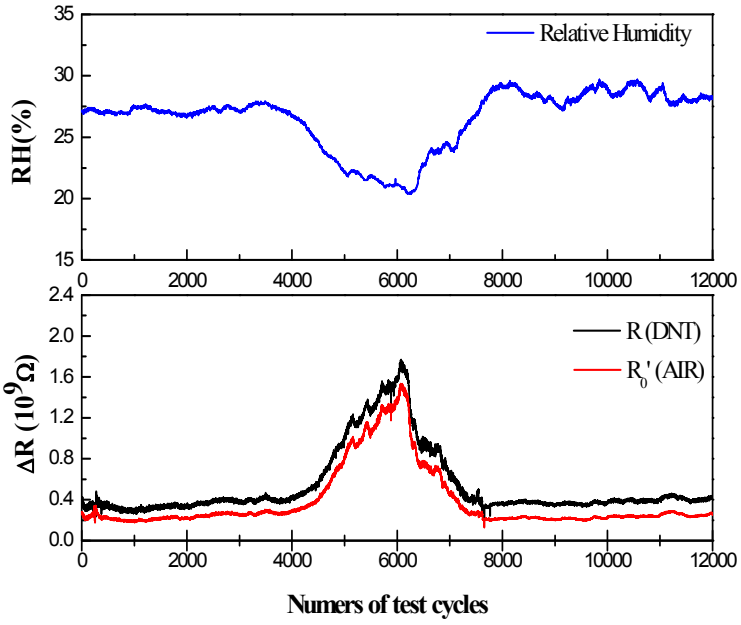

Figure 3.1 Resistance change with relative humidity.

Shown in Figure 3.2 are Fourier transform infrared spectra (FTIR) of TiO_2(B) nanowires after exposure to 2, 4-dinitrotoluene (DNT) vapour. Three main bands were detected and they were consistent with the bands described by Vargas *et al* [80]. Compared to the FTIR spectrum of the control sample, the broad band at 3370cm^{-1} is due to surface hydroxyl groups (Ti-OH) in the TiO_2 (B) thin film [81, 82]. This band is an evidence that TiO_2(B) nanowires surface is terminated with hydroxyl groups. The new band at 1625 cm^{-1} is attributed to the complex between nitro groups of DNT bonded with hydroxyl groups at TiO_2(B) surface (-O-Ti-OH—N-O-) [80]. This band did not exist in neat thin films (samples that had not been exposed to DNT). The new band at 1625 cm^{-1} after adsorption of DNT vapor onto TiO_2(B) indicates that a charge transfer pathway from the TiO_2(B) surface to nitro groups in explosives via hydroxyl groups. The bands at 2335 cm^{-1} and 2364 cm^{-1} are from carbon dioxide and aromatic groups of DNT.

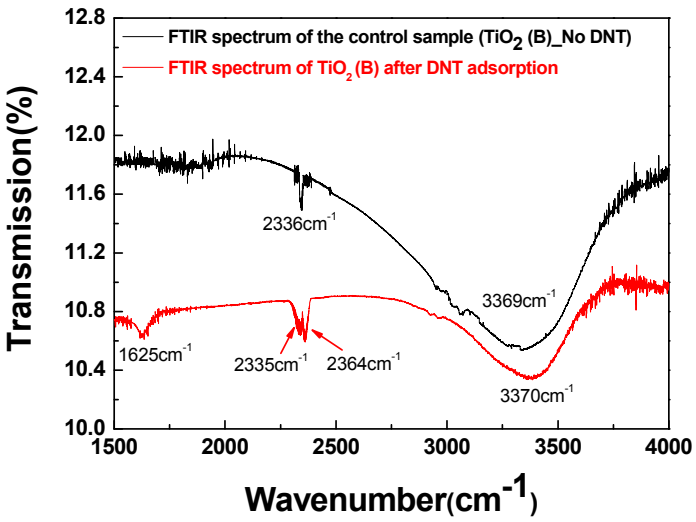

Figure 3.2 FITR Spectrum of TiO_2(B) nanowires after DNT exposure. The background was recorded by as synthesized TiO_2(B) nanowires.

1) Varying the density of surface hydroxyl groups through plasma treatment

Sensing response to explosive vapour, such as 2, 4, 6-trinitrotoluene (TNT) after plasma treatments is shown in Figure 3.3. A higher response of TiO_2(B) nanowires to TNT after an oxygen plasma treatment was observed compare to the response of the untreated TiO_2(B) nanowires and the nanowires after a surface hydrogen plasma treatment. It is noticed that the hydrogen plasma treatment did not change the sensitivity significantly. This is probably due to the competing effects of surface cleaning and reduction of hydroxyl groups.

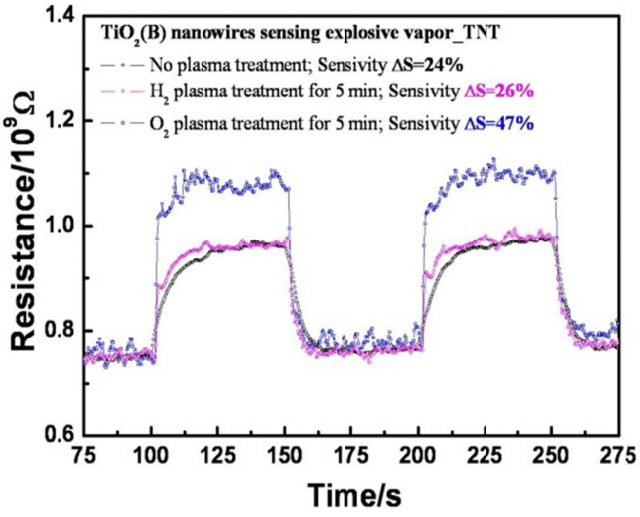

Figure 3.3 Effects of surface plasma treatments on the sensitivities of TiO_2(B) nanowires to TNT vapor.

The water wettability tests also confirmed that plasma treatments change the contact angles of water on the TiO_2 surface and therefore change the density of surface hydroxyl groups. Figures 3.4 and 3.5 show the contact angles on the TiO_2(B) nanowires surfaces after different surface plasma treatments and surface treatment with oxygen plasma for various times. It is evident that

the contact angle increases when TiO_2(B) nanowires were treated with hydrogen plasma and decreases after oxygen plasma treatment, indicating a more hydrophilic TiO_2(B) nanowire surface after an oxygen plasma treatment. These results suggest that TiO_2(B) nanowires' surface with an oxygen plasma treatment has a higher density of surface hydroxyl groups. This is because an oxygen rich nanowire surface created by oxygen plasma could enhance the dissociative adsorption of water molecules in air and increase the density of the hydroxyl groups on the TiO_2(B) surface [83]. The plasma-induced hydroxyl groups (OH^-), as additional surface defects, can trap electrons and facilitate the charge transfer between the titania nanowires and explosive compounds further [84]. Here, we should notice in Figure 3.5 that the effect of oxygen plasma treatment becomes saturated when time of oxygen plasma is longer than 5 minutes.

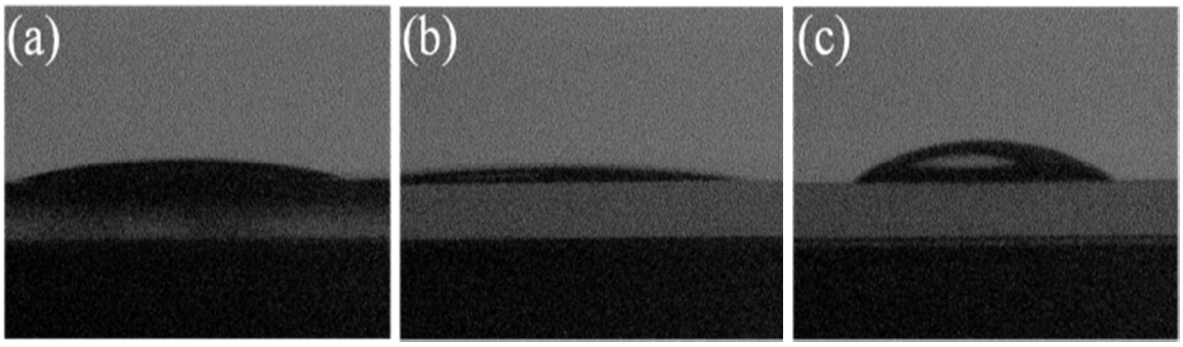

Figure 3.4 Contact angles of TiO_2(B) nanowire surfaces and water. (a) as-fabricated TiO_2(B) nanowire surface. (b) The nanowire surface after oxygen plasma treatment. (c) The nanowire surface after hydrogen plasma treatment.

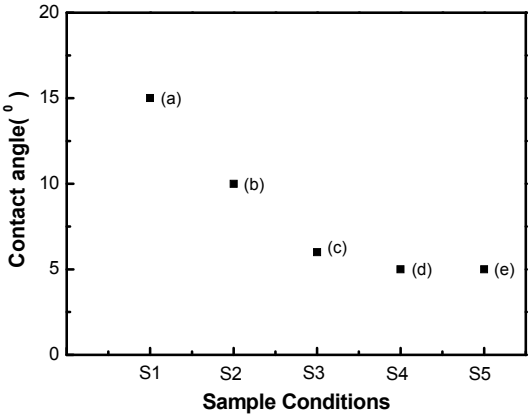

Figure 3.5 Contact angles of TiO_2(B) nanowire surface and water. (a)as-fabricated TiO_2(B) nanowire surface, (b) oxygen plasma RF power of 300 W for 3 minutes, (c) oxygen plasma RF power of 300 W for 5 minutes, (d) oxygen plasma RF power of 300 W for 9 minutes, (e) oxygen plasma RF power of 300 W for 12 minutes.

2) Varying the density of surface hydroxyl groups through self-assembled monolayer (SAM) and water treatment

The importance of surface hydroxyl groups to the chemiresistive response of TiO_2(B) nanowire was further confirmed through surface functionalization. Since surface functionalization of TiO_2(B) nanowires with a self-assembled monolayer of certain hydrophobic acids can reduce the density of surface hydroxyl groups, this treatment should result in lower sensitivity of TiO_2(B) nanowires to explosives if surface hydroxyl groups contribute to the sensitivity. As indicated in Figure 3.6(a), as-fabricated TiO_2(B) nanowires exhibited a sensitivity of 38% to DNT. After surface modification by stearic acid, the sensitivity of the same sample dropped to 10%. Similar decrease in sensitivity was also observed after the nanowire surfaces were modified with a self-assembled hydrophobic monolayer of benzoic acid. To the contrary, sensing responses of a

TiO_2(B) nanowire thin film with water treatment was designed to increase the density of surface hydroxyl groups. Water treatment was achieved by immersing the test sample into de-ionized water and letting it become completely dry in the air. As shown in Figure 3.6(b), the sensitivity of TiO_2(B) nanowire thin film to DNT vapor after the water treatment was almost two times higher than that before the water treatment. This increase in sensitivity is most likely due to water treated TiO_2(B) nanowires having higher density of surface hydroxyl groups of bonded water molecules [84, 85] and hydroxyl groups enhance the sensing properties of the TiO_2(B) nanowires.

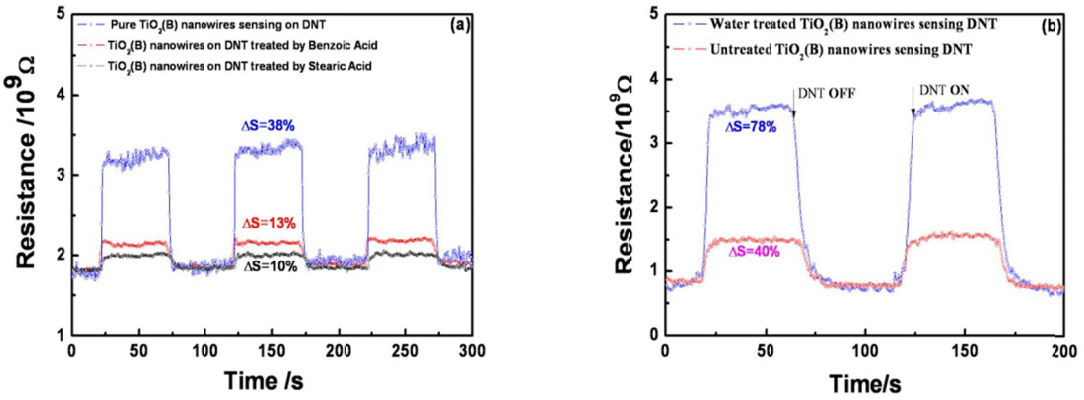

Figure 3.6 Sensitivities of TiO_2(B) nanowires to (a) DNT with surface modification (b) DNT before and after water treatment of the surfaces. (Note: The difference of resistance change, ΔR, in (a) and (b) for untreated TiO_2(B) nanowires results from the fluctuation of different batches of samples in, for example, thickness, density or porosity, etc.)

3.2.3 Mechanism Discussion

According to the above results, a stronger response was observed after increasing the density of surface hydroxyl groups. These observations indicate that surface hydroxyl groups provide a

major charge transfer pathway between nitro groups in nitroaromatic explosives and TiO_2(B) nanowires and causes the chemiresistive response. In order to understand the function of surface hydroxyl groups of TiO_2(B) nanowires on its sensing properties, it is important to know the mechanism of the effect of water vapor on the resistance of TiO_2(B) based gas sensors.

Since it is a general effect that water vapor or humidity can change the sensing properties of metal-oxide sensors, a deep study of the interaction between water and solid surface has been carried out [86]. Three types of mechanisms are proposed to explain the experimentally proven increase of surface conductivity in presence of water vapor. Two of them, called direct mechanisms, were proposed by Heiland and Kohl [87] and the third indirect was suggested by Morrison *et al* [88]. The first mechanism attributes the hydroxyl groups are "rooted" and built-up by the reaction of the neutral H atom (generated through hemolytic dissocation of water) with the lattice oxygen. Such rooted OH group, having a lower electron affinity, can become ionized and become a donor. The second mechanism considers that the reaction between hydrogen atom and the lattice oxygen and the binding the resulting hydroxyl group to metal atom in the metal oxide, for example, Ti in TiO_2(B). This reaction results in producing oxygen vacancy, by ionization, leading to additional electrons. Morrison *et al* consider that the water effect is an indirect effect. The effect could be the interaction between either the hydroxyl group or the hydrogen atom originating from the water molecule with an acid or basic group, which could also acceptor surface states. Whatever the mechanism will be, they are all proposed based on the conception that the water effect is determined by the metal-oxide surface states. **Surface defects and dopants** in the metal oxides can increase the dissociative adsorption and cause different depth of the effect of humidity.

Going back to TiO_2 semiconductor, *first of all*, we know that the structure of TiO_2(B) is less compact that that of other forms of titanium oxides and has a shear derivative of the ReO_3 type structure [89]. Therefore, TiO_2(B) has a relatively open structure with significant voids and continuous channels for electron transportation and the nanowires show relatively high charge carriers transfer ability [90]. *Also*, it was reported that the dominant defects in TiO_2 surfaces are Ti^{3+} defects and oxygen vacancies [66]. For example, Tan et al found that the adsorption of NO_2 on TiO_2 was through the Ti^{3+} sites rather than through direct adsorption of NO_2 on oxygen vacancies of TiO_2 [91]. Ti^{3+} sites in the surface of TiO_2 is an important parameter controlling its hydrophilic property [92, 93] because Ti^{4+} can be reduced to Ti^{3+} by the dissociation of water molecules, and forms OH groups on crystal surface [89]. The Ti^{3+} ions in TiO_2(B) can be coordinated by hydroxyl groups and tend to have hydroxyl terminated surfaces [94]. The surface hydroxyl groups could effectively interact with nitro groups at room temperature and facilitate TiO_2(B) surface physisorption and charge transfer interactions [80]. This is because hydroxyl groups binding to Ti atoms can give rise to additional electrons, based on the aforementioned mechanisms for the formation of hydroxyl group. The Ti-OH becomes donor surface states so as to provide electrons to strong electron deficient adsorbates such as nitro-group explosives.

Surface plasma treatments on TiO_2 not only can realize the conversion between Ti^{3+} and Ti^{4+} and change its hydrophobicity but also can clean the surface. Oxygen plasma (one of the main components of oxygen plasma is O^- due to a dissociation reaction: $O_2 + e \rightarrow O^- + O$) will convert Ti^{4+} to Ti^{3+} and make TiO_2 surface have more Ti^{3+} ions followed by the equation: $Ti^{4+} + e^- \rightarrow Ti^{3+}$, where e^- results from O^-. The local electrostatic balance is broken, and an oxygen vacancy should be introduced because of charge compensation, by ionization, resulting in additional electrons. The conversion of Ti^{4+} sites to Ti^{3+} sites and generating more oxygen vacancies

promote dissociative water adsorption and then make the surface be more hydrophilic [95]. Therefore, after oxygen plasma treatment, TiO_2(B) nanowires have higher response to explosives. While, hydrogen plasma treatment can covert Ti^{3+} to Ti^{4+} and form a relative more hydrophobic surface.

Water treatment can be explained by the mechanisms of the formation of hydroxyl groups in the metal oxides. The presence of water vapor can form higher density of surface hydroxyl groups and then cause an increase of surface conductance [87]. In the case of TiO_2 nanowires, higher density of hydroxyl groups can cause higher response to explosives. As an example, the process can be described by the equation in case of the second mechanism of hydroxyl group:

H_2O^{gas} + Ti + O (lattice oxygen) → (Ti-OH) + V_O^{2+} (oxygen vacancies) + $2e^-$

However, prolonged exposure the TiO_2 to humid environments or over-treated the nanowires with water can result in a deterioration of the sensitivity of TiO_2 nanowires to explosives. A detailed discussion in regard of this point can be found in Chapter 6.

In addition, it is interesting to know that surface hydroxyl groups in TiO_2(B) nanowires result in an increased concentration of surface dipoles [81-82, 96-97]. This provides another way to increase the efficiency of sensing interaction, which will be discussed in the following sections.

3.3 The relationship between the dipolar strength of the analyte molecule and speed of sensor response

In section 3.2, surface hydroxyl groups coordinated with Ti^{3+} on the TiO_2(B) nanowires play an important role in its sensing response to explosive detection. In this section, we focus on the influence of polar surface of TiO_2(B) nanowire thin film on its chemiresistive effects.

A series of experiments were designed to study how the molecular polarity and electron deficiency influence the charge transfer process between nitro-containing explosives and TiO_2(B). Since the polarity of analytes depends on their molecular structures with functional groups, two types of analytes have been chosen for this study. One series of analytes are positional isomers of dinitrobenzene (DNB). These positional isomers have varying dipole moments but are similar in electron deficiency. The other series of compounds are nitroanilines (NA) and nitrotoluenes (NT), such as 4-nitroaniline and 4-nitrotoluene. Although NA's and NT's have the similar molecular structures except for one functional group, their molecular polarities are quite different because the electron rich amino group ($-NH_2$) in the nitroanilines is a stronger electron donor than the methyl group ($–CH_3$) in nitrotolune.

3.3.1 Nanowire synthesis, analyte vapour generation and sensor sample testing

The synthesis of nanowires and the method of generation of analyte vapours are as same as the description in Chapter 2. Briefly, the single crystalline TiO_2(B) nanowires were synthesized by a low-cost, high efficient, hydrothermal technique [59, 60]. The length of the nanowires ranges from 1.1 μm to 2.2 μm and the diameter of nanowires is 40-100 nm, adjustable through synthesis conditions. The nanowire film was prepared by a drop-casted method on the glass substrates with

thickness about 10 μm. The thin film has a highly porous structure made of a three dimensional mesh of randomly orientated and interconnected nanowires. In order to form a good ohmic contact of low junction resistance with TiO_2(B), electric contact was made of titanium by sputtering.

3.3.2 Results and Discussion

Table 3.1 lists the response time and sensitivity of TiO_2(B) nanowires to the positional isomers of dinitrobenzene. The response time_τ (1/e time constant) is obtained by fitting the resistance change to an exponential function. The sensitivity_S is defined as the relative resistance change due to the analyte; that is, the ratio of resistance change caused by the analyte to the initial resistance without the analyte, according to a definition commonly used in chemical sensors [37, 71]. The relative position of the two nitro groups of dinitrobenzene determines the polarity of the molecule, which can be estimated theoretically by the density functional theory (DFT) [98]. As is evident in Table 3.1, the response time and the dipole moment of the analyte molecules are strongly correlated. Molecules with higher dipole moments exhibit faster responses. For example, as shown in Figure 3.7, 1,2-dinitrobenzene has the most asymmetric structure in terms of electron withdrawing group position, and therefore it has the highest dipole moment, and produces the shortest response time of 1.54s. In contrast, 1,4-dinitrobenzene has a symmetrical molecular structure, and its dipole moment is zero. As a result, its response time is the slowest (6.31 s). Another observation is that the response time is not completely correlated with the calculated lowest unoccupied molecular orbital (LUMO) level.

Table 3.1 Sensing response to positional isomers of dinitrobenzene. The dipole moments and LUMO levels were calculated using DFT method [98].

Analyte molecule	Molecular structure	μ (Debye)	LUMO (eV)	P at 20 °C (Torr) [99]*	τ (s)
1,4-DNB		0	-2.46	3.95×10^{-3}	6.31
1,3-DNB		4.22	-3.14	2.06×10^{-3}	3.15
1,2-DNB		6.67	-3.03	1.03×10^{-3}	1.54

*P: Vapor Pressure

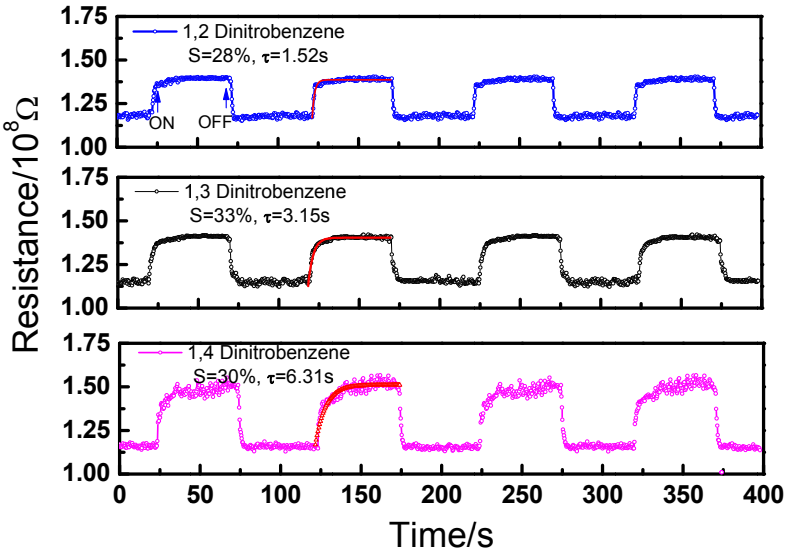

Figure 3.7 Typical resistance change of a TiO_2(B) nanowire thin film in response to positional isomers dinitrobenzene vapors.

Another factor to affect the molecular dipole moment_μ is the type of functional groups in analytes. In Table 3.2 a series of nitroanilines and corresponding nitrotoluenes are compared. Nitroanilines have an amino group (-NH_2) and a nitro group while in nitrotoluenes the amino

group is replaced by a methyl group (-CH_3). Both amino and methyl groups are electron donating, however the amino group (-NH_2) is more electropositive than the methyl group (-CH_3). The nitro group is electronegative, therefore the dipole moment of a nitroaniline is greater than the dipole moment of its corresponding nitrotoluene[100, 101]. Once again, it is observed that the response times of more polar NA's have faster response than their corresponding NT's, consistent with the trend shown in Table 3.1.

Table 3.2 A comparison of chemiresistive responses to nitroanilines and corresponding nitrotoluenes.

Analyte molecule	Molecular structure	μ (Debye)	LUMO (eV)	Pat 20 °C (Torr) [103, 104]	τ(s)
4-NA	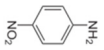	7.12	-1.96	1.50×10^{-3}	0.42
4-NT	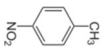	5.21	-3.14	2.06×10^{-3}	0.73
3-NA		5.65	-2.24	0.96×10^{-4}	3.18
3-NT		4.89	-2.36	2.05×10^{-1}	5.68
2-NA		4.74	-2.17	3.00×10^{-3}	6.48
2-NT		4.33	-2.31	1.88×10^{-1}	6.85

The fact that the response time is dominated by the polarity of the sensing molecules supports previous arguments that TiO_2(B) nanowires have a polar surface [46, 80-82, 102]. Since **a polar surface facilitates a stronger dipole-dipole interaction between surface dipoles and more polar analyte molecules, it can facilitate surface adsorption and result in a faster response.**

3.4 The relationship between electronegativity of the analyte molecule and the level of sensor response

3.4.1 The effect of electron deficiency on sensing properties

In order to study the effect of electron deficiency of analytes, we have measured and compared chemiresistive responses of the TiO_2(B) nanowire films with nitrotoluenes with increasing number of nitro groups, 4-nitrotoluene (NT), 2, 4-dinitrotoluene (DNT), and 2,4,6-trinitrotoluene (TNT). The electron deficiency of nitro-aromatic compounds varies with the number of nitro groups in a molecule [105]. TNT has the most number of electron withdrawing nitro groups and it leads to the lowest LUMO level. TNT is more electron deficient than both NT and DNT and tends to cause a stronger charge transfer interaction with the TiO_2(B) nanowire. As shown in Table 3.3, although the vapor pressure of TNT is about 1000 times lower than that of DNT, TNT vapor can still produce the same level of sensitivity as DNT vapor of much higher concentration. This means that TNT can induce stronger charge transfer interactions with TiO_2(B) surface than DNT. Amazingly, the sensitivity to TNT is even higher than the sensitivity to NT despite the fact that the vapor pressure of NT is almost 10^5 higher than TNT. From these results, it is clear that the sensitivity is strongly dependent on the number of nitro groups and thus electron deficiency of analyte. That is, **the degree of chemiresistivity is determined by the electron deficiency of the analytes.**

Table 3.3 A comparison of chemiresistive responses to nitrotoluenes.

Analyte molecule	Molecular structure	μ (Debye)	LUMO (eV)	P at 20 °C (Torr) [103, 106]	S (%)	τ(s)
4-NT	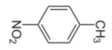	5.21	-2.46	1.2×10^{-1}	16	0.73
2,4-DNT		4.85	-2.86	1.4×10^{-4}	33	1.94
2,4,6-TNT	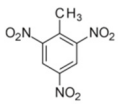	1.00	-3.40	8.0×10^{-6}	33	3.31

3.4.2 Effect of electronegative and electropositive compounds on sensing response

Another experiment was carried out to study the effect of electron deficiency of analytes by comparing the responses of analytes functionalized with electropositive amino groups and electronegative nitro groups. As shown in Table 3.4, aniline, nitrobenzene (NB), and 4-nitroanline (4-NA) were chosen to interact with nanowires and the sensing results reveal the mechanistic details of the chemiresistive effect at the interface due to nitro-compounds. Aniline is an electron rich compound (with a LUMO level of +1.44eV). Replacing the amino group with electron withdrawing nitro group results in electron deficient nitrobenzene (with a LUMO level of -0.36eV). The electron rich aniline causes a *decrease* of resistance (S= -23%). In contrast, the electron deficient nitrobenzene causes an *increase* of resistance (S=+25%). In the case that there is both an amino and a nitro group linked to the aromatic ring, as in 4-nitroaniline, the resistance still increases. Also, the response time (26.7s) of aniline is much longer than that of nitrobenzene (2.83s) although they have the similar dipole moments. All those suggest the interaction between nitro group and TiO_2(B) prevails over the interaction between the amino group and TiO_2(B). The trend can be explained by the orientation of permanent dipoles moments of analytes relative

to the hydroxylated surface dipoles of TiO_2(B) nanowires [82]. On the other hand, like most wide band-gap metal oxide semiconductors, TiO_2(B) is a n-type semiconductor with electrons as the majority charge carrier. When electron deficient nitrobenzene is adsorbed onto TiO_2(B) nanowires, its electron withdrawing nitro groups likely create localized surface states that trap TiO_2(B) to cause surface depletion of electron carriers and result in the decreasing conductivity and faster response. The observations from this study show that **the rate of surface adsorption is dominated by the molecular polarity and the degree of the charge transfer interaction is dominated by the electron deficiency of analytes**.

Table 3.4 A comparison of chemiresistive responses to nitroanilines, nitrobenzene and nitrotoluene.

Analyte molecule	Molecular structure	μ (Debye)	LUMO (eV)	P at 20 °C (Torr) [104, 107]	S (%)	τ(s)
aniline		3.5	1.44	0.60	-23	26.7
NB		3.98	-0.36	0.15	25	2.83
4-NA	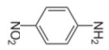	7.12	-1.96	1.5×10^{-3}	8	0.42

3.5 Conclusion

The sensing mechanism based on TiO_2(B) dominant nanowires to sub-trace explosive detection has been investigated. It was found that the unique surface characteristics of TiO_2, such as surface defects, are attributed to the excellent sensing properties of nanowires to detect low vapor pressure, high electronegative, explosive compounds. The surface defects, Ti^{3+} and oxygen vacancies, provide a charge transfer channel. In particular, Ti^{4+} can convert to Ti^{3+} sites and

make TiO_2 surface be hydrophilic via the formation of surface hydroxyl groups (Ti-OH). Such surface hydroxyl groups can effectively interact with NO_x even at low operating temperature [108], while NO_x is an important constituted group of explosive compounds. Therefore, Vargas *et al* [80] reported that nitro group interacts with TiO_2 surface *via* a hydrogen bond, arising from the complex of water molecules with the Ti^{3+} ions (Ti-OH donor) on its surface.

In a word, the sensing performance of TiO_2 nanowires to detect explosives can be determined by the following factors:

1) High surface area and porous structures

2) The surface defects Ti^{3+} sites in TiO_2 can modulate surface hydroxyl groups of TiO_2. That is, more Ti^{3+} sites can increase surface hydrophilicity of TiO_2. This makes TiO_2 have high affinity to nitrocompounds because surface hydroxyl groups as donors can efficiently give electrons to electron deficient compouns. More electron deficient analytes cause higher sensitivity.

3) The surface hydroxyl groups make TiO_2 have a polar surface. The charge transfer between TiO_2 and explosives is through surface dipole-dipole interaction. Therefore, higher molecular polarity exhibits quicker sensing response.

4) More open structure of TiO_2(B) can facilitate electron transportation and thus result in fast sensor response.

The discussion above that if we can control the conversion between Ti^{3+} and Ti^{4+} sites on TiO_2 surface, then we can modulate the density of surface hydroxyl groups and reduce the moisture

effect on its sensing performance. In Chapter 4, we will detailed discuss how UV illumination improves TiO_2 sensing response to explosives by modulating TiO_2 surface hydroxyl groups.

Chapter 4

UV ILLUMINATION TO REDUCE CROSS-SENSITIVITY OF TiO_2(B) DOMINANT NANOWIRES TO HUMIDITY

4.1 Introduction

Environmental humidity is an important factor to influence the sensing performance of metal-oxide gas sensors. This is one reason that many humidity gas sensors based on metal oxides have been developed. In Chapter 2, it mentioned that the response of TiO_2 nanowires to explosives can be modulated by environmental humidity. This is because humidity can cause a change of the density of hydroxyl groups on TiO_2 surface and then lend to significant fluctuation in background resistance of the sensor, which was described in Chapter 3. Although the cross-sensitivity to humidity can be numerically compensated with digital signal process referenced to an additional humidity senor, a technique to effectively suppress the cross-sensitivity of the TiO_2(B) nanowires to humidity is very desirable.

TiO_2(B) as one of the crystal polymorphs of TiO_2 [94], is a material of great interest not only for photocatalytic applications [109, 110] but also a UV-sensitive hydrophilic surface conversion agent [111-113]. This is because the electrons in TiO_2 can be effectively excited to create free radicals under the illumination of ultraviolet (UV) light of wavelength shorter than 388 nm. Photogenerated electrons can be trapped and tend to reduce Ti^{4+} cations to Ti^{3+} ions and holes can oxidize water on the surface of the TiO_2(B) for the formation of surface hydroxyl groups. Therefore, UV illumination should be a feasible technique to dramatically decrease the amount of water molecules that interfere with changes in chemiresistivity of the sensor.

The motivation of this Chapter is to develop a feasible method to minimize the effect of humidity on the sensing response of TiO_2 based explosive sensors. Here, we need to pay attention that the mechanism that TiO_2 nanowires are sensitive to water vapor is different to the sensing mechanism of TiO_2 to explosive vapors. The different sensing mechanisms provide some ideas to control the humidity effect and obtain the best sensing performance of TiO_2 nanowires.

4.2 Experimental section

Single crystalline TiO_2(B) nanowires were synthesized by a hydrothermal technique as described in previous chapters and our published papers [45-47, 57, 59, 61]. The length of the nanowires ranges from 1.1 μm to 2.2 μm and the diameter of nanowires is in the region of 40-100 nm, which can be adjusted by varying the synthesis conditions such as the reaction temperature, time, and the concentration of precursor solution. The as-synthesized nanowires were dispersed as a suspension in ethanol and drop-casted on a glass substrate to form a highly porous thin film about 10 μm in thickness. The electric contact pads were deposited onto the film via magnetron sputtering. The pads were made of titanium in order to form a good ohmic contact of low junction resistance with the TiO_2(B) nanowires.

Vapors of explosives in equilibrium concentration at room temperature were generated using glass beads coated with various explosives (Inert Products, LLC.) and a vapor generator as reported [70]. The concentrations of vapors of various explosives were measured by an HP 5797 gas chromatography-mass spectrometry (GC-MS). Saturated vapor of water at room temperature was generated by a heated water bubbler. Sensor testing of the explosive and water vapors was performed through a computer controlled valve system at room temperature in ambient

atmosphere. Chemiresistive response was measured with an electrometer (Keithley 617) and recorded by a computer. A schematic diagram of the test set up is shown in Figure 4.1. An UV LED (LedEngin LZ1-10U605) was used as the source of UV illumination. The intensity of the UV light ranging from zero up to 40 mW/cm^2 was used for the measurements and nominal wavelength was 368 nm.

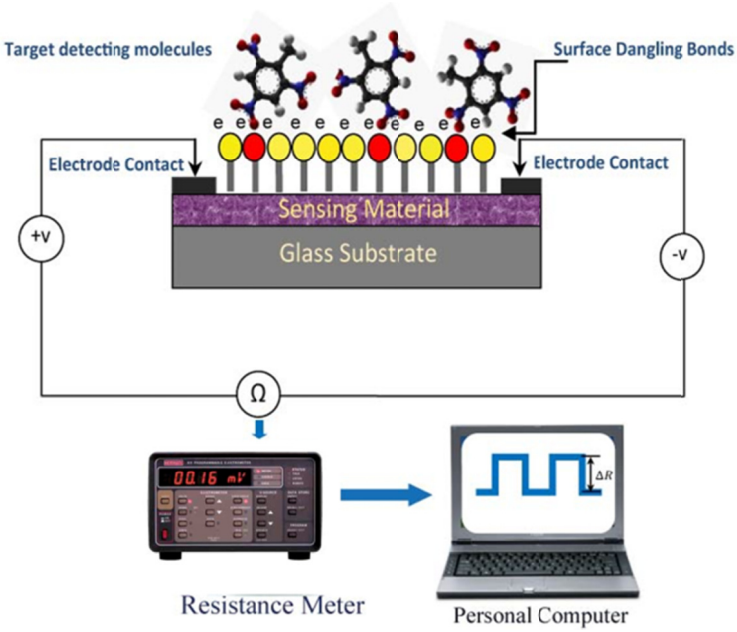

Figure 4.1 Schematic sketch of chemiresistive sensor based on TiO_2(B) nanowire thin film.

4.3 Results and discussion

As shown in Table 4.1, the resistance of nanowires increases on all nitro-related explosive compounds. The reason of causing the change of resistance was explained in Chapter 3, which is due to the charge transfer interaction between high electronegativity of explosives and TiO_2

nanowires via surface hydroxyl groups. Such interaction can result in a depletion of charge carriers in the nanowires due to localized surface states created by the adsorbed explosive molecules. Since humidity in the air can affect the density of hydroxyl groups on the surface of TiO_2(B) nanowires, it can cause cross-sensitivity to the sensor. As shown in Figure 4.2, it is clear that humidity indeed cause a significant shift to the base resistance.

Table 4.1 Sensing response to electron deficient compounds.

Explosives	Response Time (s)	Sensitivity (%)
2-nitrotoluene	4.85	16
3-nitrotoluene	3.18	18
4-nitrotoluene	0.73	16
2,4-dinitrotoluene (DNT)	3.94	33
2,4,6-trinitrotoluene (TNT)	4.31	33
1,3,5-trinitrobenzene (TNB)	2.60	33
2,4,6-Trinitrophenylmethylnitramine	5.85	14
2,4,6-trinitrophenol (TNP)	4.20	14

The effect of humidity can also be reflected by the result of a sensing test using saturated water vapor at room temperature without UV illumination as shown in Figure 4.3, where a significant response of TiO_2(B) to air with saturated water vapor (air of relative humidity of 100%) exhibits. The sensor response to saturated water vapor is about 50% higher than the response to saturated (1 ppb) TNT vapor. The rather high response of TiO_2(B) to water vapor is suggested to be a result of adsorption of water molecules on the surface of TiO_2(B) nanowires [114, 115]. According to the second mechanism of the water vapor effect on the metal oxide sensing performance [87, 88], discussed in Chapter 3, the formation of hydroxyl groups in the presence of water on the TiO_2(B) nanowire surface can act as doping charges and change the charge

concentration of TiO_2 and thus shrunk the depletion region [90, 116]. As a result, the resistance *decreased* when TiO_2(B) nanowires were exposed to the water vapor. The resistance "bump" observed in Figure 4.2 when the humidity in air is lower. In view of the fact that the sensor response to water vapor with high relative humidity (RH) is almost on the same order of magnitude as that to explosive vapors, finding a way to reduce the influence of humidity becomes critically necessary.

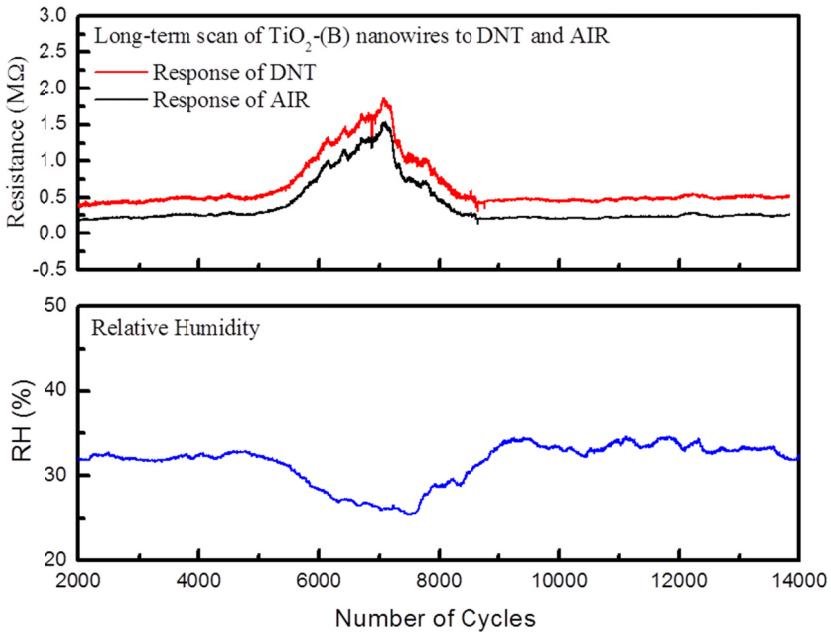

Figure 4.2 Baseline resistance change over 12000 continuous test cycles between vapor of 100 ppb of DNT and pure air. Each test cycle consists of 6 s of vapor followed by 6 s of air. The total time of the test is 33 hours.

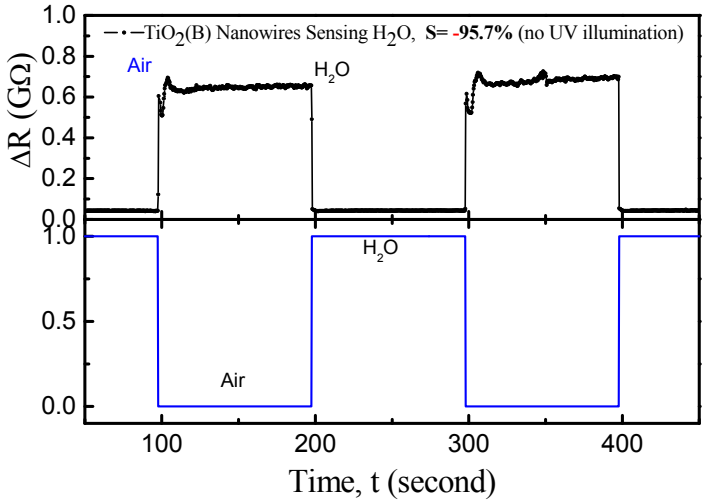

Figure 4.3 Typical resistance change of a TiO_2(B) nanowires thin film in response to saturated water vapor at room temperature.

UV illumination has been adopted in this study to solve the cross-sensitivity problem of the TiO_2(B) sensor arising from the influence of humidity, based on the consideration that titanium dioxide (TiO_2) is a good photocatalyst with the capability to split water under UV light illumination [117, 118]. A photocatalyst is characterized by its capability to adsorb simultaneously two reactants, which can be reduced and oxidized by a photonic activation through an efficient absorption in the case of $h\nu \geq E_g$, where $h\nu$ is the energy of photons and E_g is the energy band gap of the photocatalyst. For TiO_2, its band gap is 3.02 eV for rutile phase and 3.20 eV for anatase phase, both of which are larger than the required energy for water splitting, 1.23 eV, and more importantly the conduction band bottom of TiO_2 is more negative (vs NHE) than the reduction potential (H_2/H_2O) while the valence band top is more positive than the oxidization potential (O_2/H_2O) (Figure 4.4), enabling the water to be split into H^+ and O^{2-} under illumination and thus reduce the influence of humidity.

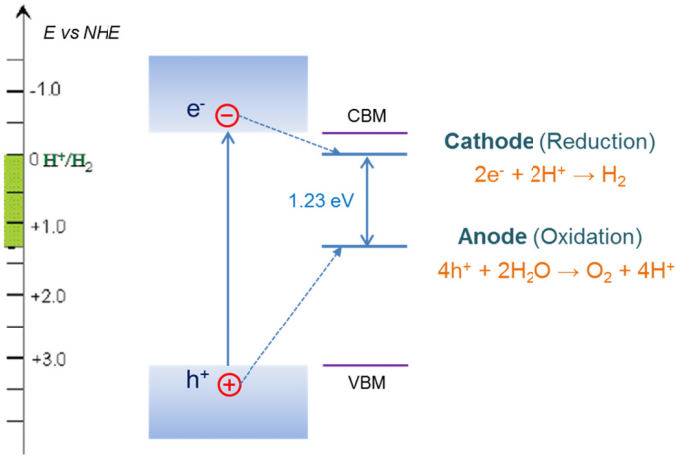

Figure 4.4 Mechanism of photo-induced water splitting.

Therefore, the photoexcitation of TiO_2 photocatalyst can be very effective when it is illuminated by UV light with the photon energy greater than the band-gap of TiO_2 corresponding to the wavelength of 384 nm, however the sensing response of TiO_2 to explosives will not be impaired by such an illumination of UV light. With this consideration, in our study, an UV light source with wavelength of 368 nm (corresponding to photon energy of 3.3 eV) was employed. During the testing, the UV light remained on but its intensity was tuned from zero to 40 mW/cm^2. The performance of TiO_2 nanowires to detect humidity was evaluated by resistance measurement at different UV power. The results shown in Figure 4.5 reveal that the cross-sensitivity of TiO_2(B) nanowires to humidity was reduced down to 51% when the UV light with intensity of 40 mW/cm^2 was applied. Under the same UV illumination, the overall sensitivity to TNT presents little change, about 17% fluctuation over the entire range of UV illumination. The reduced response of the TiO_2(B) nanowire thin film to humidity when illuminated by UV light can be explained by water splitting effect of the TiO_2(B) under UV photoexcitation.

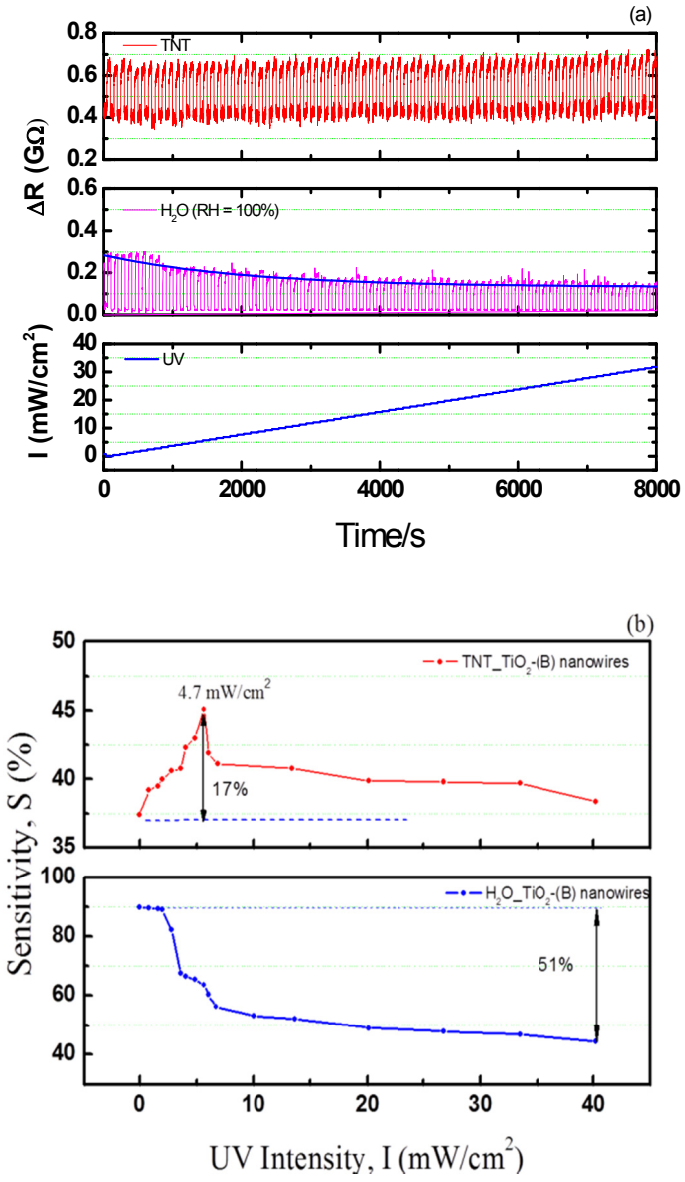

Figure 4.5 (a) Sensing response (Resistance change, ΔR) to 1ppb concentration of TNT and saturated water vapor at room temperature based on TiO_2(B) nanowires under controlled UV intensity from zero to 40 mW/cm^2. (b) The variation of sensitivity to TNT and H_2O at different UV current.

As shown in Figure 4.6, the effective photoexcitation of TiO_2(B) can result in the formation of electrons (e^-) in the conduction band and holes (h^+) in the valence band [119]. It is known that

the electron-hole pairs can be trapped at the TiO_2 surface. The holes oxidize O^{2-} anion to form reactive **oxygen species** such as superoxide ion ($O_2^{\bullet-}$), atomic oxygen (O), O^-, hydroxyl radicals (OH^*) radicals by interacting with O_2 and H_2O on the surface of TiO_2 [120, 121]. The electrons tend to reduce Ti^{4+} to Ti^{3+}. The general mechanism of photocatalytic oxidation of water and the formation of hydrophilic surface on TiO_2 is described in Figure 4.7.

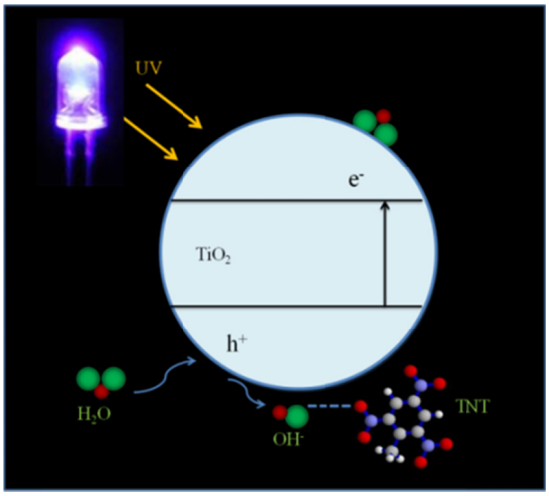

Figure 4.6 Schematic drawing showing water splitting on the surface of TiO_2 (B) nanowires under UV irradiation.

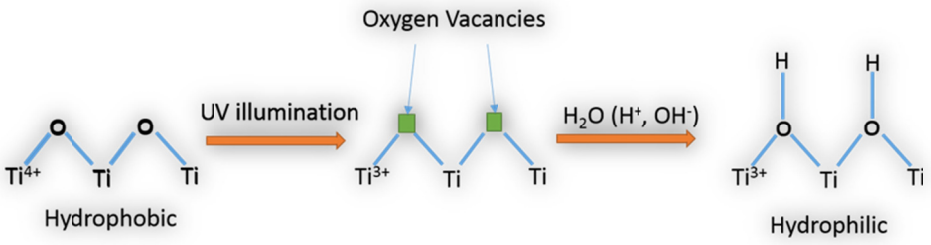

Figure 4.7 Mechanism of photoinduced hydrophilicity of TiO_2.

The hydroxyl groups on the TiO_2 surface are highly active, which not only lend to an increase of van der Waals forces and make the surface more hydroxylated but also increase the hydrogen bonding interaction between –OH and nitro-group in explosive compounds [81]. In other words, the hydroxyl radicals act as a bridge for the charge transfer interaction between the TiO_2(B) and explosive molecules. The whole process indicates that UV illumination of TiO_2(B) nanowires during the sensing of explosives has two impacts on minimizing the humidity: 1) the UV illumination excites n-type semiconducting TiO_2 nanowires to enable the generation of holes and electrons photocatalytically at TiO_2 surface and; 2) The electron-hole pairs (e^-- h^+) on the TiO_2 surface effectively interact with water on the surface to produce hydroxyl radicals, as shown in equations (1) through (4). Here, hydroxide ions are dissociated from water coming from air.

1) Charge-carrier generation by UV:

$$TiO_2 + h\nu \rightarrow e^-_{CB} + h^+_{VB} \quad (1)$$

2) Charge-carrier trapping and formatting hydrophilic :

$$e^-_{CB} + Ti^{4+} \rightarrow Ti^{3+} \quad \text{(deep electron traps)} \quad (2)$$

$$e^-_{CB} + Ti^{4+}\text{-}OH \rightarrow Ti^{3+}\text{-}OH \quad \text{(shallow electron traps)} \quad (3)$$

$$h^+_{VB} + OH^- \rightarrow OH^* \quad (4)$$

Therefore, the increased concentration of hydroxyl groups on the surface of TiO_2 (B) nanowires due to the increase of Ti^{3+} via UV illumination and the removal of water in view of photo-oxidation lead to a significant reduction of cross-sensitivity to humidity. It is noted in Figure

4.5(b) that when the UV intensity is below 4.7 mW/cm^2, the response to explosives increases with the UV intensity. This is likely due to the increased coverage of hydroxyl radicals on the surfaces of nanowires. However, when UV intensity increases too high, UV radiation could photochemically decompose or break down the explosives or desorb the explosives from the TiO_2(B) nanowires surface, causing a decrease in response. This scenario implies that a proper intensity of UV illumination for the as-discussed application should be carefully chosen.

In order to further confirm that the increased concentration of surface hydroxyl groups on the TiO_2(B) nanowires originates from UV photocatalysis, a water wettability test was performed by measuring the surface contact angles. Figure 4.8 shows the change of contact angles on TiO_2(B) nanowires surfaces with and without UV light illumination. It can be seen that the contact angle of TiO_2(B) nanowires becomes smaller under UV radiation. When the UV density is 26.7 mW/cm^2, the contact angle is less than 10°, which indicates a more hydrophilic TiO_2 (B) nanowire surface due to the UV illumination. A Fourier transform infrared spectrum (FTIR) in Figure 4.9 shows the change of a spectroscopic feature characteristic after TiO_2(B) nanowire illuminated by UV light with power density of 40 mW/cm^2 for 5 minutes. The peak at 3300 cm^{-1} due to surface hydroxyl groups (Ti-OH) [81, 82] in the TiO_2(B) thin film became higher after UV illumination. A slight increase can be observed at the band with wavenumber of 1625cm^{-1} due to the formation of bond (-O-Ti-OH-N-O-) [80]. These results clearly suggest that the UV illumination can increase concentration of surface hydroxyl groups with generated hydroxyl radicals from water dissociated on the TiO_2 (B) surfaces [111, 122, 123]. We also notice that the peaks at 2335 cm^{-1} and 2364 cm^{-1} due to carbon dioxide and aromatic groups of DNT become smaller after UV illumination. It is likely that UV light can clean TiO_2(B) nanowire surface and photochemically decompose the explosives. According to our previous studies, the increase of

hydroxyl groups can enhance interaction between the nanowires and electron deficient molecules with nitro groups [46]. The hydroxyl groups provide a charge transfer pathway between the nitro groups in nitroaromatic explosives and TiO_2(B) nanowires, resulting in the measured chemiresistive responses.

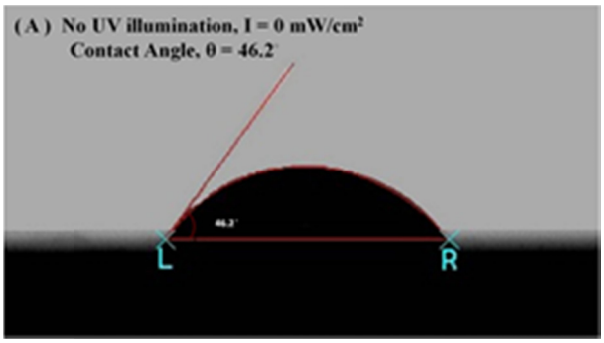

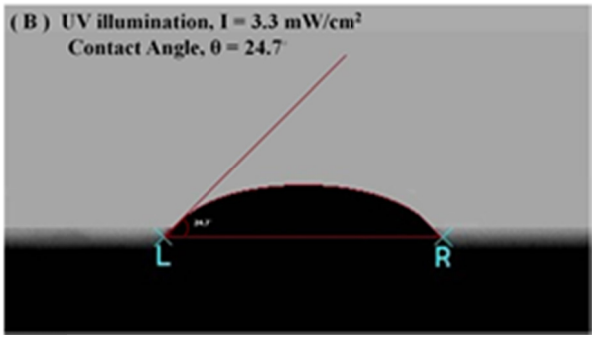

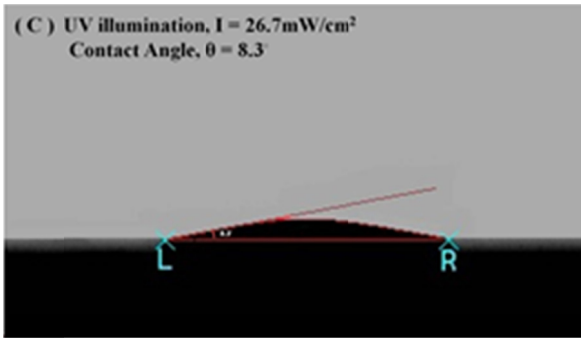

Figure 4.8 Contact angles of TiO_2(B) nanowires surface and water with and without UV irradiation. (a)As-fabricated TiO_2(B) nanowires surface. (b) The nanowires surface under 3.3 mW/cm^2 of UV illumination for 4 minutes. (c) The nanowires surface under 26.7 mW/cm^2 of UV illumination for 4 minutes.

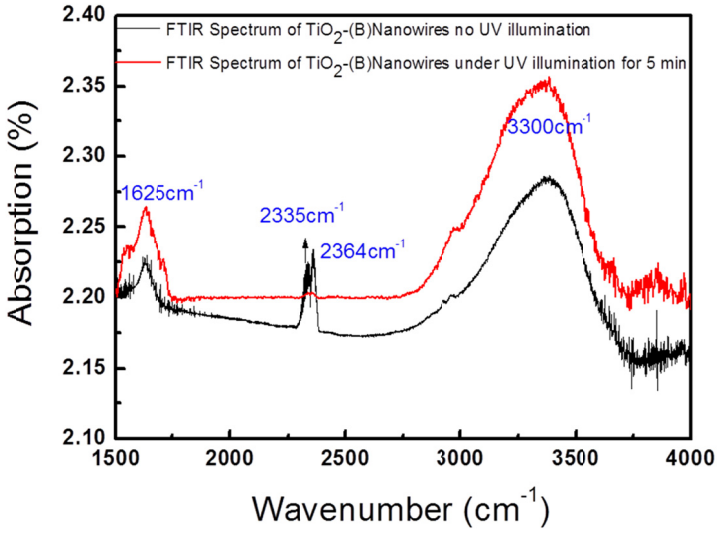

Figure 4.9 FTIR Spectra of control sample and TiO_2(B) nanowires after UV illumination for 5 minutes.

4.4 Conclusion

The effect of UV illumination on the response of TiO_2(B) nanowires to vapors of water and TNT was studied using a UV LED of wavelength of 368 nm. The results show a significant reduction of cross-sensitivity to humidity from UV illumination. The response to TNT has moderate increase at 4.7 mW/cm^2 intensity of UV radiation. Photocatalytic oxidation of water on the surface of films of TiO_2(B) nanowires under UV illumination can be used to increase surface

hydroxyl groups that suppress the cross-sensitivity of the nanowires toward environmental humidity while preserving a stable response to explosives.

Chapter 5

CHEMIRESISTIVE RESPONSE OF SILICON NANOWIRES TO TRACE VAPOR OF NITRO EXPLOSIVES

5.1 Introduction

In previous Chapters, an explosive sensor based on TiO_2(B) dominant nanowires is reported. It exhibits excellent sensing properties to detect explosive trace vapor. However, the synthesis of TiO_2(B) dominant nanowires like most semiconductor nano-materials were used a bottom-up approach, which is based on solution phase reactions and produces random nanowires. Random nanowires suffer from difficulties in controlling position and diameters of individual nanowires and in making reliable ohmic contacts, and incorporating random nanowires in integrated electronic circuiting remains a challenge [124, 125]. Silicon nanowires fabricated with a lithography process can overcome these problems and provide advantages in sensor designs and especially in integration with microelectronic circuits that interfaces with the sensor [126-129]. Since silicon is the most important and the most commonly used semiconductor, its material properties such as doping and charge carrier distribution near the surface can be precisely controlled and characterized with well-developed techniques in the semiconductor industry. The surface can be further functionalized through silanol chemistry to achieve improved selectivity [23]. The lithography and nano-fabrication process provides freedom in the geometry of nanowires.

In this Chapter, silicon nanowires were fabricated with lithography and etching processes commonly used in the microelectronic industry. The chemiresistive response to vapors of several

common explosive chemicals, including DNT (2, 4-dinitrotoluene), TNT (2,4,6-trinitrotoluene), RDX (cyclotrimethylenetrinitramine), PETN (pentaerythritol tetranitrate), picric acid (2,4,6-trinitrophenol), and an explosive degradation by-product, 2-nitrotoluene, was studied. The width of nanowires was varied to study the interaction between the surface adsorbed chemicals and the charge transport in the nanowires. Treating the surface of nanowires with oxygen and hydrogen plasma is found to significantly change the carrier characteristics and the chemiresistive behavior. Properties important to practical applications, such as long-term stability, were also investigated.

5.2 Experimental Section

5.2.1 Silicon Nanowires Fabrication

The silicon nanowires were fabricated on a commercial silicon-on-insulator (SOI, from Soitec) wafer (Figure 5.1a). The thickness of the top silicon layer for the nanowires is 220 nm and the buried oxide (BOX) between the top silicon and the handle wafer is 3 μm thick. The top silicon is lightly doped with boron to make it a p-type semiconductor with conductivity of 14~22 Ω·cm. The wafer is oriented in the <100> crystal plane. Nanowires were fabricated in the top silicon and they are parallel to the <100> direction. Nanowires of three different widths, 100, 200 and 400 nm, respectively, were fabricated. The length of the nanowires between the two aluminum contact pads for electrical measurements is 100 μm. There are about 20 identical nanowires between two contact pads. To pattern the silicon nanowires, negative resist (XR-1541 from Dow Corning) was spin coated on the SOI wafer and the nanowire patterns were exposed with electron beam. The patterns were further transferred to the top silicon layer with inductive coupled plasma reactive ion etching (ICP-RIE, PlasmaTherm PT770) and the resist served as the

etching mask. The residual e-beam resist after reactive ion etching was removed with buffed oxide etching. Aluminum contact pads covering the two ends of the silicon nanowires were fabricated with a lift-off process and were annealed to form Ohmic contact with the silicon nanowires.

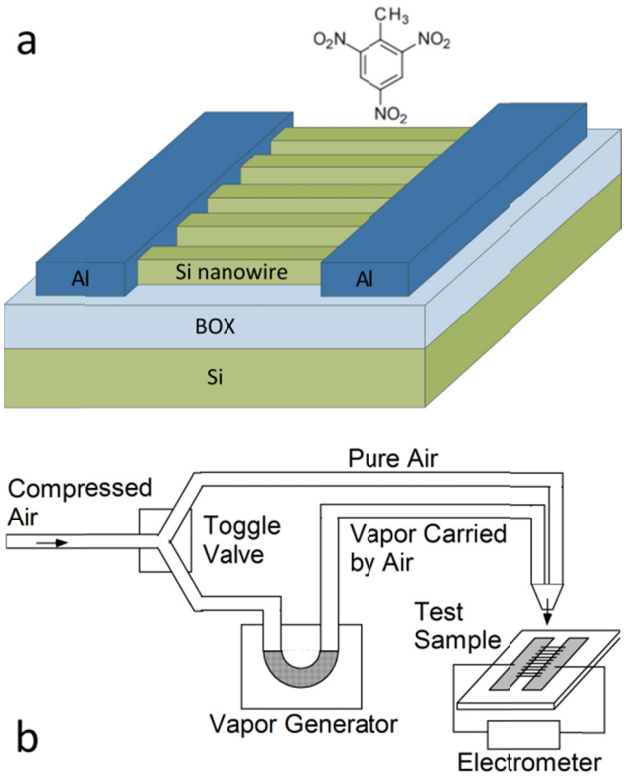

Figure 5.1 (a) Schematic drawing of the silicon nanowire sensor. (b) The setup for explosive vapor generation and electrical measurement.

5.2.2 Test of Sensor Samples

The nanowire samples were tested in the ambient environment (Figure 5.1b). During the test, the sample under test was alternatively exposed to pure air and air that carries explosive vapors for 100 seconds each, and the resistance between the two contact pads was continuously monitored

with a programmable electrometer (Keithley 617). The air from a compressed air pump flows in two alternate paths controlled by a solenoid toggle valve which in turn is controlled by a computer. Air of one path flows through a vapor generator [70] that produces vapor of the chemicals used in the test. The chemical was heated at 60 °C to enhance evaporation to ensure that when the vapor is cooled down to room temperature as air flows from vapor generator to the test samples, the vapor contains enough molecules of the chemicals and can reach a stable saturated concentration at room temperature. Excess molecules condense on the wall of the tubing between the vapor generator and the test sample. According to literatures, the saturated concentrations of TNT, DNT and RDX are 5 ppb, 100 ppb, and 5 ppt, respectively [130]. The vapor concentrations at room temperature were verified by collecting a known volume of vapor with a thermal desorber. The amount of absorbed chemicals was determined by an analytical laboratory (Columbia Analytical Services, www.caslab.com) and the measured vapor concentrations are in agreement to the order-of-magnitude of the values reported in the literatures [129]. The nanowire samples were tested for sensitivity and response time to the chemicals. Sensitivity is defined as the relative resistance change due to the chemicals, i.e. the ratio of resistance change caused by the chemicals to the initial resistance without the chemicals, a definition commonly used in chemical sensor research [71]. The response time is time constant of the exponential transient response of the sensor after the sensor is exposed to the air containing explosive vapor.

5.2.3 Surface Modifications of Sensor Samples

Oxygen and oxygen plasma treatments of nanowires were carried out in a microwave plasma cleaner/etcher (Plasma-preen). The plasma treatments were made at pressure of 1 Torr and rf power of 300 W for 5 minutes.

5.3 Results and Discussion

Figure 5.2 shows a typical response of the silicon nanowire sensors to DNT vapors. No surface treatment was done on the nanowires. The resistance is in the mega-ohm range and the vapor caused a decrease in resistance. The decreased resistance (i.e., increased conductance) in *p*-type silicon nanowires indicates that electron-deficient nitro compounds traps electrons and generate more hole carriers, i.e. accumulate majority carriers in the *p*-type silicon nanowires. This is in contrast with the response of *n*-type semiconductor nanowires to explosive vapors, where a depletion of electron majority carrier causes the resistance to increase [46]. Table 5.1 lists the measured sensitivities to DNT for silicon nanowires of three different widths. The higher sensitivities observed in the nanowires of smaller width confirm the correlation between sensitivity and surface-to-volume ratio of nanowires.

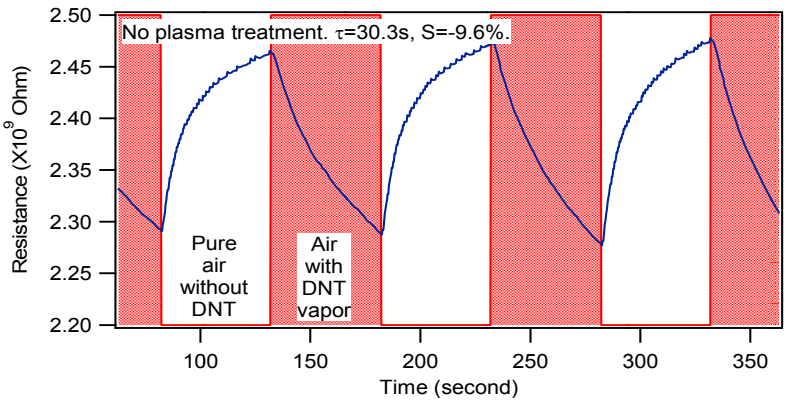

Figure 5.2 Responses of the silicon nanowires (400 nm in width) to DNT vapor without surface treatment.

Table 5.1 Sensitivities of the silicon nanowires with different widths to DNT.

Nanowire width/nm	Sensitivity (%)
100	6
200	5
400	4

Since the interaction of explosive molecules and silicon takes place on the surface of the nanowires, the condition of the silicon surface is expected to have a strong impact to the sensing property. The silicon nanowires were treated with oxygen and hydrogen plasmas to study the effect of the surface treatments on the sensitivity and response time. The treatments were carried out at the following condition: the pressure of the chamber of 1 Torr, the RF power of 300 Watts, and the process time of 5 minutes. As shown in Figures 5.3a and 5.3b, both oxygen and hydrogen plasmas greatly improve the sensitivity and response time of the sensors, and oxygen plasma changes the sign of resistance change.

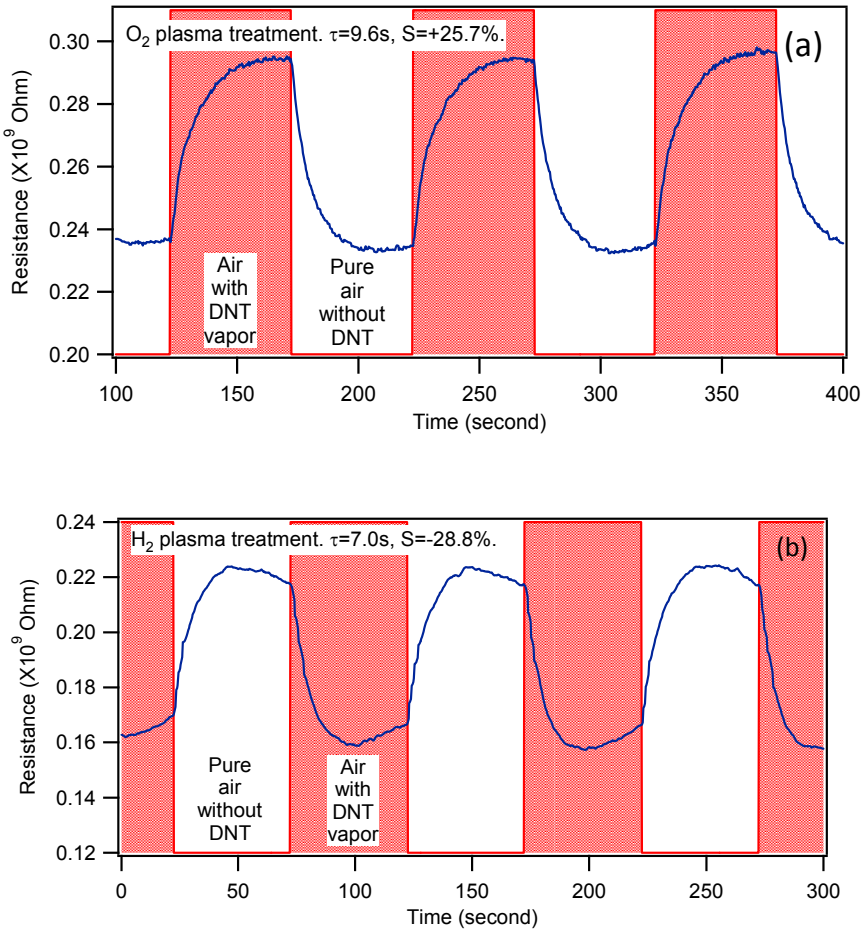

Figure 5.3 Responses of the silicon nanowires (400 nm in width) after surface plasma treatments to DNT vapor. (a) Treated with oxygen plasma. (b) Treated with hydrogen plasma.

The first effect of the oxygen or hydrogen plasma treatment would be the cleaning of the nanowire surfaces, which provides more adsorption and binding sites for the target molecules and leads to stronger and faster responses [131, 132]. Because oxygen plasma is more efficient in cleaning organic contaminants than hydrogen plasma, the higher sensitivity after the oxygen plasma treatment is expected. Exposure to oxygen plasma and subsequently to air is known to result in formation of hydroxyl groups on the surface [133], and previously we have found that surface hydroxyl groups form charge transfer complexes with nitro groups of nitro explosives

and strengthen chemiresistive effect in TiO_2(B) nanowires [46]. Hydroxyl groups on the surface of silicon nanowires could have similar effects but not exact same. In TiO_2(B) nanowires, the hydroxyl groups are coordinated with Ti^{3+}, which make surface Ti-OH more easily to interact with high electron deficient explosive compounds. While, in silicon nanowires, the interaction between surface hydroxyl groups and nitro-group in explosive should be much weaker. This is the reason even after oxygen plasma treatment, the sensing response of silicon nanowires to explosive vapor is still weaker than that of TiO_2(B) nanowires. Further discussion will be reported in next Chapter.

We attribute the reversed change of the resistance to the conversion of the type of the majority carrier on the silicon nanowires surface after the oxygen plasma treatment. To confirm the assumption, surface studies such as X-ray photoelectron spectra (XPS) and Hall measurements at room temperature were carried out on pristine as well as plasma treated pieces from the same SOI wafer that were used to fabricate the silicon nanowires. The Hall measurement results in Table 5.2 indicate that the oxygen plasma treatment with short exposure time (5 min.) changed the top silicon layer of the low doping SOI wafer (hole concentration about ~10^{15} cm^{-3}) from p-type to n-type semiconductor. The reverse of the type of majority carriers gradually fades away after the sample is kept in the ambient environment for a few days, and afterwards the sample behaves the same as before plasma treatment. The spectra of XPS in Figure 5.4 show two oxygen peaks. One O 1s peak at the binding energy around 535 eV is from surface oxygen species on SOI wafer; the other peak with binding energy at 105 eV is the element from SiO_2. The intensities of both peaks increased after post-oxygen plasma treatment. After oxygen-treated SOI wafer was rinsed in deionized (DI) water, the intensity of the peak at 535 eV decreased. This indicates that plasma treatment produced more oxygen species adsorbed on the surface, and the

adsorbed oxygen does not form covalent bond with silicon because the oxygen species can be removed by rinsing in DI water. The intensity of the peak at 105 eV increased after plasma treatment, and was not affect by DI water rinsing. This means that oxygen plasma treatment permanently increased the thickness of SiO_2, and the increase of SiO_2 does not contribute to the reversal of majority carriers. These observations further explained that post-oxygen plasma treatment of the SOI wafer can introduce a change in the type of majority carriers as well as cause a growth of thin layer of silicon oxide [134, 135]. According to references [133, 136-138], this may be explained by the formation of electron donors associated with removing the negatively charged oxygen species (O^-, O^{2-}) adsorbed on the silicon surface and the electron acceptor trapping sites from the low doping SOI surface under short exposure time of O_2 plasma. As discussed previously, p-type and n-type semiconductor nanowires exhibit different response to electron-deficient explosive compounds. Therefore the reversed resistance change and the change of majority carrier type are in agreement.

Table 5.2 Hall measurement results of SOI wafer with and without plasma treatments.

	Untreated SOI	**O_2 plasma treated SOI**	**H_2 plasma treated SOI**
Hall coefficient (cm^3/C)	2.688×10^3	-1.673×10^4	9.857×10^2
Carriers Concentration ($1/cm^3$)	2.323×10^{15}	-3.730×10^{14}	6.333×10^{15}

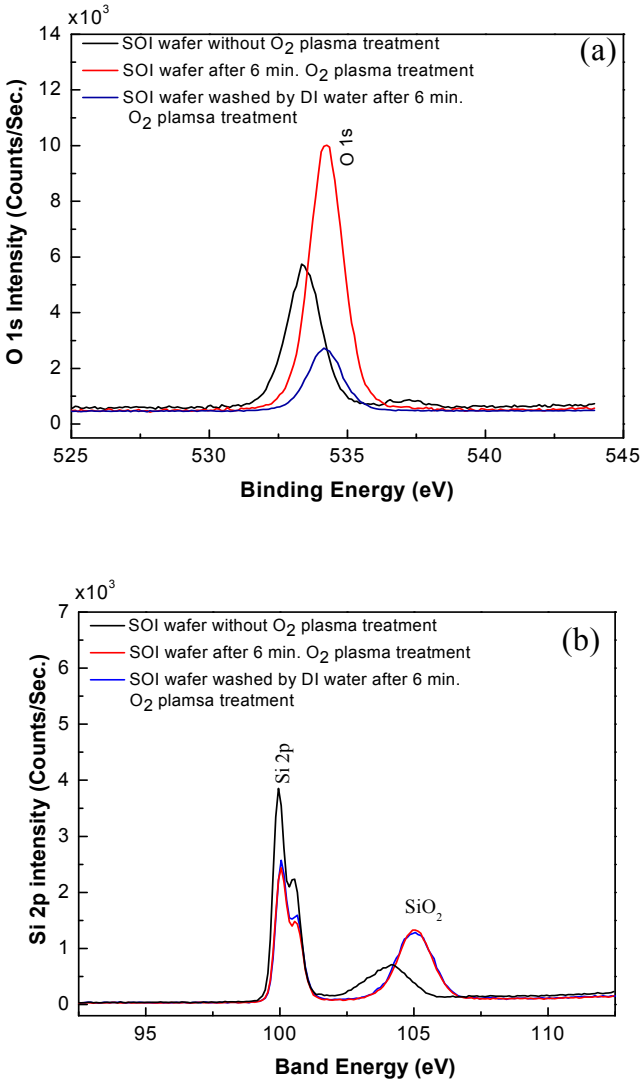

Figure 5.4 The O(1s) and Si(2p) peaks of XPS spectra of the top silicon surface before and after oxygen plasma treatment, and after rinsing with DI water after the plasma treatment. (a) O(1s) peak of surface adsorbed oxygen. (b) Si(2p) peak of surface SiO_2 layer.

In addition to DNT, the nanowires were found to respond to several other nitro explosives and nitro compounds related to explosives. The responses of silicon nanowires to saturated vapors of DNT, TNT, RDX, PETN, picric acid, and 2-nitrotoluene as well as effects of the plasma treatments are summarized in Table 5.3. The chemiresistive response of silicon nanowires was

found to be stable in the ambient atmosphere. The sensor responses to DNT with and without oxygen plasma treatment were continuously tested over 2000 cycles and, in both cases, no significant drift is observed (Figure 5.5).

Table 5.3 Responses of the silicon nanowires (200 nm in width) to different explosive compounds.

Explosive compounds	*No plasma*		*Hydrogen plasma*		*Oxygen plasma*	
	S* (%)	T§ (s)	S (%)	T (s)	S (%)	T (s)
DNT	-6	29.6	-20	3.4	50	7.1
TNT	-2	38.4	-15	12.07	28.5	10.3
RDX	-8	33.4	-4	2.93	24	7.82
Picrid Acid	-4	85.4	-5	2.6	15.3	21.8
PETN	-1.5	9.7	-16	174	30	2.3
2-Nitrotoluene	-11	25.18	-14.5	7.2	20	12.4

* S: Sensitivity

§ T: Response Time

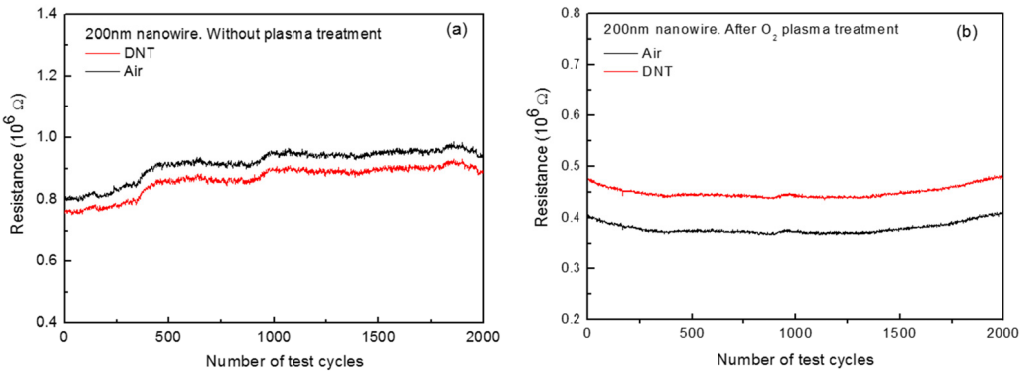

Figure 5.5 Test results of the silicon nanowires (200 nm in width) through 2000 testing cycles of alternating between DNT vapor and air. (a) Without plasma treatment. (b) Treated with oxygen plasma.

5.4 Conclusion

Silicon nanowires exhibit significant chemiresistive effect in response to common nitro explosives and their degradation by-products, including DNT, TNT, RDX, PETN, picric acid, and 2-nitrotoluene. Oxygen and hydrogen plasma treatments are found to significantly improve sensitivity and response time. In particular, oxygen plasma treatment changes the type of majority carriers from *p* to *n* and inverts the sign of the resistance change. Nanowires of smaller cross sections exhibit higher sensitivity. These observations indicate that surface physics/chemistry plays a critical role in the chemiresistive response of silicon nanowires. By exploring different doping levels and other surface modification techniques, including plasma of other reactive gases and self-assembled monolayers of functional molecules, nanowire sensors of higher sensitivity and selectivity can be expected.

Chapter 6

FURTHER INVESTIGATION OF SENSING MECHANISM BASED ON TiO_2 NANOWIRES

6.1 Motivation

In the previous Chapters, we investigated an explosive sensor based on TiO_2(B) dominant nanowires. Good sensing performance such as very low detection limit up to sub-trace concentration and much quicker response on the order of 1 second, is observed. Preliminary mechanism of sensing response has been discussed. It is attributed to the interaction between the surface Ti-OH groups and nitro groups in explosives through a strong charge transfer process. Since gas sensing properties based on TiO_2(B) dominant nanowires can be modulated by microstructure, morphology, surface modification and doping, and different crystal phases, more experiments are carried out in this chapter to gain more insightful understanding regarding 1) the moisture effect on sensing performance; 2) surface modification and doping effect on sensing performance; 3) the impacts of microstructure and crystal phases of TiO_2 on sensing properties; In addition, 4) the use of some more materials other than TiO_2(B) and silicon nanowires for explosive detection.

Specifically, we studied on sensor response under different humidity with TiO_2(B) nanowires; we compared sensor response when TiO_2 is in the forms of nanoparticles and nanowires, and in the case of different crystal phases, i.e., anatase, rutile, and TiO_2(B). We also outreached the materials to ZnO nanowires, V_2O_5 nanowires and non-oxide semsiconductors such as CdS

nanowires. Based on these research, we can build up an explosive sensor device based on nanostructured TiO_2 with improved sensing performance.

6.2 Moisture effects

In Chapter 3, we mentioned the effect of water on the sensing response of TiO_2(B) nanowires to detect explosives and can be summarized as follows:

- The effect of water vapor or moisture lends to the decrease in resistance of TiO_2 or baseline shift. This effect can be explained by an increased coverage of surface hydroxyl groups as suggested by the mechanism proposed by Heiland and Kohl [87] and the appearance of donors.

- Relative high humidity results in higher sensitivity. This improvement is due to specific surface characteristics of TiO_2. The surface hydroxyl group can be coordinated with Ti^{3+} and form surface Ti-OH sites, which build an effective bridge to realize surface charge transfer between explosive molecules and TiO_2.

Therefore, in case of TiO_2 nanowires as explosive gas sensor, the level of humidity in ambient air needs to be controlled in order to avoid a loss in the response to a target gas if the level of humidity is too high or too low. However, it is not easy to quantify the effect of moisture. In order to characterize the influence of water based on TiO_2 nanowires to detect trace explosives, such as TNT vapor, a series of experiments to have been carried out with different concentrations of water vapor (or different relative humidity, RH) at room temperature. As shown in Figure 6.1,

the optimal sensitivity of TiO_2 nanowires to DNT vapor was obtained when relative humidity was 25%.

The reason that there exists an optimal humidity for TiO_2(B) sensor response is due likely to the factor, in the case of low humidity, as mentioned above an increase of humidity may result in enriched hydroxyl groups formed on the TiO_2(B) nanowire surface; however, in the case of high humidity, an increase of humidity leads to the adsorption of water molecules, which act as a barrier against the explosive molecules to adsorb on TiO_2(B). The superficial charge migration of the explosive molecules on the TiO_2 surface becomes difficult, thus the sensitivity decreases. Such a deteriorative effect of water vapor has been also observed on SnO_2 sensor to C_2H_2 [136].

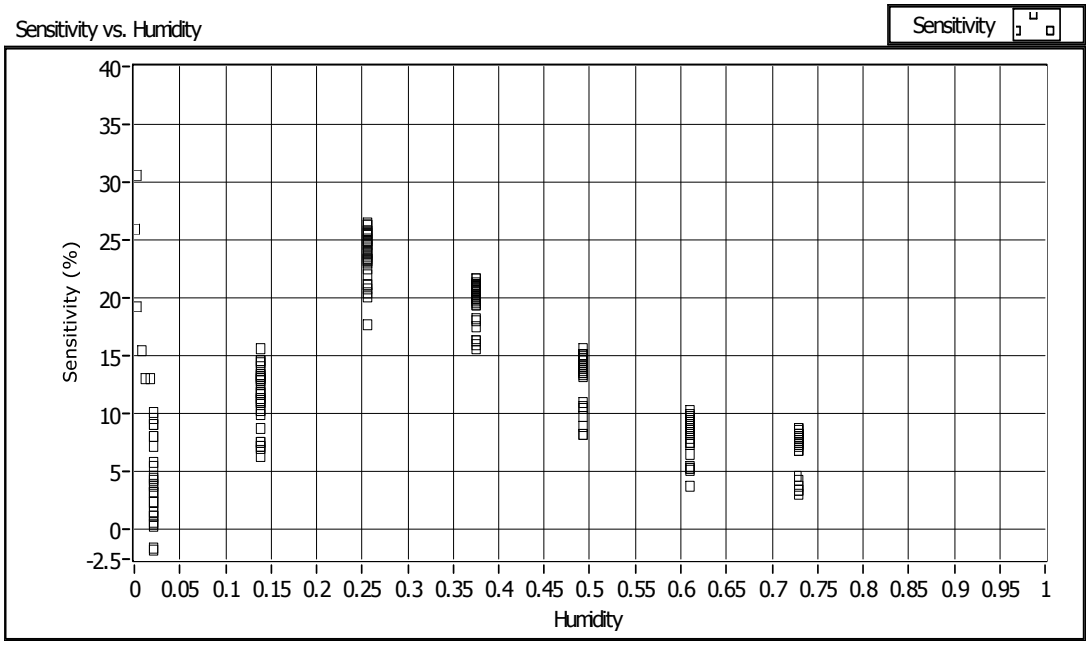

Figure 6.1 Sensing response to TNT vapor under different relative humidity.

6.3 Surface modification of TiO_2(B) dominant nanowires and anatase TiO_2 nanoparticles

6.3.1 Au/TiO_2(B) nanocomposite films for explosive detection

Surface modification (functionalizing) is one of the effective methods for improvement of gas-sensing properties of metal-oxides, aimed for application in various gas sensors. Metals, in particular, noble metals such as Pd, Pt and Au nanoparticles, play both passive and active roles to enhance the reactions on gas sensor surface and then improve the sensing properties [137, 138]. This is because the presence of metal nanoparticles increases the active surface area and improves gas diffusion inside the film. In this study, a surface modification by introducing noble metals in TiO_2(B) nanowires to form nanocomposite films was used to detect explosives. The nanocomposite films consist of small metal nanoparticles in the range of a few to several nanometers embedded in TiO_2(B)

Au/TiO_2(B) nanocomposite was prepared by fabricating Au nanoparticles and then adsorbing the Au nanoparticles onto TiO_2(B) nanowires in a solution environment [139]. Typically, 100 mg of chloroauric acid ($HAuCl_4$) are added into 50 mL of ethylene glycol (EG) to form Solution 1, and to the Solution 1 was added 0.5 M NaOH till the pH value reached 11. The solution 1 was then refluxed at 160 °C for 3 h and cooled down to room temperature. In another separate step, 0.2 g of TiO_2(B) dominant nanowire powder was dispersed in 2 mL of EG and the suspension was fully mixed by sonication for at least 10 min to Solution 2. The solution 2 was then added into Solution 1, and the mixture was stirred for 24 h. The Au-coated TiO_2(B) dominant nanowires were separated from the EG through centrifuging and were then dried at 100 °C. Sensor film

made of Au/TiO_2(B) nanocomposite was annealed at 450 °C for 1 h in air before metal electrodes were deposited. The XRD pattern of Au/TiO_2(B) nanocomposite is shown in Figure 6.2.

The results as shown in Figure 6.3 (a) and (b), the sensitivity with Au/TiO_2(B) nanocomposite film shows higher sensitivity (84%) than the one with TiO_2(B) dominant nanowire film (55%). Besides this, Au/TiO_2(B) nanocomposite film has much lower resistance ~ 100 MΩ than the resistance of TiO_2(B) dominant nanowire ~ 4 GΩ. The enhancement of sensitivity and decrease of resistance because of Au nanoparticules can be explained by "electronic mechanism" [140, 141]. That is, as shown in Figure 6.4, an electron-depleted layer formed around the Au nanoparticles and then modulated the nano-Schottky barriers, which can change the charge transfer process between analytes and TiO_2(B) dominant nanowires.

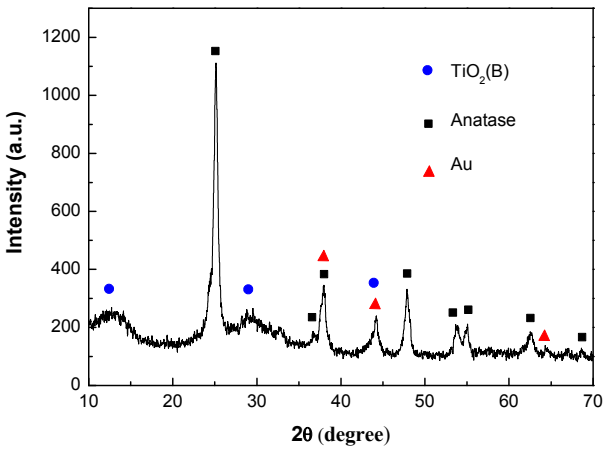

Figure 6.2 XRD pattern of Au/TiO_2(B) nanocomposite.

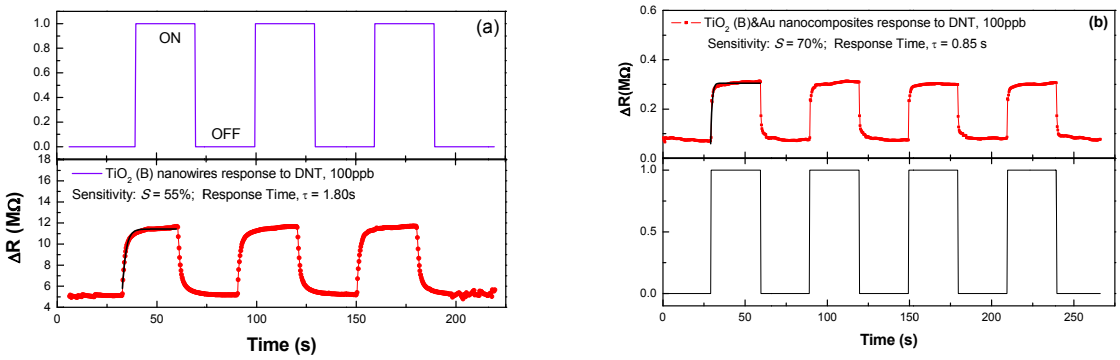

Figure 6.3 Sensing response to DNT, 100ppb; (a) TiO_2(B) dominant nanowires to DNT; (b) Au-TiO_2 (B) nanocomposite to DNT.

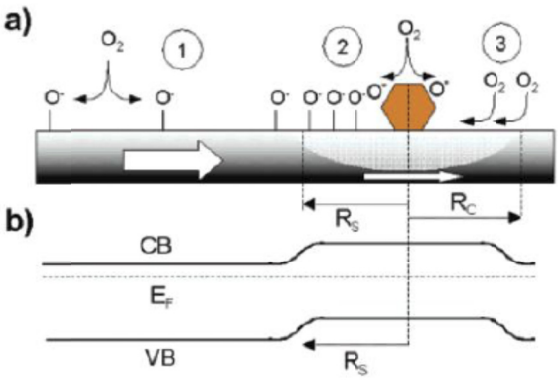

Figure 6.4 (a) Schematic depiction of the major process taking place at a TiO_2 nanowire surface when exposed to O_2. (b) Band diagram of the bare TiO_2 nanowire and in the vicinity (and beneath) an Au nanoparticle. The depletion region is determined by the spillover zone. [139]

6.3.2 Doping Effect

Another way to improve TiO_2(B) sensing performance was done by doping transition metals such as Fe (group III transition metal), V (group V transition metal). Usually, the purpose of doping is to enhance catalytic activity and adjust electrical resistance of the intrinsic metal oxide

[142-145]. In our case, doping is to change the doping level, thus, modifying the bulk Fermi level position, and hence, the equilibrium carrier population at the surfaces [145].

Fe doped TiO_2 nanoparticles (Fe-TiO_2)

Fe doped TiO_2 nanoparticles were prepared with a sol-gel based hydrothermal method. In a typical synthesis, 0.341 g of $Fe(NO_3)_3 \cdot 9H_2O$ dissolved in 5 mL of water was added into a mixture of 5 mL of titanium isopropoxide (TTIP) and 10 mL of acetic acid (HAc). A precipitate formed in the solution when the $Fe(NO_3)_3 \cdot 9H_2O$ aqueous solution was added, and it disappeared after the solution was stirred for 30 min, resulting in the formation of a clear sol in dark red. The sol was then transferred into an autoclave and was heated at 230 °C for 24 h. The resultant precipitate was washed with DI-water to remove residual $Fe(NO_3)_3$. Afterwards, the precipitate was dried at 100 °C and then ground to fine powder for use. Sensor film was prepared on glass substrate followed by a thermal treatment at 450 °C for 1 h.

V doped TiO_2 nanoparticles (V-TiO_2)

V doped TiO_2 nanoparticles were also prepared with a sol-gel based hydrothermal method. 0.0768 g of V_2O_5 powder was dispersed in 5 mL of DI-water and, after the solution was stirred for about 10 min, 1 mL of H_2O_2 was then added, resulting the formation of a clear sol of V_2O_5. The V_2O_5 sol was then added into 10 mL of HAC which contains 5 mL of TTIP. The mixture was then transferred into an autoclave for hydrothermal growth at 230 °C for 24 h. The precipitate was washed with DI-water, dried at 100 °C, and ground to fine powder. The sensor film was annealed at 450 °C for 1 h. Figure 6.5(a) and (b) are XRD patterns of V-TiO_2 and Fe-TiO_2 nanoparticles.

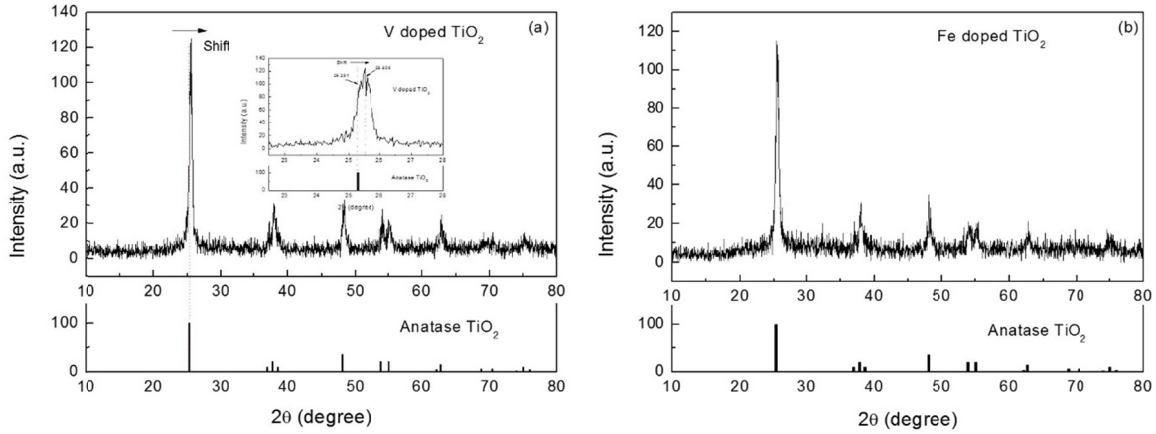

Figure 6.5 XRD spectra of (a) V doped TiO_2 nanoparticles (the inset is zoom-in spectrum) and (b) Fe doped TiO_2 nanoparticles.

We noticed that there is a peak position shift in V-TiO_2 nanoparticles. Such shift is considered due to the change of lattice spaces, which reflects a replacement of Ti by V in the TiO_2 matrix. As for Fe doped TiO_2 nanoparticles, no obvious peak position shift is observed. It can be explained by the Fe is interstitial in the TiO_2 matrix.

The sensing test of pure anatase TiO_2 nanoparticles and nanoparticles with doping on explosive vapor such as DNT has been performed. As shown in Figure 6.6, the conductivity of V-doped TiO_2 and Fe-doped TiO_2 is higher than that of pure anatase TiO_2 at room temperature. Also, a relative faster response to DNT has been observed after nanoparticles doped by transition metals, V and Fe. This can be explained that the substitutional Ti by V or interstitial Fe in cationic positions results in a charge imbalance, which creates oxygen vacancies [146].

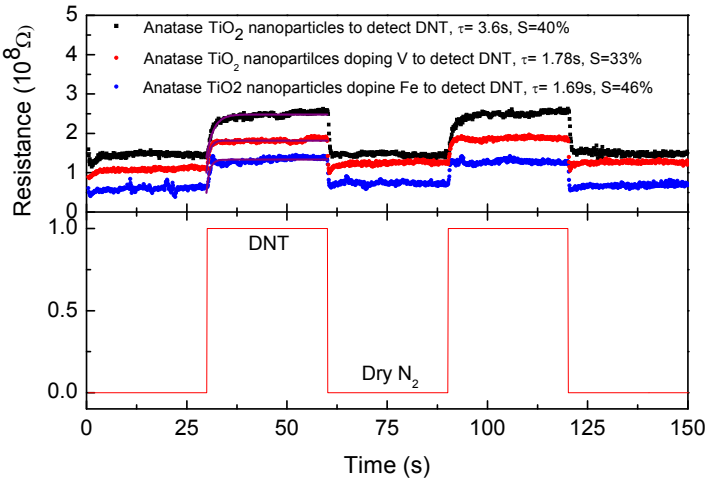

Figure 6.6 Sensing response to DNT with anatase TiO_2 nanoparticles without and with doped by V and Fe at room temperature.

It is interested to notice that the sensitivity to DNT shows decrease after anatase TiO_2 nanoparticles doped by V but has increase after anatase TiO_2 nanoparticles doped by Fe. In order to further understand the reason, a sensing test to saturated water vapor has been carried out. As indicated in Figure 6.7, the sensitivity of water vapor based on doped TiO_2 nanoparticles is slightly decreased. These results may show that the substitution of Ti by V can lead to lower concentration of Ti^{3+} to form Ti-OH. While, in Fe doped TiO_2, Fe is interstitial in the TiO_2 and then introduces extrinsic defects which can lead to a shift of Fermi level and then causes the change of the electrical properties of TiO_2. The detailed reason regarding the Fe-TiO_2 still needs to study. Going back to the sensing mechanism of TiO_2 to explosive vapors, surface Ti-OH on TiO_2 is an important functional group to effectively interact with nitro groups in explosives. In this case, doping transition metals in TiO_2 provides a way to reduce the cross-interference of humidity. This is because cationic doping of TiO_2 such as V not only can modify the

concentration of Ti^{3+}-OH but also, like Fe doping, could affect the conduction band of TiO_2 by either shifting the edge of the conduction band to be more positive, or introducing new electron states in the band gap at the position near to the conduction band bottom [147-149]. The UV-visible spectra shown in Figure 6.8 prove that the doping of TiO_2 with the transition metals such Fe and V can shift the adsorption onset of TiO_2 from UV to visible region [150]. All the effect can result in the photocatalytic water splitting of TiO_2 under visible light and a less sensitive to environmental humidity. Figure 6.9 shows the sensing response to saturated water vapor based on V doped and Fe doped TiO_2, respectively. The sensitivity of TiO_2 to water vapor, in particular, V-TiO_2 shows a very obvious decrease under visible light illumination.

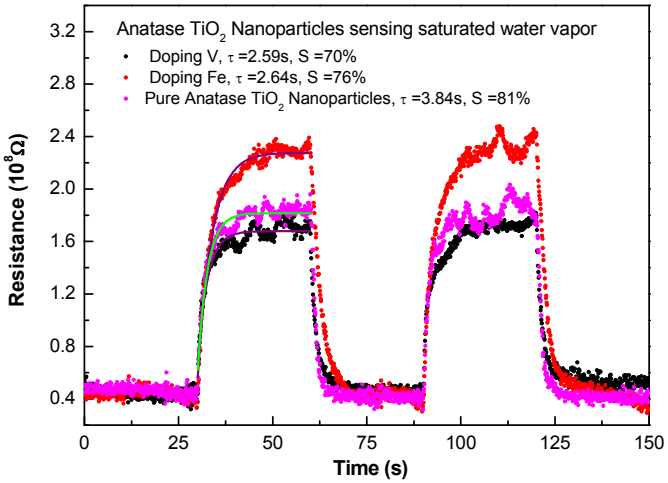

Figure 6.7 Sensing test on saturated water vapor based on anatase TiO_2 nanoparticles and V or Fe doped TiO_2 nanoparticles.

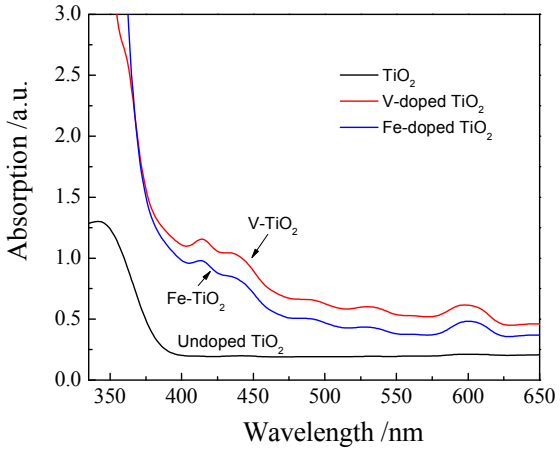

Figure 6.8 Optical absorption spectra of undoped TiO_2, Fe-TiO_2, and V-TiO_2.

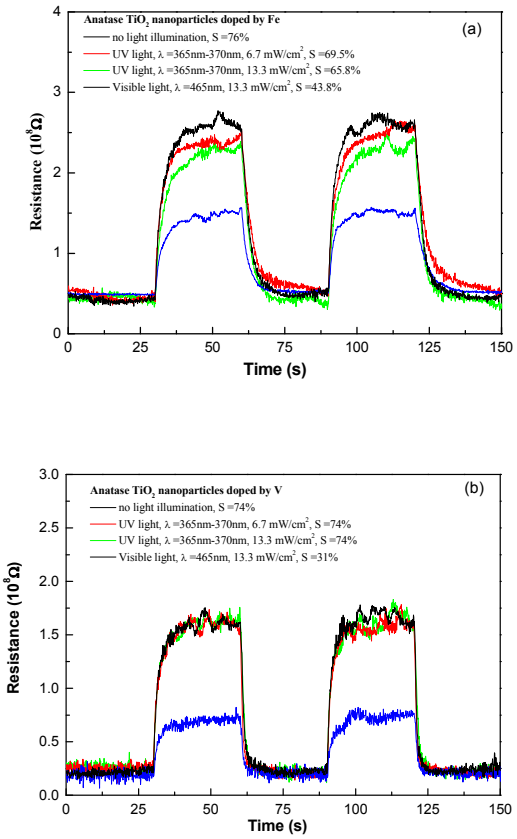

Figure 6.9 Sensing test on saturated water vapor based on doped anatase TiO_2 nanoparticles under UV and visible light illumination; (a) Fe-TiO_2; (b) V-TiO_2.

6.4 Microstructure effect

In order to understand the effect of microstructure on the sensor performance, we purposely prepared TiO_2(B) nanoparticles and compared the sensing response between the pure TiO_2(B) nanoparticles and nanowires.

TiO_2(B) nanoparticles were prepared by firstly dispersing 0.72 g of Ti powder in a mixture of 70 mL of H_2O_2 and 20 mL of $NH_3 \cdot OH$ and keeping stirred in an ice-water bath (0 °C) for about 3 h to allow a complete dissolution of Ti powder, and then adding 1.71 g of glycolic acid to the solution and keeping at 80 °C for another 3-4 h. The as-prepared precursor solution was then transferred to an autoclave for hydrothermal growth at 160 °C for 5 h. The resultant precipitate was washed with DI-water and ethanol before being dried at 100 °C. The sensor film was prepared on glass substrate and annealed at 300 °C for 1 h.

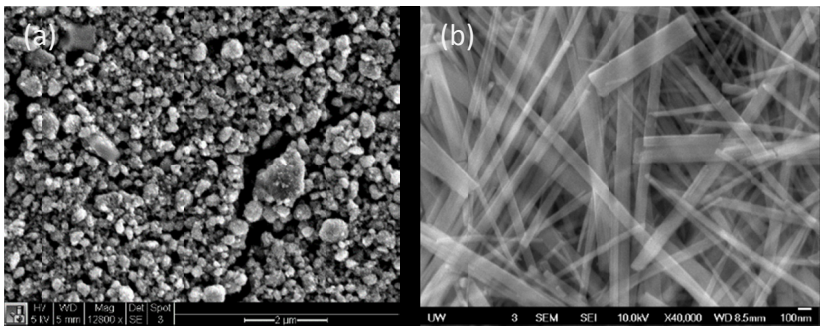

Figure 6.10 SEM images TiO_2(B) nanoparticles (a) and nanowires (b).

The fabrication of single crystalline pure TiO_2(B) nanowires is similar to that for the synthesis of TiO_2(B) dominant nanowires described in Chapter 2 except the temperature for hydrothermal growth being 200 ºC, higher than 180 ºC used for the latter. Figure 6.10 is the SEM images of

pure TiO_2(B) nanoparticles and nanowires. As we can see, the diameter of nanoparticle is ranging from 20 nm to 1 μm. Comparing to the SEM image of TiO_2(B) nanowires, nanoparticle thin film is more dense.

Shown in Figure 6.11 (a) is XRD pattern of as-synthesized TiO_2(B) nanosparticles, and (b) is XRD pattern of as-synthesized TiO_2(B) nanoswires, which are in line with the pattern of pure TiO_2(B) in literature[151].

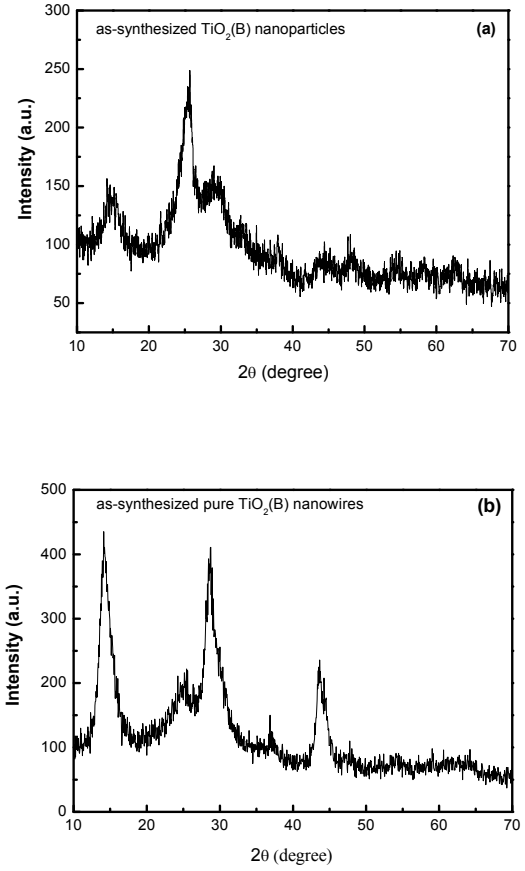

Figure 6.11 XRD patterns of as-synthesized pure TiO_2(B) nanoparticles(a) and the XRD pattern of TiO_2(B) nanowires(b).

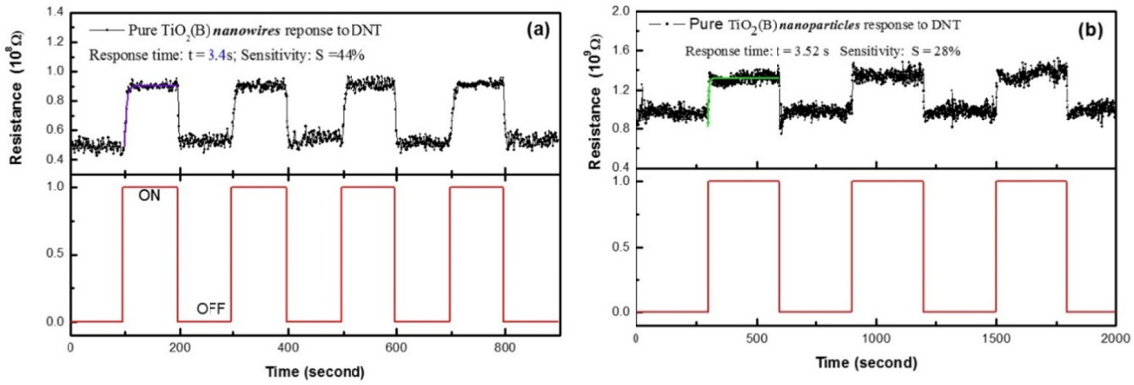

Figure 6.12 Sensing response to DNT based on (a) pure TiO_2(B) nanowires; (b) pure TiO_2(B) nanoparticles.

Figure 6.12 shows a comparison of sensing response to DNT between TiO_2(B) nanoparticles and TiO_2(B) nanowires. Nanowires exhibit a quicker response and higher sensitive to DNT vapor (3.2 s) than that of nanoparticles (4.1 s). This improvement is because nanowires not only have higher surface-to-volume ratios but also higher porous structures as seen in SEM images. These advantages can participate in gas diffusion and therefore cause rapid gas response.

6.5 Crystal Phase Effect

The sensing properties can be tailored by different crystal phases of TiO_2. This is because different crystal phase will have different crystal facets exposed on the surface of a nanocrystal and result in different surface structure and different surface reactivity with different adsorption abilities. For example, considering ammonia adsorption, anatase TiO_2 {001} facets are highest reactive [152] and rutile {110} facets are the most reactive facets [153]. Recently, Guo *et al*. studied that facets {100} of TiO_2(B) are more reactive to adsorb ammonia. Therefore, it is important to know the effect of TiO_2 crystal phase on its sensing performance. It benefits better

understanding of sensing mechanism based on TiO_2(B). Here, different crystal phases of TiO_2 nanoparticles were prepared to perform the sensing test on explosives. In addition, sensing tests based on pure TiO_2(B) nanoparticles and anatase/TiO_2(B) bicrystalline nanoparticles to DNT are compared.

The fabrication of pure TiO_2(B) nanoparticles was already described in section 6.3. It is worth being addressed that the nanoparticles with pure TiO_2(B) phase was obtained by annealing film samples at 300 °C. The preparation of anatase/TiO_2(B) bicrystalline nanoparticles was achieved with the same method except that the temperature for film annealing was at 450 °C, higher than the 300 °C for pure TiO_2(B) nanoparticles. Annealing at high temperature such as 450 °C leads to a partial conversion of the TiO_2 from TiO_2(B) to anatase phase, as what are shown in Figure 6.11(a) mentioned above and Figure 6.13 listed below. In this section, we mainly describe the fabrication of anatase and rutile TiO_2 nanoparticles. Both the anatase and rutile TiO_2 nanoparticles were prepared with a sol-gel based hydrothermal method. For the synthesis of anatase TiO_2 nanoparticles, 5 mL of TTIP was dispersed into 10 mL of HAc, and to this mixture was 5 mL of DI-water added. The resultant sol was transferred into an autoclave for hydrothermal growth at 225 °C for 24 h. The fabrication of rutile TiO_2 nanoparticle was done by however using HCl instead of HCl. Typically, 5 mL of HCl was dissolved into 20 mL of DI-water, and 5 mL of TTIP was then added into the HCL solution, leading to the formation of a clear TiO_2 sol. A hydrothermal treatment at 225 °C for 24 h was then carried out to result in the formation of rutile TiO_2 nanoparticles. Shown in Figures 6.13 to 6.15 are the SEM images and XRD patterns for anatase TiO_2 nanoparticles, rutile TiO_2 nanoparticles, and anatase/TiO_2(B) bicrystalline nanoparticles, respectively. Beside different crystal phase of TiO_2, the particle size of rutile is much larger than anatase TiO_2 nanoparticle.

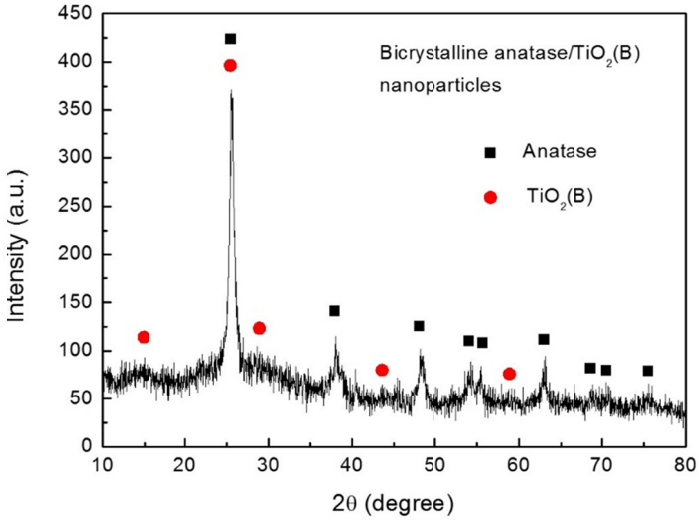

Figure 6.13 XRD pattern of anatase/TiO_2(B) bicrystalline nanoparticles

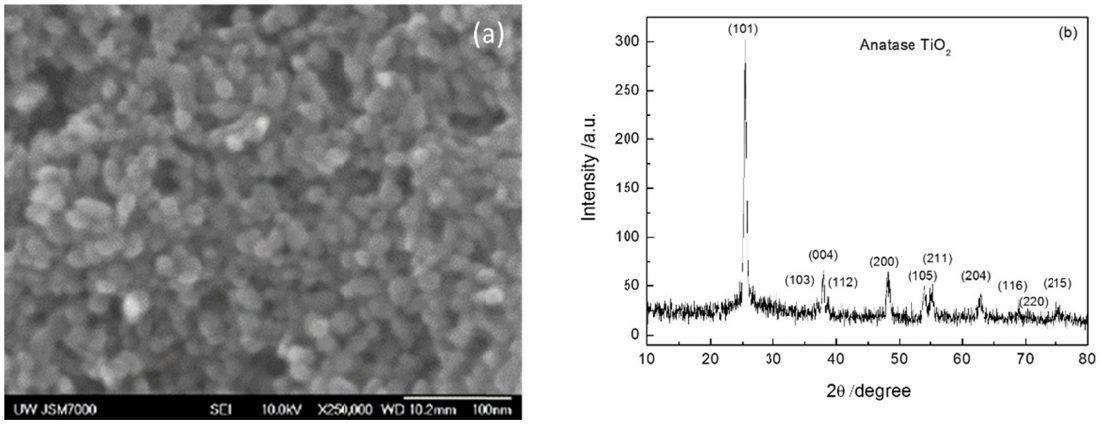

Figure 6.14 SEM image and XRD pattern of anatase TiO_2 nanoparticles.

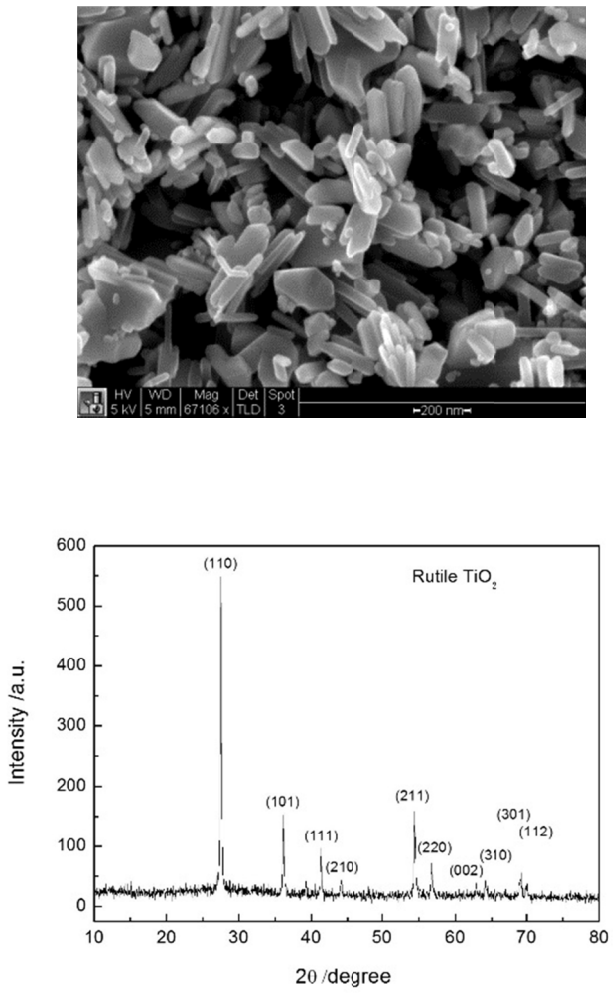

Figure 6.15 SEM image and XRD pattern of rutile TiO_2 nanoparticles

Figure 6.16 shows sensing test on DNT (100 ppb) based on different crystal phase of TiO_2 nanoparticles and a comparison of sensing response to DNT vapor based on pure TiO_2(B) nanoparticles and anatase/TiO_2(B) bicrysalline nanoparticles have been done. It indicates that anatase/TiO_2(B) bicrystalline nanoparticles have the highest sensitivity and fastest response compared to other crystal phase. Also, the conductivity of anatase/TiO_2(B) bicrystalline nanoparticles is 10 times lower than that of pure TiO_2(B) nanoparticles. The reason of the sensing performance of anatase/TiO_2(B) bicrystalline nanoparticles superior to the performance

of pure TiO_2(B) nanoparticles is still under investigation. However, according to the literatures [58, 154, 155], the anatase/TiO_2(B) bicrystalline nanoparticles can show enhanced charge transport efficiency. It might cause a relative faster response of anatase/TiO_2(B) bicrystalline nanowires to DNT molecules.

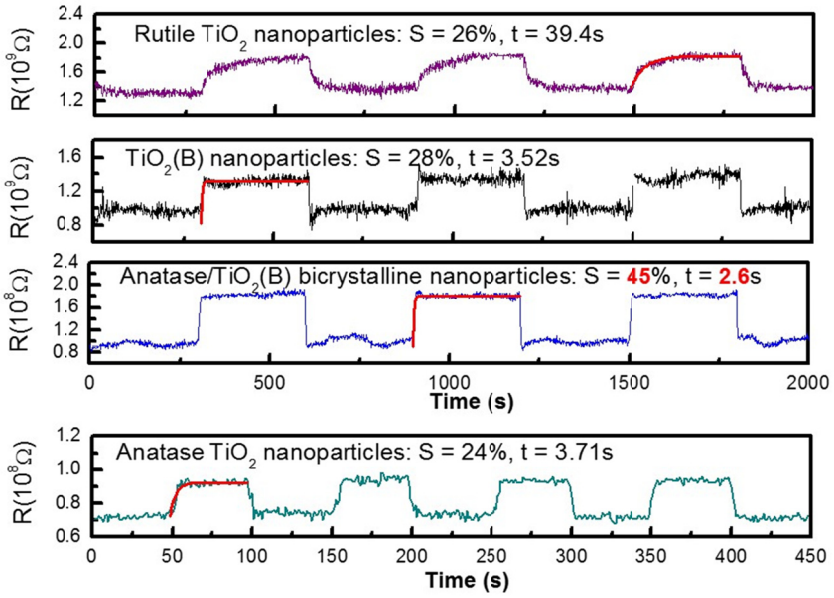

Figure 6.16 Sensing test on DNT based on different crystal phase of TiO_2 nanoparticles at room temperature.

6.6 Other materials

1) ZnO nanowires and TiO_2 coated ZnO nanowires

ZnO nanowires were prepared with a precipitation method [156]. 1.1 g of $ZnAc{\cdot}2H_2O$ was dissolved in 200 mL of ethanol to form Solution 1, and 4 g of NaOH was dissolved in 100 mL of ethanol to form Solution 2. These two solutions were then mixed and kept in an oven at 100 °C

for 24 h in a sealed bottle, yielding white precipitate at the bottle bottom. The precipitate was washed with Di-water and ethanol for several times and dried at 100 °C. The sensor film was prepared on glass substrate and annealed at 350 °C for 1 h.

To coat TiO_2 onto ZnO nanowires, a TiO_2 sol containing 0.742 g of $(NH_4)_2TiF_6$ and 0.618 g of H_3BO_3 in 50 mL of DI-water was prepared. ZnO nanowire film deposited on glass substrate annealed at 350 °C was then immersed into the TiO_2 sol for 30 min. After the film was dried at room temperature, it was heated at 450 °C for 1 h to convert the TiO_2 from amorphous to crystalline phase.

Shown in Figures 6.17 and 6.18 are the SEM images ZnO nanowires and TiO_2 coated ZnO nanowires. The as-fabricated ZnO nanowire thin film also shows an interconnected three-dimensional mesh of randomly orientated nanowires.

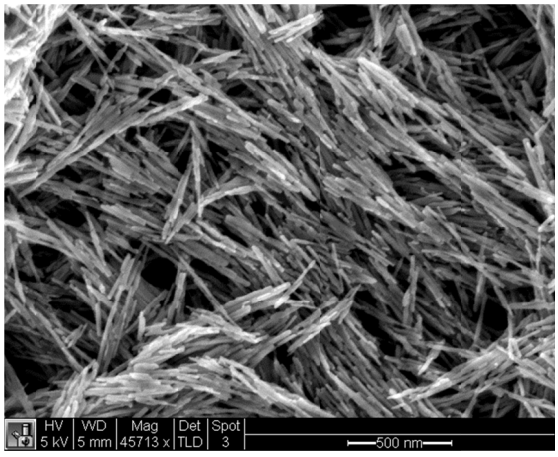

Figure 6.17 SEM image showing an interconnected 3D mesh structure of a ZnO thin film.

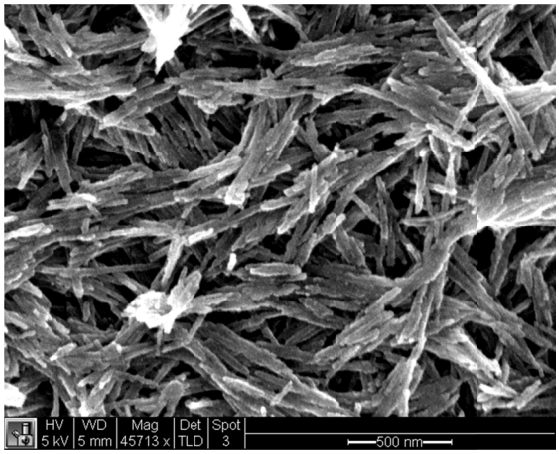

Figure 6.18 SEM image showing an interconnected 3D mesh structure of a TiO_2 coated ZnO thin film

Zinc Oxide (ZnO) like other metal oxides, is a chemically and thermally stable n-type semiconductor with large bandgap energy of 3.37eV and widely applied in gas sensors. Generally, the sensing mechanism based on nanostructured ZnO gas sensor involves the chemisorption of oxygen on the oxide surface, followed by charge transfer during the reaction between chemisorbed oxygen and target gas molecules, changing the surface resistance of the sensor element [157].

The sensing test to DNT vapor at room temperature based on ZnO nanowires is shown in Figure 6.19. Compared to TiO_2(B) nanowires to DNT (Figure 6.3a), ZnO nanowires show very weak response to DNT. This result double confirms that the chemisorption of high electronegative explosive compounds onto TiO_2(B) nanowires is mainly due to the Ti-OH groups on TiO_2 (B) surface.

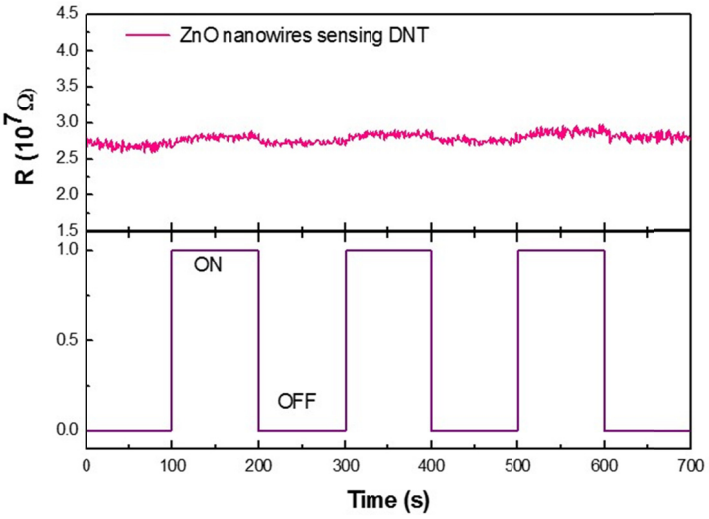

Figure 6.19 Sensing response to DNT, 100 ppb based on ZnO nanowires at room temperature.

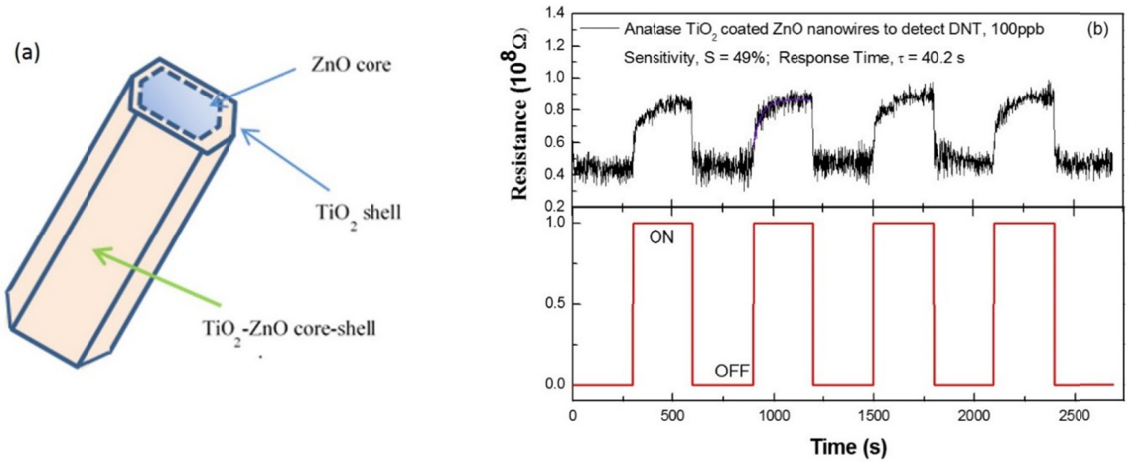

Figure 6.20 Schematic draw of TiO_2 coated ZnO nanowires. (a) structure of TiO_2 coated ZnO nanowires, and (b)sensing response to 100 ppb DNT at room temperature based on anatase TiO_2 coated ZnO nanowires.

However, ZnO nanowires have much higher conductivity, which can further reduce the sensor power consumption. Based on these findings, a novel explosive sensor device can be built by using TiO_2 coated ZnO nanowires to form ZnO-TiO_2 core-shell structured nanotubes in Figure 6.20(a). The sensing test to DNT based on such core shell structure is shown in Figure 6.20(b).

2) V_2O_5 nanowires

V_2O_5 nanowires were chosen to do the explosive sensing test due to the reason that it is also a transition metal oxide like TiO_2 and widely used in catalytic application and gas sensing devices [158]. V_2O_5 is an n-type semiconductor with an electronic conductivity in the order of 0.5 Scm^{-1} at room temperature. The charge transport takes place in electron hopping between V^{IV} (impurities) and V^{V} centers. This property makes V_2O_5 is well suited for the construction of functional materials or novel devices, which can be operated under ambient conditions. The purpose of this experiment to exam if other transition metal oxide such as V_2O_5 can exhibit similar surface reaction like Ti^{4+} reducing to Ti^{3+} and form surface Ti-OH groups in TiO_2 when is exposed by high electronegative explosives.

V_2O_5 nanowires were synthesized with a hydrothermal method [159]. Typically, 0.364 g of V_2O_5 powder was dispersed in 30 mL of DI-water, and to this solution was added 5 mL of H_2O_2, resulting in the formation of a clear V_2O_5 sol. The V_2O_5 sol was transferred to an autoclave for hydrothermal growth at 205 °C for 3 days. After hydrothermal reaction, a dark grey gel was formed. The gel was dried at 100 °C for 24 h and then dispersed in ethanol for the preparation of sensor film, which was followed by a thermal treatment at 500 °C for 1 h. Shown in Figure

6.21(a) is the SEM image of the V_2O_5 nanowires. Sensing test on DNT based on V_2O_5 is shown in Figure 6.21(b).

Although the V_2O_5 nanowires in SEM image in Figure 6.21(a) have very porous structure and even larger surface-to-volume ration than that of TiO_2 nanowires, it still shows a very week response to DNT vapor in Figure 6.21(b) under the same experimental condition as TiO_2 nanowires had. As an n-type semiconductor like ZnO and TiO_2, V_2O_5 nanowires should interact with high electronegative compounds like explosive molecules. Compared to the sensing response of ZnO nanowires to DNT, V_2O_5 nanowires show a little bit higher response which may be attributed to the variable valence of V (V^{4+} and V^{5+}), similar to the case of TiO_2, as discussed previously, the valance of which is also variable. However, based on the sensing result, this kind of electron transfer is much less efficient than the transfer between nitro-group in explosives and hydroxyl groups in coordinated with Ti in TiO_2.

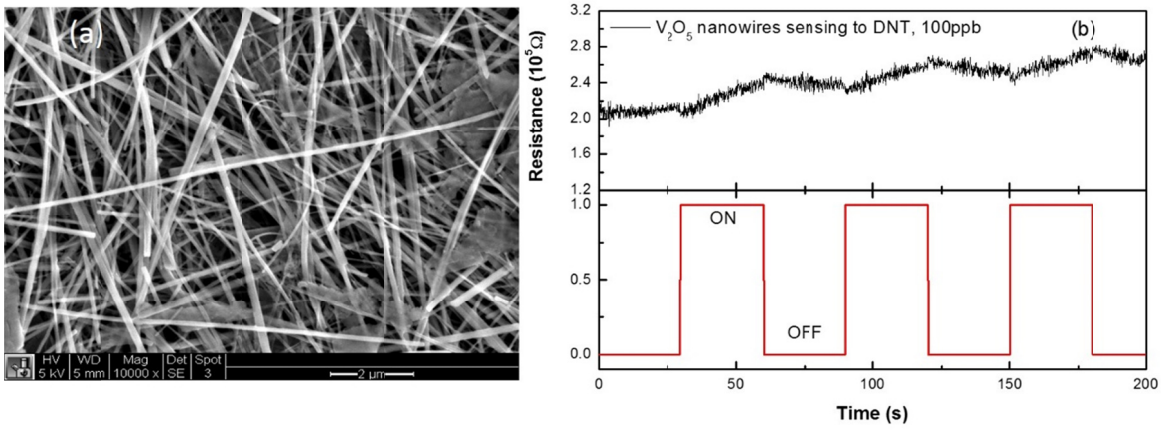

Figure 6.21 SEM image and sensing test on DNT vapor based on V_2O_5 nanowires. (a) SEM image of V_2O_5 nanowires, and (b) sensing test on DNT vapor at room temperature.

3) CdS nanowires

CdS nanowires were synthesized using a hydrothermal method with a precursor solution containing 1 g of $CdAc{\cdot}2H_2O$ and 0.24 g of S in 60 mL of ethylenediamine [160]. The temperature for hydrothermal growth is 200 °C while the duration is 10 h. After reaction, the CdS nanowires were collected by centrifuging and washed with toluene and ethanol to get rid of residual S. The product was then dried at 60 °C for 24 h. The sensor film was deposited onto glass substrate followed by a thermal treatment at 400 °C for 1 h in N_2. Shown in Figure 6.22 is the SEM image of the as-prepared CdS nanowires.

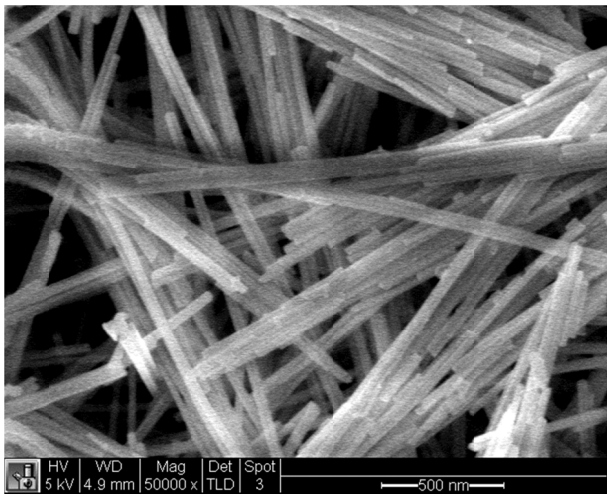

Figure 6.22 SEM image of CdS nanowires.

Sensing test on DNT vapor based on CdS nanowires is shown in Figure 6.23. Our initial motivation of employing CdS nanowires is to check (1) if they can have the capability to detect explosives with the considerations that the CdS nanowires have the similar nanostructure to the TiO_2(B) nanowires which we have studied, and (2) if non oxides may possibly respond explosives. However, from Figure 6.23, we can see that there is no response to DNT vapor when

the CdS nanowires were used as sensing material for explosive detection. We can therefore conclude that (1) the one dimensional nanostructure is not the inherent reason for the good response of TiO_2(B) nanowires to explosives that we investigated previously, and (2) the oxides of titanium as well as some of other oxides such as ZnO and SiO_2 are advantageous in responding explosives (However, the oxides of titanium are far superior to other metal oxides).

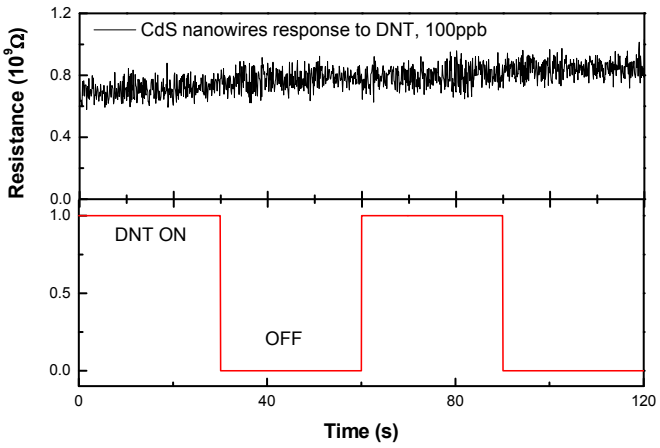

Figure 6.23 Sensing response of CdS nanowires to DNT.

6.7 Conclusions

In this Chapter, we systematically studied:

1) The factors of influence on the sensing performance on the explosive detection based on nanostructured TiO_2, including microstructure, surface modification, and crystal phases. We can see that nanowires due to higher surface area and more porous structure show better response than nanoparticles. Surface modification including composite thin film or doping can change the electrical properties of TiO_2 and then result in an improvement of sensing response. Different crystal phase has different crystal facets which can affect TiO_2 surface energy to adsorb

explosive molecules and such cause a change of sensitivity and response time. We observed that anatase/TiO_2(B) bicrystalline nanowires shown the best sensing response to explosive and doping or Au/TiO_2(B) nanocomposite can further improve TiO_2 sensing properties.

2) Other nanostructured semiconductors such as ZnO, V_2O_5, and CdS nanowires as sensor material to detect explosives. Oxide nanowires show very week response to DNT and non-oxide nanowires have no response to DNT at all. These results further confirm that the unique surface hydroxyl groups (Ti-OH) in nanostructure TiO_2 play a very important role in efficiently response to nitro-related explosives.

6.8 Prospective research

Prospective Research 1:

Our study demonstrates that TiO_2 is a very promising material for explosive detection. As a follow-up of the already well conducted study on the material issues, the next work is suggested to be focused on the development of sensor device with these materials for possibly practical application. A potential approach is shown in Figure 6.24, in which TiO_2 is coated on either porous SiO_2 or glass based on our investigation of TiO_2 coated ZnO nanowires, which present decent response to explosives. Porous SiO_2 may be created using an etching method to be produced on a silicon-based substrate. A coating treatment of the porous silicon with TiO_2 will allow the integration of explosive sensor into a chip.

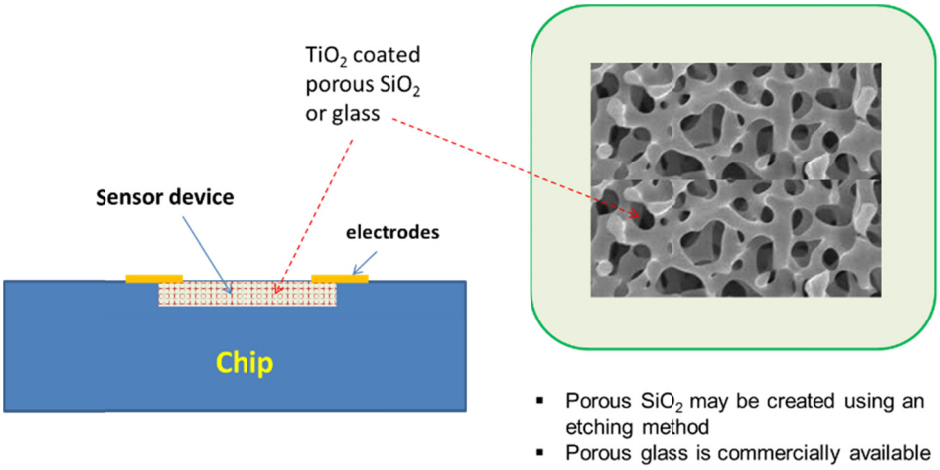

Figure 6.24 A proposed structure to integrate TiO_2-based explosive sensor into a chip.

Prospective Research 2:

Our previous study has clearly revealed that the material consisting of a mixed phases of anatase and TiO_2(B) or the TiO_2(B) mixed with gold nanoparticles present much better performance for the detection of explosives than the TiO_2(B) alone. It is speculated that the TiO_2(B) plays a role in providing suitable sites for explosive adsorption while the anatase TiO_2 or gold nanoparticles may possibly contribute to enhancing the electron transport in some way. With this consideration, to boost the sensing response of TiO_2(B), an optimal structure which is comprised of TiO_2(B)-coated anatase TiO_2 nanowires with gold nanoparticles adsorbed on the surface is shown in Figure 6.25. To achieve such a core-shell structure, it is suggested that the anatase TiO_2 nanowire core can be prepared using an electrospinning method, the formation of a TiO_2(B) shell can be achieved with either the development of TiO_2(B) sol for coating or the fabrication through a hydrothermal method. The adsorption of gold nanoparticles can be accomplished by treating the

TiO_2(B)-coated anatase TiO_2 nanowires with a chloroauric acid ($HAuCl_4$) solution followed by a reduction reaction in NaOH solution.[161]

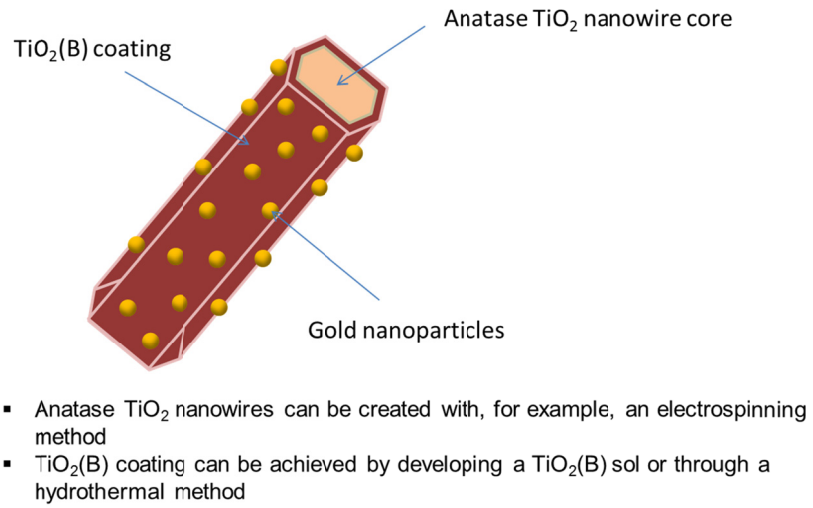

Figure 6.25 Core-shell structured TiO_2 nanowires with gold nanoparticles adsorbed.

BIBLIOGRAPHY

[1] L.Senesac and T.G.Thundat, "Nanosensors for trace explosive detection", Materials today, 11, 28, 2008.

[2] R.J. Colton and J.N.Russell, "Counterterrorism. Making the world a safer place", Science, 299, 1324, 2003.

[3] B.C.Dionne, D.P.Roundbehler, E.K.Achter, J.R.Hobbs and D.H.Fine, "Vapor Pressure of Explosives", Journal of Energy Materials, 4, 447, 1986.

[4] L.Senesac and T.G.Thundat, "Nanosensors for trace explosive detection", Materials today, 11, 28, 2008.

[5] A.M.Jimenez, and M.J.Navas, "Chemiluminescence detection systems for the analysis of explosives", Journal of Hazardous Material, 106, 1, 2004.

[6] D. S. Moore, "Instrumentation for trace detection of high explosives", Review of Scientific Instruments, 75, 2499, 2004.

[7] R.C.Phillips, "Training dogs for explosives detection".

[8] J.E.McFee and A.A.Faust, "Nuclear methods for explosive detection", SPIE, Newsroom, DOI: 10.1117/2.1201108.003761, 2011.

[9] G.A.de Nolfo, S.D.Hunter, L.M.Barbier, J.T.Link, S.Son, S.R.Floyd, N.Guardala, M.Skopec and B.Stark, "Gamma-ray imaging for explosive detection", Proceedings of SPIE, 6954, 695404, 2008.

[10] M.C.Kemp, P.F.Taday, B.E.Cole, J.A.Cluff, A.J.Fitzgerald, and W. R. Tribe, "Security applications of terahertz technology," Proceedings of SPIE, 5070, 44, 2003.

[11] Michael C. Kemp, "Explosives Detection by Terahertz Spectroscopy—A Bridge Too Far?", IEEE transactions on terahertz science and technology, 1, 282, 2011.

[12] A.Rose, Z.Zhu, C.F.Madigm, T.M.Swager and V.Bulovic, "Sensitivity gains in chemosensing by lasing action in organic polymers", Nature, 434, 876, 2005.

[13] J.V.Goodpaster and V.L.McGuffin, "Fluorescence quenching as an indirect detection method for nitrated explosives", Analytical Chemistry, 73, 2004, 2001.

[14] E.J.Houser, T.E.Misna, V.K.Nguyen, R.Chung, R.L.Mowery and R.A.McGill, "Rational materials design of sorbent coatings for explosives: applications with chemical sensors", Talanta, 54, 469, 2001.

[15] M.Kirchner, E.Matisova, S.Hrouzkova and R.Huskova, "Fast GC and GC-MS analysis of explosives", Petroleum & Coal, 49, 72, 2007.

[16] F.Rock, N.Barsan and U.Weimar, "Electronic Nose: Current Status and Future Trends", Chemical Reviews, 108, 705, 2008.

[17] Q.L.Fang, J.L.Geng, B.H.Liu, D.M.Gao, F.Li, Z.Y.Wang, G.J.Guan and Z.P.Zhang, "Inverted Opal Fluorescent Film Chemosensor for the Detection of Explosive Nitroaromatic Vapors through Fluorescence Resonance Energy Transfer", Chemistry – A European Journal, 15, 11507, 2009.

[18] F.Rock, N.Barsan and U.Weimar, "Electronic Nose: Current Status and Future Trends", Chemical Reviews, 108, 705, 2008.

[19] R.G.Ewing and C.J.Miller, "Detection of Volatile Vapors Emitted from Explosives with a Handheld Ion Mobility Spectrometer", Field Analytical Chemistry & Technology, 5, 215, 2001.

[20] X.J.Huang and Y.K.Choi, "Chemical sensors based on nanostructured materials", Sensors and Actuators B: Chemical, 122, 659, 2007.

[21] A.D.Aguilar, E.S.Forzani, M.Leright, F.Tsow, A.Cagan, R.A.Iglesias, L.A.Nagahara, I.Amlani, R.Tsui and N.J.Tao, "A hybrid nanosensor for TNT vapor detection", Nano Letters, 10, 380, 2010.

[22] Y.H.Gui, C.S.Xie, J.Q.Xu and G.Q.Wang, "Detection and discrimination of low concentration explosives using MOS nanoparticle sensors", Journal of Hazardous Material, 164, 1030, 2009.

[23] M. W. Ahn, K. S. Park, J. H. Heo, J.G.Park, D.W.Kim, K.J.Choi, J.H.Lee and S.H.Hong, "Gas sensing properties of defect-controlled ZnO-nanowire gas sensor," Applied Physics Letters, 93, 263103, 2008.

[24] O.K.Varghese and C.A.Grimes, "Metal Oxide Nanoarchitectures for Environmental Sensing", Journal of Nanoscience and Nanotechnology, 3, 277, 2003.

[25] A.Rothschild and Y.Komem, "The effect of grain size on the sensitivity of nanocrystalline metal-oxide gas sensors", Journal of Applied Physics, 95, 6374, 2004.

[26] N.Barsan and U.Weimar, "Fundametals of Metal Oxide Gas Sensors", The 14th Internaltional Meeting on Chemical Sensors, IMCS 2012, 618.

[27] A.Biaggi-Labiosa, F.Sola, M.Lobron-Colon, L.J.Evans, J.C.Xu, G.W.Hunter, G.M.Berger and J.M.Gonzalez, "A novel methane sensor based on porous SnO_2 nanorods: room temperature to high temperature detection", Nanotechnology, 23, 455501, 2012.

[28] M.E.Franke, T.J. Koplin and U.Simon, "Metal and Metal Oxide Nanoparticles in Chemiresistors: Does the Nanoscale Matter?", Small, 2, 36, 2006.

[29] W.H.Brattain and J.Bardeen, "Surface properties of Germanium", Bell System Technical Journal, 32, 1, 1953.

[30] T.Seiyama, A.Kate, K.Fujiishi and M.Nagatani, "A New Detector for Gaseous Components Using Semiconductive Thin Films", Analytical Chemistry, 34, 1502, 1962.

[31] A.L.Linsebigler, G. Lu and J.T.Yates, "Photocatalysis on TiO_2 surfaces: principles, mechanisms, and selected results". Chemical Reviews, 95, 735, 1995.

[32] K. Gesheva, A. Szekeres and T. Ivanova, "Optical properties of chemical vapor deposited thin films of molybdenum and tungsten based metal oxides", Solar Energy Materials and Solar Cells, 76, 563, 2003.

[33] T.Kamegawa, R.Takeuchi, M.Matsuoka and M. Anpo, "Photocatalytic oxidation of CO with various oxidants by Mo oxide species highly dispersed on SiO2 at 293 K", Catalysis Today, 111, 248, 2006.

[34] I.K. Battisha, "Visible up-conversion photoluminescence from IR diode-pumped SiO_2–TiO_2 nano-composite films heavily doped with Er^{3+}-Yb^{3+} and Nd^{3+}-Yb^{3+}. Journal of Non-Crystalline Solids, 353, 1748, 2007.

[35] Z.Yang, L.-M. Li, Q.Wan, Q.-H.Liu and T.-H Wang, “High-performance ethanol sensing based on an aligned assembly of ZnO nanorods”, Sensors and Actuators B: Chemical, 135, 57, 2008.

[36] C.Wang, X.Chu, and M.Wu, “Detection of H2S down to ppb levels at room temperature using sensors based on ZnO nanorods”, Sensors and Actuators B: Chemical, 113, 320, 2006.

[37] G.Sakai, N.Matsunaga, K.Shimanoe and N.Yamazoe, “Theory of gas-diffusion controlled sensitivity for thin film semiconductor gas sensor”, Sensors and Actuators B: Chemical, 80, 125, 2001.

[38] N.Matsunaga, G.Sakai, K.Shimanoe and N.Yamazoe, “Formulation of gas diffusion dynamics for thin film semiconductor gas sensor based on simple reaction–diffusion equation”, Sensors and Actuators B: Chemical, 96, 226, 2003.

[39] M.Hafeez, U. Manzoor and A.S.Bhatti A.S, “Morphology tuned ZnS nanostructures for hydrogen gas sensing”, Journal of Materials Science: Materials in Electronics, 22, 1772, 2011.

[40] Z.Bielecki, J.Janucki, A.Kawalec., J.Mikolajczyk, N.Palka, M.Pasternak, T.Pustelny, T.Stacewicz and J.Wojtas, “Sensors and Systems for the Detection of Explosive Devices – An Overview”, Metrol.Meas.Syst., XIX, 3, 2012.

[41] G.Korotcenkov, “Metal oxides for solid-state gas sensors: What determines our choice?”, Materials Science and Engineering: B, 139, 1, 2007.

[42] E.S.Snow, F.K.Perkins, E.J.Houser, S.C.Badescu and T.L.Reinecke, “Chemical Detection with a Single-Walled Carbon Nanotube capacitor”, Science, 307, 1942, 2005.

[43] S.Banerjee, S.K.Mohapatra, M.Misra and I.B.Mishra, “The detection of improvised nonmilitary peroxide based explosives using a titania nanotube array sensor”, Nanotechnology, 20, 075502, 2009.

[44] Y.Engel, R.Elnathan, A.Pevzner, G.Davidi, E.Flaxer and F.Patolsky, “Supersensitive detection of explosives by silicon nanowire arrays”, Angewandte Chemie International Edition, 49, 6830, 2010.

[45] D.Wang, A.Chen, Q.Zhang and G.Cao, “Room-temperature chemiresistive effect of TiO_2-B nanowires to nitroaromatic and nitroamine explosives”, IEEE Sensors Journals, 11, 1352, 2011.

[46] D.Wang, A.Chen, S.-H.Jang, H.-L.Yip and A. K.-Y. Jen, “Sensitivity of titania(B) nanowires to nitroaromatic and nitroamino explosives at room temperature via surface hydroxyl groups”, Journal of Materials Chemistry, 21, 7269, 2011.

[47] D.Wang, A.Chen, S.-H.Jang, J.Davies and A. K.-Y. Jen, “The effect of dipole moment and electron deficiency of analytes on the chemiresistive response of TiO_2(B) nanowires”, Analyst, 136, 4179, 2011.

[48] D.Wang, H.Sun, A.Chen, S.-H.Jang, A.K.-Y.Jen and A.Szep, “Chemiresistive response of silicon nanowires to trace vapor of explosives”, Nanoscale, 4, 2628, 2012.

[49] D.Wang, A.Chen and A.K.-Y.Jen, “Reducing cross-sensitivity of TiO_2-(B) nanowires to humidity using ultraviolet illumination for trace explosive detection”, Physical Chemistry Chemical Physics, 15, 5017, 2013.

[50] F. Millot, M.G.Blanchin, R.Tetot, J.F.Marucco, B.Poumellec, C.Picard and B.Touzelin, "High temperature nonstoichiometric rutile TiO_{2-x}", Progress in Solid State Chemistry, 17, 263, 1987.

[51] L.Sun, H.Zhao, S.Gao and J.Zhao, "Preparation and gas-sensing property of a nanosized titania thin film towards alcohol gases", Sensors and Actuators B: Chemical, 114, 387, 2006.

[52] O.K.Varghese, D.Gong, M.Paulose, K.G.Ong and C.A.Crimes, "Hydrogen sensing using titania nanotubes", Sensors and Actuators B: Chemical, 93, 338, 2003.

[53] A.Rothschild, F.Edelman, Y.Komem and F.Cosandey, "Sensing behavior of TiO_2 thin films exposed to air at low temperatures", Sensors and Actuators B: Chemical, 67, 282, 2000.

[54] A.Fujishima and X.Zhang, "Titanium dioxide photocatalysis: present situation and future approaches", Comptes Rendus Chimie, 9, 750, 2006.

[55] M.Gratzel, "Photoelectrochemical cells", Nature, 414, 338, 2001.

[56] N.Ruzycik, G.S.Herman, L.A.Boatner and U.Diebold, "Scanning tunneling microscopy study of the anatase (1 0 0) surface", Surface Science, 828, A4.6.1, 2005.

[57] A.R.Armstrong, G.Armstrong, J.Canales, and P.G.Bruce, "TiO_2-B nanowires", Angewandte Chemie International Edition, 43, 2286, 2004.

[58] Z.Yang, G.Du, Z.Guo, X.Xu, Z.Chen, T.Guo, N.Sharma and H.Liu, "TiO_2(B)@anatase hybrid nanowires with highly reversible electrochemical performance", Electrochemistry Communications, 13, 46, 2011.

[59] S. Pavasupree, Y. Suzuki, S. Yoshikawa and R. Kawahata, "Synthesis of titanate, TiO_2 (B), and anatase TiO_2 nanofibers from natural rutile sand", Journal of Solid State Chemistry, 178, 3110, 2005.

[60] R.Yoshida, Y.Suzuki and S.Yoshikawa, "Syntheses of TiO_2(B) nanowires and TiO_2 anatase naowires by hydrothermal and post-heat treatment", Journal of Solid State Chemistry, 178, 2179, 2005.

[61] A.R.Armstrong, G.Armstrong, J.Canales, R.Garcia and P.G.Bruce, "Lithium-Ion Interaction into TiO_2-B Nanowires", Advanced Materials, 17, 862, 2005.

[62] G. Armstrong, A. R. Armstrong, J. Canales, P. G. Bruce, "Nanotubes with the TiO_2-B structure", Chemical Communications, 19, 2454, 2005.

[63] Y. Q. Wang, G. Q. Hu, X. F. Duan, H. L. Sun, Q. K. Xue, "Microstructure and formation mechanism of titanium dioxide nanotubes", Chemical Physics Letters, 365, 427, 2002.

[64] J.Park, S.Bauer, P.Schmuki and K.Mark, "Narrow window in nanoscale dependent activation of endothelial cell growth and differentiation on TiO_2 nanotube surface", Nano Letters, 9, 3157, 2009.

[65] F.Guilemot, M.C.Porte, C.Labrugere, and Ch.Baquey, "Ti^{4+} to Ti^{3+} conversion of TiO_2 uppermost layer by low-temperature vacuum annealing: interest for titanium biomedical applications", Journal of Colloid and Interface Science, 255, 295, 2002.

[66] H.Liu, H.T.Ma, X.Z.Li, W.Z.Li, M.Wu and X.H.Bao, "The enhancement of TiO_2 photocatalytic activity by hydrogen thermal treatment", Chemosphere, 50, 39, 2003.

[67] A.Sirisuk, E.Klansorn and P.Praserthdam, "Effects of reaction medium and crystallite size on Ti^{3+} surface defects in titanium dioxide nanoparticles prepared by solvothermal method", Catalysis Communications, 9, 1810, 2008.

[68] G.B.Raupp and J.A.Dumesic, "Adsorption of CO, CO_2, H_2, and H_2O on titania surface with different oxidation states", The Journal of Physical Chemistry, 89, 5240, 1985.

[69] T.Berger, M.Sterrer, O.Diwald et al., "Light-induced charge separation in anatase TiO_2 particles", The Journal of Physical Chemistry B, 109, 6010, 2005.

[70] P. A. Pella, "Generator for producing trace vapor concentrations of 2, 4, 6-trinitrotoluene, 2, 4-dinitrotoluene, and ethylene-glycol dinitrate for calibrating explosives vapor detectors", Analytical Chemistry, 48, 1632, 1976.

[71] S. Ahlers, G. Muller, and T. Doll, "A rate equation approach to the gas sensitivity of thin film metal oxide materials", Sensors and Actuators B: Chemical, 107, 587, 2005.

[72] N. R. C. Committee on the Review of Existing and Potential Standoff Explosives Detection Techniques, *Existing and Potential Standoff Explosives Detection Techniques*, Washington, D.C.: THE NATIONAL ACADEMIES PRESS, 2004.

[73] J. Yinon, "Trace analysis of explosives in water by gas chromatography mass spectrometry with a temperature-programmed injector", Journal of Chromatography A, 742, 205, 1996.

[74] Y.J.Choi, I.S.Hwang and J.G.Park et al, "Noval fabrication of an SnO2 nanowire gas sensor with high sensitivity", Nanotechnology, 19, 095509, 2008.

[75] L.O.Peres and J.Gruber, "The use of block copolymeters containing PPV in gas sensors for electronic noses", Materials Science and Engineering: C, 27, 67, 2007.

[76] H.Ge amd J.Liu, "Identification of gas mixtures by a distributed support vector machine network and wavelet decomposition from temperature modulated semiconductor gas sensor", Sensors and Actuators B: Chemical, 117, 408, 2006.

[77] A. Rothschild, and Y. Komem, "The effect of grain size on the sensitivity of nanocrystalline metal-oxide gas sensors", Journal of Applied Physics, 95, 6374, 2004.

[78] G.J.Cadena, J.Riu, and F.X.Rius, "Gas sensors based on nanostructred materials," Analyst, 132, 1083, 2007.

[79] N.Barsan and U.Weimar, "Understanding the fundamental principles of metal oxide based gas sensors; the example of CO sensing with SnO_2 sensors in the presence of humidity", Journal of Physics: Condensed Matter, 15, R813, 2003.

[80] R. Vargas and O. Nunez, "Hydrogen bond interactions at the TiO_2 surface: Their contribution to the pH dependent photo-catalytic degradation of *p*-nitrophenol", Journal of Molecular Catalysis A-Chemical, 300, 65, 2009.

[81] K. S. Finnie, D. J. Cassidy, J. R. Bartlett and J. L. Woolfrey, "IR Spectroscopy of Surface Water and Hydroxyl Species on Nanocrystalline TiO_2 Films", Langmuir, 17, 816, 2001.

[82] A. S. Vuk, R. Jese, B. Orel and G. Drazic, "The effect of surface hydroxyl groups on the adsorption properties of nanocrystalline TiO_2 films", International Journal of Photoenergy, 7, 163, 2005.

[83] B. Meyer, D. Marx, O. Dulub, U. Diebold, M. Kunat, D. Langenberg and C. Woll, "Partial Dissociation of Water Leads to Stable Superstructures on the Surface of Zinc Oxide", Angewandte Chemie International Edition, 43, 6641, 2004.

[84] H. W. Ra, R. Khan, J. T. Kim, B. R. Kang, K. H. Bai and Y. H. Im, "Effects of surface modification of the individual ZnO nanowire with oxygen plasma treatment", Materials Letters, 63, 2516, 2009.

[85] J. M. Pan, B. L. Maschhoff, U. Diebold, T. E. Madey, "An isotope approach to characterization of microwave water plasma modified polyimide surfaces", Journal of Vacuum Science&Technology A, 10, 248, 1992.

[86] N.Baram amd U.Weimar, "Conduction model of metal oxide gas sensors", Journal of Electroceramics, 7, 143, 2001.

[87] G. Heiland and D.Kohl, " *Chemical Sensor Technology* 1, ed T Seiyama (Tokyo: Kodansha) ch 2 pp 15–38.

[88] S.R.Morrison 1990 *The Chemical Physics of Surfaces* 2nd edn (New York: Plenum).

[89] R.Schaub, P.Thostrup, N.Lopez, E.Lagsgaard, I.Stensgaard, J.K.Norskov and F.Besenbacher, "Oxygen Vacancies as Active Sites for Water Dissociation on Rutile TiO_2(110)", Physical Review Letter, 87, 266104, 2001.

[90] G.Wang, Q.Wang, W.Lu and J.H.Li, "Photoelectrochemical Study on Charge Transfer Properties of TiO_2-B nanowires with an Applications of Humidity Sensors", The Journal of Physical Chemistry B, 110, 22029, 2006.

[91]J.Tan, W.Wlodarski and K.K.Zadeh, "Nitrogen dioxide gas sensors based on titanium dioxide thin films deposited on langasite", Thin Solid Films, 515, 8738, 2007.

[92] N.Sakai, R.Wang, A.Fujishima, T.Watanabe and K.Hashimoto, "Effect of ultrasonic treatment on highly hydrophilic TiO_2 surfaces", Langmuir, 14, 5918, 1998.

[93] N.Sakai, A.Fujishima, T.Watanabe and K.Hashimoto, "Enhancement of the photoinduced hydrophili conversion rate of TiO_2 film electrode surfaces by anodic polarization", The Journal of Physical Chemistry B, 105, 3023, 2001.

[94] R.Marchand, L.Brohan and M.Tournoux, "TiO_2 (B) a new form of titanium dioxide and the potassium octatitanate $K_2Ti_8O_{17}$", Materials Research Bulletin, 15, 1129, 1980.

[95] Y.C.Lee, Y.P.Hong, H.Y.Lee, H.Kim, Y.J.Jung, K.H.Ko, H.S.Jung and K.S.Hong, "Photocatalysis and hydrophilicity of doped TiO_2 thin film," Journal of Colloid and Interface Science, 267, 127, 2003.

[96] O. A. El Seoud, A. R. Ramadan, B. M. Sato and P. A. R. Pires, "Surface Properties of Calcinated Titanum Dioxide Probed by Solvatochromic Indicators: Relevance to Catalytic Application", Journal of Physical Chemistry C, 114, 10436, 2010.

[97] R.Muller, H.K.Kammler, K.Wegner and S.E.Prtsinis, "OH Surface Density of SiO_2 and TiO_2 by Thermogravimetric Analysis", Langmuir, 19, 160, 2003.

[98] R. G. Parr, "Density Functional Theory", Annual Review of Physical Chemistry, 34, 631, 1983.

[99] D. Ferro, V. Piacente, R. Gigli and G. D'Ascenzo, "Determination of the vapour pressures of o-, m-, and p- dinitrobenzene by the torsion-effusion method", Journal of Chemical Thermodynamics, 8, 1137, 1976.

[100] J. E. Abbott, X. Z. Peng and W. Kong, "Symmetry properties of electronically excited states of nitroaromatic compounds", Journal of Chemical Physics, 117, 8670, 2002.

[101] T. Tanaka, A. Nakajima, A. Watanabe, T. Ohno and Y. Ozaki, "Surface-enhanced Raman scattering spectroscopy and density functional theory calculation studies on adsorption of o-, m-, and p-nitroaniline on silver and gold colloid", Journal of Molecular Structure: THEOCHEM, 661, 437, 2003.

[102] G. Munuera, V. Rivesarnau and A. Saucedo, "Photo-adsorption and photo-desorption of oxygen on highly hydroxylated TiO_2 surfaces. Part 1.—Role of hydroxyl groups in photo-adsorption", Journal of the Chemical Society-Faraday Transactions I, 75, 736, 1979.

[103] K. Aim, "Saturated Vapor Pressure Measurements on Isomeric Mononitrotoluenes at Temperatures between 380 and 460 K", J.Chem.Eng.Data, 39, 591, 1994.

[104] http://actrav.itcilo.org/actrav-english/telearn/osh/ic/100016.htm.

[105] H. Carlsson, G. Robertsson and A. Colmsjo, "Response Mechanisms of Thermionic Detectors with Enhanced Nitrogen Selectivity", Analytical Chemistry, 73, 5698, 2001.

[106] P. L. Edmiston, D. P. Campbell, D. S. Gottfried, J. Baughman and M. M. Timmers, "Detection of vapor phase trinitrotoluene in the parts-per-trillion range using waveguide interferometry", Sensors and Actuators B: Chemical, 143, 574, 2010.

[107] A. Kawski, B. Kuklinski and P. Bojarski, "Dipole moment of aniline in the excited S1 state from thermochromic effect on electronic spectra", Chemical Physics Letters, 415, 251, 2005.

[108] T.Pustelny, M.Procek, E.Maciak, A.Stolarczyk, S.Drewniak, M.Urbanczyk, M.Setkiewicz, K.Gut and Z.Opilski, "Gas sensors based on nanostructures of semiconductors ZnO and TiO_2," Bulletin of the polish academy of sciences technical sciences., 60, 853, 2012.

[109] A. Fujishima, T. N. Rao and D. A. Tryk, "Are the five natural DNA/RNA base monomers a good choice from natural selection?: A photochemical perspective", Journal of Photochemistry and Photobiology C: Photochemistry Reviews, 1, 1-21, 2000.

[110] A. Hakki, R. Dillert and D. Bahnemann, "Photocatalytic conversion of nitroaromatic compounds in the presence of TiO_2", Catalysis Today, 144, 154-159, 2009.

[111] R.Wang, K.Hashimoto, A.Fujishima, M.Chikuni, E.Kojima, A.Kitamura, M.Shimohigoshi and T.Watanable, "Light-induced amphilic surfaces", Nature, 388, 431, 1997.

[112] R.Wang, K.Hashimoto, A.Fujishima, M.Chikuni, E.Kojima, A.Kitamura, M.Shimohigoshi and T.Watanable, "Photogeneration of highly amphiphilic TiO_2 surfaces", Advanced Materials, 10, 135, 1998.

[113] J.G.Yu and X.J.Zhao, "Effect of surface treatment on the photocatalytic activity and hydrophilic property of the sol-gel derived TiO_2 thin films", Materials Research Bulletin, 36, 97, 2001.

[114] O. Carp, C. L. Huisman and A. Reller, "Photoinduced reactivity of titanium dioxide", Progress in Solid State Chemistry, 32, 33, 2004.

[115] K. W. Kim, E. H. Lee, Y. J. Kim, M. H. Lee, K. H. Kim and D. W. Shin, "A relation between the non-stoichiometry and hydroxyl radical generated at photocatalytic TiO_2 on 4CP decomposition", Journal of Photochemistry and Photobiology A: Chemistry, 159, 301, 2003.

[116] W. Janusz, A. Sworska and J. Szczypa, "The structure of the electrical double layer at the titanium dioxide/ethanol solutions interface", Colloids and Surfaces A: Physicochemical and Engineering Aspects, 152, 223, 1999.

[117] A. Fujishima, K. Honda, "Electrochemical Photolysis of Water at a Semiconductor Electrode", Nature, 238, 37, 1972.

[118] A. Mills and S. Le Hunte, "An overview of semiconductor photocatalysis", Journal of photochemistry and photobiology. A, Chemistry, 108, 1, 1997.

[119] M. R. Hoffmann, S. T. Martin, W. Choi and D. W. Bahnemann, "Environmental Applications of Semiconductor Photocatalysis", Chemical reviews, 95, 69, 1995.

[120] H. Jamil, S. S. Batool, Z. Imran, M. Usman, M. A. Rafiq, M. Willander and M. M. Hassan, "Electrospun titanium dioxide nanofiber humidity sensors with high sensitivity", Ceramics International, 38, 2437, 2012.

[121] D. P. Smetaniuk, M. T. Taschuk and M. J. Brett, "Photocatalytic Titanium Dioxide Nanostructures for Self-Regenerating Relative Humidity Sensors", IEEE Sensors Journals, 11, 1713, 2011.

[122] Y. H. Tseng and C. H. Kuo, "Photocatalytic degradation of dye and NO_x using visible-light-responsive carbon-containing TiO_2", Catalysis Today, 174, 114, 2011.

[123] Y. M. Lin, Y. H. Tseng, J. H. Huang, C. C. Chao, C. C. Chen and I. Wang, "Photocatalytic Activity for Degradation of Nitrogen Oxides over Visible Light Responsive Titania-Based Photocatalysts", Environmental science & technology, 40, 1616, 2006.

[124] C.Cummings, in Proc.of the 1st Olfactory-Based Systems for Security Applications meeting (OBSSA), London, UK 2004.

[125] F.Patolsky, G.F. Zheng and C.M. Lieber, "Fabrication of silicon nanowire devices for ultrasensitive, label-free, real-time detection of biological and chemical species", Nature Protocols, 1, 1711, 2006.

[126] O.H.Elibol, D.Morisette, D.Akin, J.P.Denton and R.Bashir, "Integrated nanoscale silicon sensors using top-down fabrication", Applied Physics Letters, 83, 4613, 2003.

[127] A. Talin, L.L.Hunter, F.Leonard and B. Rokad, "Large area, dense silicon nanowire array chemical sensors", Applied Physics Letters, 89, 153102, 2006.

[128] M.C.MaALPINE, H.Ahmad, D.W.Wang and J.R.Heath, "Highly ordered nanowire arrays on plastic substrates for ultrasensitive flexible chemical sensors", Nature Materials, 6, 379, 2007.

[129] E.Stern, A.Vacic and M.A.Reed, "Semiconducting Nanowire Field-Effect Transistor Biomolecular Sensors", IEEE Transactions on Electron Devices, 55, 3119, 2008.

[130] N. M. A. Board, in National Academy of Science, Washington, D. C. 2004.

[131] J. Koo and S. Kim, "Charge transport modulation of silicon nanowire by O_2 plasma", Solid State Sciences, 11, 1870, 2009.

[132] A.N.Nazarov,V.S.Lysenko and T.M.Nazarova, "Hydrogen plasma treatment of silicon thin-film structures and nanostructured layers", Semiconductor Physics, Quantum Electronics & Optoelectronics, 11, 101, 2008.

[133] Y.-L. Loo, R.L.Willett, K.W.Baldwin and J.A.Rogers, "Additive, nanoscale patterning of metal films with a stamp and a surface chemistry mediated transfer process: Applications in plastic electronics", Applied Physics Letters, 81, 562, 2002.

[134] T.Yasuda, Y.Ma, S.Habermehl and G.Lucovsky, "Low-temperature preparation of SiO_2/Si(100) interfaces using a two-step remote plasma-assisted oxidation-deposition process", Applied Physics Letters, 60, 434, 1992.

[135] S.Taylor, J.F.Zhang and W.Eccleston, "A review of the plasma oxidation of silicon and its applications", Semiconductor Science and Technology, 8, 1426, 1993.

[136] M.Egashira, S.Kawasumi, S.Kagawa and T. Seiyama, "Temperature Programmed Desorption Study of Water Absorbed on Metal Oxides. I. Anatase and Rutile", Bulletin of the Chemical Society of Japan, 51, 3144, 1978.

[137] N.Yamazoe, Y.Kurokawa and T.Seiyama, "Effects of additives on semiconductor gas sensors", Sensors and Actuators, 4, 283, 1983.

[138] G.Korotcenkov, V.Brinzari, Y.Boris, M.Ivanov, J.Schwank and J.Morante, "Surface Pd doping influence on gas sensing characteristics of SnO_2 thin films deposited by spray pyrolysis", Thin Solid Films, 436, 119, 2003.

[139] A.A. Athawale, S.V. Bhagwat, P.P. Katre, A.J. Chandwadkar and P. Karandikar, "Aniline as a stablizer for metal nanoparticles", Materials Letters, 57, 89, 2003.

[140] A.Kolmakov, D.O.Klenov, Y.Lilach, S.Stemmer and M. Moskovits, "Enhanced Gas Sensing by Individual SnO_2 Nanowires and Nanobelts Functionalized with Pd Catalyst Particles", Nano Letters, 5, 667, 2005.

[141] S.Basu and P.K.Basu, "Nanocrystalline Metal Oxides for Methane Sensors: Role of Noble Metals", Journal of Sensors, 2009, 861968, 2009.

[142] G.Korotcenkov "Gas response control through structural and chemical modification of metal oxide films: State of the art and approaches", Sensors and Actuators B: Chemical, 107, 209, 2005.

[143] K.Jain, R.P.Pant and S.T.Lakshmikumar, "Effect of Ni doping on thick film SnO_2 gas sensor", Sensors and Actuators B: Chemical, 113, 823, 2006.

[144] I.T.Weber, A.Valentini, L.F.D.Probst, E.Longo and E.R. Leite, "Influence of noble metals on thestructural and catalytic properties of Ce-doped SnO_2 systems", Sensors and Actuators B: Chemical, 97, 31, 2004.

[145] J. Marien, T. Wagner, G. Duscher, A. Koch and M. Rühle, "Nb on (110) TiO_2 (rutile): growth, structure, and chemical composition of the interface", Surface Science, 446, 219, 2000.

[146] Y.J.Choi, Z.Seeley, A.Bandyopadhyay, S.Bose and S.A.Akbar, "Aluminum-doped TiO_2 nanpowders for gas sensors", Sensors and Actuators B: Chemical, 124, 111, 2007.

[147] M. S.Park, S.Kwon and B.Min, "Electronic structures of doped anatase TiO_2: $Ti_{1-x}M_xO_2$(M= Co, Mn, Fe, Ni)", Physical Review B, 65, 161201, 2002.

[148] J.Choi, H.Park and M.R.Hoffmann, "Effects of single metal-ion doping on the visible-light photoreactivity of TiO_2", The Journal of Physical Chemistry C, 114, 783, 2009.

[149] C.Wang, C.Bottcher, D. W.Bahnemann and J. K.Dohrmann, "A comparative study of nanometer sized Fe (III)-doped TiO_2 photocatalysts: synthesis, characterization and activity", Journal of Materials Chemistry, 13, 2322, 2003.

[150] Q.F.Zhang, E.Uchaker, D.Myers, G.Z.Cao, "Visible light-driven water splitting using TiO_2 nanocrystallite aggregates doped with transition metals", 2013 (In preparation).

[151] Y.Ren, Z.Liu, F.Pourpoint, A.R.Armstrong, C.P.Grey, and P.G.Bruce, "Nanoparticulated TiO_2(B): An Anode for Lithium-Ion Batteries", Angewandte Chemie International Edition, 51, 2164, 2012.

[152] A.Selloni, “Anatase shows its reactive side”, Nature, 7, 613, 2008.

[153] W. K. Siu, R. A. Bartynski and S. L. Hulbert, “The role of defects at low concentrations in the $NH_3/TiO_2(110)$ adsorption system: An Auger–photoelectron coincidence spectroscopy study”, The Journal of Chemical Physics, 113, 10697, 2000.

[154] Y.Bai, W.Li, C.Liu, Z.Yang, X.Feng, X.Lu and K.-Y.Chan, “Stability of Pt nanoparticles and enhanced photocatalytic performance in mesoporous Pt-(anatase/TiO_2(B)) nanoarchitecture”, Journal of Materials Chemistry, 19, 7055, 2009.

[155] T.Beuvier, M.R.Plouet and L.Brohan, “Accurate Methods for Quantifying the Relative Ratio of Anatase and TiO_2(B) Nanoparticles”, The Journal of Physical Chemistry C, 113, 13706, 2009.

[156] Y.Xiao, L.Li, Y.Li, M.Fang and L.Zhang, “Synthesis of mesoporous ZnO nanowires through a simple in situ precipitation method”, Nanotechnology, 16, 671, 2005.

[157] P. Mitra, A. P. Chatterjee, and H. S. Maiti, “ZnO thin film sensor”, Materials Letters, 35, 33, 1998.

[158] B.H.Kim, A.Kim, S.-Y.Oh, S.-S.Bae, Y.Yun, and H.Yu, “Energy gap modulation in V_2O_5 nanowires by gas adsorption”, Applied Physics Letters, 93, 233101, 2008.

[159] F.Zhou, X.M.Zhao, C.G.Yuan and L.Li, “Vanadium Pentoxide Nanowires: Hydrothermal Synthesis, Formation Mechanism, and Phase Control Parameters”, Crystal Growth & Design, 8, 723, 2008.

[160] S.Yan, L.Sun, Y.Sheng, N.Huang and Z.Xiao, “Novel regrowth mechanism of CdS nanowire in hydrothermal synthesis”, New Journal of Chemistry, 35, 299, 2011.

[161] T.-D.Nguyen, C.-T.Dinh and T.-O.Do, “A general procedure to synthesize highly crystalline metal oxide and mixed oxide nanocrystals in aqueous medium and photocatalytic activity of metal/oxide nanohybrids”, Nanoscale, 3, 1861, 2011.

VITA

Danling Wang was born in Hanzhong City, Shaanxi Province, China. She graduated from Peking University and earned her Ph.D. degree from Physics Department in 2003. After graduation, she went to US and joined Prof. John C. Wright group in Department of Chemistry at University of Wisconsin, Madison as a research associate. Later, she worked in Prof. Xingde Li group in Department of Bioengineering at University of Washington in Seattle as sensor fellow. In fall 2008, she started pursuing her second Ph.D. in the Electrical Engineering Department at University of Washington in Seattle, WA and joined the photonics group under the supervision of Dr. Antao Chen in Applied Physics Laboratory and Prof. Lih Yuan Lin in the Electrical Engineering Department. In Autumn 2013, she received her Ph.D. in Electrical Engineering. Her research was focused on explosive sensor based on nanostructured semiconductors.

LIST OF PUBLICATIONS

- **Journal Papers**

1. **D.L.Wang**, A.T.Chen, and Alex K-Y.Jen, "Reducing cross-sensitivity of TiO_2-(B) nanowires to humidity using ultraviolet illumination for trace explosive detection", Phys.Chem.Chem.Phys., Vol.15, pp.5017-5021.
2. **D.L.Wang**, A.T.Chen, S-H. Jiang, J.J.Davies, and Alex K-Y.Jen, "The effect of dipole moment and electron deficiency of analytes on the chemiresistive response of TiO_2(B) nanowires", Analyst, vol.136, pp. 4179-4182.
3. **D.L.Wang**, A.T.Chen, S-H. Jiang, H.Yip, and Alex K-Y.Jen, "Sensitivity of Titania(B) nanowires to nitroaromatic and nitroamino explosives at room temperature via surface hydroxyl groups", Journal of Materials Chemistry, vol.21, pp. 7269-7273.
4. **D.L.Wang**, Q.F.Zhang, G.Z.Cao, and A.T.Chen, "Room-Temperature Chemiresistive Effect of TiO2-B Nanowires to Nitroaromatic and Nitroamine Explosives", IEEE Sensors Journal, vol.11, pp. 1352-1358.
5. **D.L.Wang**, S.H.Sun, A.T.Chen, S.H.Jang, and Alex K-Y.Jen, "Chemiresistive response of silicon nanowires to trace vapor of nitro explosives", Nanoscale, vol.4, pp. 2628-2632.
6. **D. L. Wang**, B. V. Hunter, M. J. Cobb, and X. D. Li, "Super-achromatic rapid scanning microendoscope for ultrahigh-resolution OCT imaging", IEEE Journal of Selected Topics in Quantum Electronics, vol. 13, pp. 1596-1601, Nov-Dec 2007 (invited).
7. **D.L.Wang**, Q.F.Zhang, G.Z.Cao and A.T.Chen., "Chemiresistive response of TiO_2-B nanowires: the effect of polar strength of analyte molecules", Proc. of SPIE Vol. 8024 80240W-1, 2011.
8. **D. L. Wang**, J. F. Xiang, H. B. Jiang, G. Z. Xu, and Q. H. Gong, "Photoinduced electron transfer between dye IR-140 and TiO_2 colloids by femtosecond pump supercontinuum probing", Journal of Optics A-Pure and Applied Optics, vol. 5, pp. 123-127, Mar 2003.
9. **D. L. Wang**, H. B. Jiang, S. J. Wu, H. Yang, Q. H. Gong, J. F. Xiang, and G. Z. Xu, "An investigation of solvent effects on the optical properties of dye IR-140 using the pump supercontinuum-probing technique", Journal of Optics A-Pure and Applied Optics, vol. 5, pp. 515-519, Sep 2003.

10. **D. L. Wang**, H. B. Jiang, H. Yang, C. L. Liu, Q. H. Gong, J. F. Xiang, and G. Z. Xu, "Investigation on photoexcited dynamics of IR-140 dye in ethanol by femtosecond supercontinuum-probing technique", Journal of Optics A-Pure and Applied Optics, vol. 4, pp. 155-159, Mar 2002.
11. **D. L. Wang**, H. Yang, H. B. Jiang, Q. H. Gong, Q. F. Zhang, and J. L. Wu, "Optical transient relaxation of an Ag-BaO composite thin film with a supercontinuum probe", Chinese Physics Letters, vol. 19, pp. 1115-1118, Aug 2002.
12. **D. L. Wang**, C. D. Li, L. Luo, H. Yang, and Q. H. Gong, "Sub-diffraction-limit voids in bulk quartz induced by femtosecond laser pulses", Chinese Physics Letters, vol. 18, pp. 65-67, 2001.
13. **D. L. Wang**, Q. H. Gong, K. G. Wang, and G. J. Yang, "Quantum nondemolition measurement in degenerate optical parametric oscillator", Acta Physica Sinica, vol. 49, pp. 1484-1489, Aug 2000.
14. J. S. Brown, **D. L. Wang**, X. L. Li, F. Ballyot, B. Iliakis, T. D. Lindquist, R. Shirakawa, T. T. Shen and X. D. Li, "Situ Ultrahigh-resolution Optical Coherence Tomography Characterization of Eye Bank Corneal Tissue Processed for Lamellar Keratoplasty", Cornea, vol. 27, pp. 802-810, Aug.2008.
15. J. Y. Chen, **D. L. Wang**, J. F. Xi, L. Au, A. Siekkinen, A. Warsen, Z. Y. Li, H. Zhang, Y. N. Xia, and X. D. Li, "Immuno gold nanocages with tailored optical properties for targeted photothermal destruction of cancer cells", Nano Letters, vol. 7, pp. 1318-1322, May 2007.
16. S. J. Wu, **D. L. Wang**, H. B. Jiang, H. Yang, Q. H. Gong, Y. L. Ji, and W. Lu, "Transient saturation absorption spectroscopy excited near the band gap at high excitation carrier density in GaAs", Chinese Physics, vol. 13, pp. 111-114, Jan 2004.
17. Q. F. Zhang, **D. L. Wang**, Q. H. Gong, and J. L. Wu, "Investigation on transient relaxation in Ag-BaO composite thin film with pump supercontinuum-probe technique", Journal of Physics D-Applied Physics, vol. 35, pp. 1326-1329, Jun 2002.
18. L. Luo, **D. L. Wang**, C. D. Li, H. B. Jiang, H. Yang, and Q. H. Gong, "Formation of diversiform microstructures in wide-bandgap materials by tight-focusing femtosecond laser pulses", Journal of Optics a-Pure and Applied Optics, vol. 4, pp. 105-110, Jan 2002.

19. Y. D. Qin, **D. L. Wang**, S. F. Wang, and Q. H. Gong, "Spectral and temporal properties of femtosecond white-light continuum generated in H_2O", Chinese Physics Letters, vol. 18, pp. 390-392, Mar 2001.
20. C. D. Li, **D. L. Wang**, L. Luo, H. Yang, Z. J. Xia, and Q. H. Gong, "Feasibility of femtosecond laser writing multi-layered bit planes in fused silica for three-dimensional optical data storage", Chinese Physics Letters, vol. 18, pp. 541-543, Apr 2001.
21. Q. F. Zhang, W. M. Liu, Z. Q. Xue, J. L. Wu, S. F. Wang, **D. L. Wang**, and Q. H. Gong, "Ultrafast optical Kerr effect of Ag-BaO composite thin films", Applied Physics Letters, vol. 82, pp. 958-960, Feb 2003.
22. Q. F. Zhang, Q. Y. Shao, S. M. Hou, G. M. Zhang, W. M. Liu, Z. Q. Xue, J. L. Wu, S. F. Wang, R.S. Liang, W. T. Huang, **D. L. Wang**, and Q. H. Gong, "Large and extremely fast third-order nonlinearity of Ag nanoparticles embedded into a CsxO semiconductor matrix", Chinese Physics, vol. 10, pp. S65-S69, Jul 2001.

- **Conference Proceedings and Presentations:**

1. **Wang, D. L.,** Zhang, Q. F., Cao, G. Z. and Chen, A. T., "Strong room-temperature chemiresistive effect of TiO2-B nanowires to nitro-aromatic compounds", Accepted by SPIE Defense, Security, and Sensing conference, 25-29 April 2011 in Orlando, Florida, United States.
2. **Wang, D.L.,** Feng, X.C., Yang, H., Xia, Z.J. and Gong, Q.H., "Femtosecond time-resoved photodynamical study on Ag-O-Ba thin film", Accepted by IEEE QELS 2001, United States.

- **Patents**

US Patents:

1. A.Chen, **D. Wang**, Q. Zhang, and G. Cao, "Detection of Trace Chemicals and Method Therefor", G01N 27/12 ed US and PCT Countries, 2009.
2. A.Chen, A.K.-Y.Jen, S.H.Jang, and **D.Wang**, "Reduction of Cross Sensitivity to Air Humidity by UV Illumniation".

China Patents:

J. L. Wu, Q. F. Zhang, Z. Q. Xue, W. M. Liu, Q. D. Wu, **D. L. Wang**, and Q. H. Gong, "Fabrication of metal nanoparticle-semiconductor composite film and application to all-optical Kerr switch", in State Intellectual Property Office of P. R. China, G02F1/025; H04B10/12 ed China, 2002.

Technical Disclosures at UW:

A. T. Chen, **D. L. Wang**, Q. F. Zhang, and G. Z. Cao, "Trace explosive sensor using nanostructured chemoresistive thin film (No. 8049D, UW)".